

AMERICAN UNIVERSITY OF BEIRUT

DECORTICATION VS MICROPERFORATIONS:  
A FINITE ELEMENT ANALYSIS

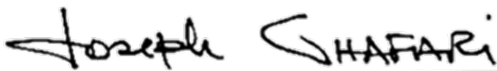
by  
SARAH ALI KHAMIS

A thesis  
submitted in partial fulfillment of the requirements  
for the degree of Master of Science in Orthodontics  
to the Department of Otolaryngology- Head and Neck Surgery  
of the Faculty of Medicine  
at the American University of Beirut

Beirut, Lebanon  
June, 2020

DECORTICATION VS MICROPERFORATIONS:  
A FINITE ELEMENT ANALYSIS

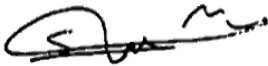
by  
SARAH ALI KHAMIS



---

Dr. Joseph Ghafari, Professor and Head  
Orthodontics and Dentofacial Orthopedics

Primary Advisor



---

Dr. Samir Mustapha, Assistant Professor  
Department of Mechanical Engineering

Co-Primary Advisor



---

Dr. Jason Amatoury, Assistant Professor  
Department of Mechanical Engineering

Member of Committee



---

Dr. Kinan Zeno, Assistant Professor  
Orthodontics and Dentofacial Orthopedics

Member of Committee

Date of thesis defense: June 19, 2020



# ACKNOWLEDGMENTS

**Alone we can do so little; together we can do so much**

*Hellen Keller*

This thesis is the product of an enormous amount of teamwork and cooperation. Therefore, I would like to express my deepest appreciation to all the individuals who have contributed to this journey. I am genuinely grateful to:

*Dr. Joseph Ghafari*, for being a great teacher and role model in exploring innovative research ideas and giving me the chance to contribute in integrating engineering into the world of orthodontics, providing expert guidance and invaluable support;

*Dr. Samir Mustapha*, for teaching me the basics of engineering and introducing me to FEA, and sharing his intellectual and engineering knowledge to guide me through each step;

*Dr. Makram Ammouy*, for providing the ground base of this research with his thesis; "A Finite Element Analysis Study", and for always being there to answer my questions;

*Dr. Kinan Zeno*, for sharing his engineering and orthodontic input in various aspects of this work and for his valuable comments in correcting the thesis;

*Dr. Ingrid Karam*, for her assistance in the statistical analysis and interpretation;

*Christophe Zoughaib*, for being my partner in engineering, and for all the memories we made over the last three years;

*Residents and staff*, for being my second family, and creating a fun and encouraging atmosphere at the department;

And finally, last but not least, *my beloved family and friends*, for all the love and emotional support in my life.



## AN ABSTRACT OF THE THESIS OF

Sarah Ali Khamis for Master of Science  
Major: Orthodontics

Title: Decortications Vs microperforations: A finite element analysis

### Introduction:

Adjunctive corticotomies such as decortication and microperforations reportedly reduce the duration of orthodontic treatment, but their effectiveness remains controversial.

### Aims:

1. Compare the stresses and displacements generated by canine distalization against orthodontic miniscrews with and without decortication and microperforations. 2. Determine the conditions under which both techniques lead to similar effects. 3. Test the influence of individual variation in cortical bone properties through thickness and stiffness.

Our hypothesis was that increasing the extent of the corticotomy leads to higher stress and initial displacement, and that cortical bone thickness and stiffness influence stress generation.

### Methods:

A 3D model of the maxilla containing teeth, PDL, cortical and trabecular bone was prepared for finite element analysis (FEA) using first ScanIP™ 7.0 software (Simpleware Ltd., Exeter UK) to construct the model and later ABAQUS 6.13 for mechanical modeling. Distalization of the buccal segment was simulated with a force (150 grams) directed from a miniscrew placed between the 2<sup>nd</sup> premolar and 1<sup>st</sup> molar to the canine bracket. With DEC and MOP introduced distal to the canine, six models were generated: Control, DEC, and 4 MOP (with 3, 4, 5 and 6 perforations). Initial canine and first premolar displacement and stress distribution on the PDL of the canine, first premolar, and trabecular bone were compared.

### Results:

The stress distribution pattern was similar in all the models, being highest on the canine, more precisely on the cervical region, and progressively decreasing in magnitude from the canine to the second molar. Stresses on all PDL surfaces and displacement of the canine were significantly higher (with the highest stress registered on the distal surface) than the stresses and displacement of the 1<sup>st</sup> premolar except for the palatal surface. Statistically significant differences were found for the stress and displacement between modalities in both the stiffness and thickness variations. Stress and displacement increased as the number of perforations increased. The 6MOP modality yielded the highest initial displacement and stress on all PDL surfaces and the trabecular bone. However, when

compared with decortications, greater stresses and displacements were found except for the stress on the buccal surface where it was significantly reduced. DEC and 6MOP led to almost the same effect on distal surface stress and initial canine displacement (25% increase). The difference was in the stress on the buccal surface.

High correlations were present between the total stress on the PDL and initial tooth displacement. No correlations were found between PDL stress and thickness, and between initial displacement and cortical bone properties. At the 1<sup>st</sup> premolar, high and negative correlations were present with the palatal stiffness components of the premolar. Moreover, stress on the trabecular bone underlying the corticotomy showed a negative correlation with the buccal cortical bone stiffness and a positive correlation with the thickness in the microperforation modalities.

### Conclusions:

1. By removing a continuous shear band of cortical bone with decortication, resistance to tooth movement is decreased thereby facilitating initial displacement
2. Six microperforations could be as efficient as decortication when extended over the same distance.
3. By introducing individual variation in cortical bone properties, we were able to determine the effect of stiffness and thickness on stress generation, proving that the response of the dentoalveolar structures depends not only force magnitude and vectors, but also on individual anatomy.
4. Future research should elucidate other clinical setups and time-dependent orthodontic movement, beyond the present initial static FEA conditions.

# CONTENTS

ACKNOWLEDGEMENTS.....	iii
ABSTRACT.....	iv
LIST OF ILLUSTRATIONS.....	x
LIST OF TABLES.....	xii
LIST OF ABBREVIATIONS.....	xiv
1. INTRODUCTION	1
2. LITTERATURE REVIEW	5
2.1. Alveolar bone.....	5
2.2. Orthodontic tooth movement .....	6
2.2.1. Theories of orthodontic mechanisms .....	6
2.2.2. Phases of tooth movement .....	7
2.2.3. Biology of tooth movement .....	7
2.2.4. Bone modeling and remodeling .....	9
2.3. Regional acceleratory phenomenon .....	10
2.3.1. Definition .....	10
2.3.2. Nature .....	10
2.3.3. Contributing factors .....	11
2.3.4. Duration .....	11
2.4. Accelerating orthodontic tooth movement .....	12
2.4.1. Non-surgical methods .....	12
2.4.1.1. Low-intensity laser therapy (LLLT) .....	12
2.4.1.2. Electric currents and electromagnetic fields .....	13
2.4.1.3. Resonance vibration .....	14
2.4.1.4. Pharmacological approaches .....	14
2.4.1.5. Gene therapy .....	15
2.4.2. Surgical methods .....	16
2.4.2.1. Distraction of the PDL and the dento-alveolus .....	16

2.4.2.2. Corticotomy .....	18
2.4.2.2.1. The “bony block” concept .....	19
2.4.2.2.2. Wilckodontics .....	20
2.4.2.2.3. Corticision .....	23
2.4.2.2.4. Piezocision .....	24
2.4.2.2.5. Micro-osteoperforation (MOP) .....	25
2.4.2.2.6. Comparison between the different techniques .....	30
2.5. Finite Element Analysis .....	32
2.5.1. Definition .....	33
2.5.2. Development of FEA in dentistry.....	34
2.5.3. FEA in orthodontics .....	35
2.5.4. Limitations .....	37
2.5.4.1. Sensitivity of the meshing process .....,.....	37
2.5.4.2. Inaccurate assumptions .....	38
2.5.4.3. 3D modeling of human tissues .....	39
2.5.4.4. Tooth movement simulation over time .....	40
2.5.4.5. Applicability of results .....,.....	41
2.5.4.6. Generalizability of results .....	41
2.6. Progress in bone modeling .....	42
2.7. Significance .....	43
2.8. Specific aims .....	45
2.9. Hypothesis .....	46
<b>3. MATERIAL AND METHODS</b> .....	<b>47</b>
3.1. Material .....	47
3.1.1. Anatomical records .....	47
3.1.2. Individual data acquisition .....	47
3.2. Methods .....	49
3.2.1. 3D model .....	49
3.2.1.1. Model construction .....	49
3.2.1.2. CAD processing .....	50
3.2.1.3. Individual variations .....	52
3.2.1.4. Decortications and microperforations .....	54
3.2.1.5. Meshing .....	57
3.2.2. Finite element analysis (FEA) .....	58
3.2.2.1. Definition of material properties .....	58
3.2.2.2. Analysis type definition .....	60
3.2.2.3. Interactions .....	60

3.2.2.4. Loading setup and boundary conditions .....	62
3.2.2.5. Data collection and export .....	66
3.2.3. Statistical analysis .....	68
<b>4. RESULTS</b> .....	<b>71</b>
4.1. Stiffness variation .....	71
4.1.1. Stress comparison between teeth and modalities .....	71
4.1.2. Displacement comparison between teeth and modalities .....	78
4.2. Thickness variation .....	80
4.2.1. Stress comparison between teeth and modalities .....	80
4.2.2. Displacement comparison between teeth and modalities .....	83
4.3. Correlation between stress and displacement .....	84
4.3.1. Stiffness variation .....	84
4.3.2. Thickness variation .....	85
4.4. Correlation between cortical bone properties and stress .....	87
4.4.1. Correlation with cortical bone stiffness .....	87
4.4.1.1. Canine .....	87
4.4.1.2. 1 <sup>st</sup> Premolar .....	87
4.4.1.3. Trabecular bone .....	88
4.4.2. Correlation with cortical bone thickness .....	89
4.4.2.1. Canine .....	89
4.4.2.2. 1 <sup>st</sup> Premolar .....	89
4.4.2.3. Trabecular bone .....	89
4.5. Correlation between cortical bone properties and displacement .....	90
4.5.1. Correlation with cortical bone stiffness .....	90
4.5.1.1. Canine .....	90
4.5.1.2. 1 <sup>st</sup> Premolar .....	91
4.5.2. Correlation with cortical bone thickness .....	91
4.5.2.1. Canine .....	91
4.5.2.2. 1 <sup>st</sup> Premolar .....	92
4.6. Correlation between cortical bone removal, stress and displacement .....	92
4.6.1. Stiffness variation .....	92
4.6.2. Thickness variation .....	93
4.7. Data normalization .....	94

5. DISCUSSION	97
5.1. Strengths	97
5.1.1. Individual variation	97
5.1.2. Effect of bone characteristics on tooth movement	98
5.1.3. Orthotropic material properties	98
5.2. Comparison with FEA corticotomy studies	100
5.2.1. Comparison between teeth	105
5.2.1.1. Stress	105
5.2.1.2. Displacement	106
5.2.2. Comparison between modalities	106
5.2.3. Correlation between stress and displacement	112
5.2.4. Correlation between stress, displacement and cortical bone properties	113
5.2.5. Correlation between stress, displacement and volume of bone removed	117
5.3. Clinical implications	118
5.4. Limitations	121
5.5. Future research	122
6. CONCLUSION	125
7. BIBLIOGRAPHY	128

## ILLUSTRATIONS

Figure	Page
2.1 A theoretical model describing the stages of tooth movement .....	8
2.2 Bone modeling and remodeling processes .....	9
2.3 Different surgical techniques for acceleration of tooth movement .....	16
2.4 Periodontal distraction technique .....	17
2.5. Surgical technique of dento-alveolar distraction .....	
18	
2.6 Bony block osteotomies by Köle (1959) .....	19
2.7 “Wilckodontics” surgical cuts and bone grafting .....	21
2.8. The process by which corticotomies accelerate tooth movement .....	21
2.9 Clinical case of a patient treated with “Wilckodontics” .....	22
2.10 Follow up after accelerated osteogenic orthodontics surgery .....	23
2.11 Animal study on corticision .....	24
2.12 Piezocision surgical technique .....	25
2.13 The Propel Excellerator device .....	26
2.14 Role of microperforations on bone remodeling .....	27
2.15. Follow up on canine retraction after microperforations .....	28
2.16 Protocol of microperforations application during canine retraction .....	29
2.17 Microperforations performed between the mandibular anterior teeth .....	29
2.18 Finite element mesh generated for ceramics veneer simulation .....	35
2.19 A three-dimensional model of a lower first premolar .....	36
3.1 Cortical bone sites in the maxilla in the study by Peterson et al. (2006) .....	48
3.2 Segmentation of the teeth mask .....	49
3.3 Smoothing of the teeth, PDL and bone masks .....	49
3.4 Sketching and placement of the CAD objects (brackets, TAD) .....	50
3.5 Bracket imported and added to the FE model .....	51
3.6 Division of the cortical bone in the model according to the areas of the dentate maxilla as described by Peterson et al. (2006) .....	52
3.7 Axial cuts of the template model and the models with variation in cortical bone thickness .....	53
3.8 The template model .....	54
3.9 Corticotomy cut created using the 3D editing tool .....	54
3.10 Positioning of the cylindrical object on the cortical bone mask .....	55
3.11 Subtraction of the cylindrical object from the cortical bone mask to simulate the microperforation .....	56
3.12 The six generated models representing the different clinical scenarios .....	56
3.13 The meshed template model .....	58
3.14 The 3D model imported into Abaqus .....	58
3.15 Creation and positioning of ellipsoid shapes representing interactions between teeth .....	61
3.16 “Surface to surface” interactions between teeth .....	62
3.17 Clinical application of the direct distalization modality .....	62

3.18	Node set created on the canine bracket for load application .....	63
3.19	Lateral view of the direct load from the miniscrew to the bracket .....	64
3.20	Boundary conditions on the upper and posterior part of the maxilla .....	64
3.21	Datum axis parallel to the long axis of the teeth to simulate the archwire .....	64
3.22	Boundary conditions on the maxilla and the teeth .....	65
3.23	Selection of element sets on the canine .....	67
3.24	Selection of the set of elements on the trabecular bone .....	67
3.25	Selection of node sets representing the centroid of the canine and premolar ...	68
4.1	Von mises stress distribution on the PDL in each modality .....	71
4.2	Graphic representation of the stress on the canine and 1 <sup>st</sup> premolar in the stiffness variation .....	73
4.3	PDL stress on the buccal surface of the canine and 1 <sup>st</sup> premolar in each modality .....	75
4.4	Von mises stress on the trabecular bone in each modality .....	75
4.5	Initial tooth displacement in each modality .....	79
4.6	Graphic representation of the stress on the canine and 1 <sup>st</sup> premolar in the thickness variation .....	81
4.7	Bar graph showing the metric measures for stress/volume of bone removed in the stiffness and thickness variations .....	95
4.8	Bar graph showing the metric measures for displacement /volume of bone removed in the stiffness and thickness variations .....	96
5.1	Designs of corticotomy approaches with variation in position, width, and distance from canine (Yang et al. (2015) .....	101
5.2	Models in Pacheco et al. (2016) study .....	102
5.3	Corticotomy models in Samgir et al. (2018) study .....	102
5.4	FE corticotomy models in Gupta et al. (2019) study .....	103
5.5	Stress distribution with the different corticotomy modifications in Yang et al. (2015) study .....	109
5.6.	Line graphs showing the percentage of increase in canine stress and initial displacement on stiffness variations in the different modalities .....	111
5.7	Anatomical differences between the canine and 1 <sup>st</sup> premolar .....	114
5.8	Total incisor displacement in both control and corticotomized models .....	115



## TABLES

Table	Page
3.1 Density, cortical thickness and ash weight (Peterson et al. 2006) .....	48
3.2 Calculated volume of bone removed in each modality .....	57
3.3 Material properties of anatomical components used in orthodontic FEA studies .....	59
3.4 Orthotropic material properties at the site of buccal cortical bone in the 15 cadavers (Peterson et al. 2006) .....	60
4.1 Comparison of the stress generated on the PDL of the teeth in each modality (stiffness variation) .....	72
4.2 Comparison of the stress on the teeth and trabecular bone among the different microperforation modalities (stiffness variation) .....	73
4.3 Pairwise comparison for stress between each microperforation modality (stiffness variation) .....	74
4.4 Teeth and trabecular bone stresses comparison between the decortication and microperforations (stiffness variation) .....	74
4.5 Comparison of the stress generated on the PDL sections of the canine .....	76
4.6 Pairwise comparison for stress on the PDL sections of the canine between each microperforation modality (stiffness variation) .....	77
4.7 Canine PDL sections stress comparison with the decortication .....	77
4.8 Comparison of the initial displacement between the teeth (stiffness variation)	78
4.9 Comparison of the initial teeth displacement among the different microperforation modalities (stiffness variation).....	79
4.10 Pairwise comparison for displacement between each microperforation modality (stiffness variation) .....	79
4.11 Displacement comparison with decortication (stiffness variation) .....	79
4.12 Comparison of the stress generated on the PDL of the teeth in each modality (thickness variation) .....	80
4.13 Comparison of the stress on the teeth and trabecular bone among the different microperforation modalities (thickness variation) .....	81
4.14 Pairwise comparison for stress between each microperforation modality (thickness variation) .....	82
4.15 Teeth and trabecular bone stresses comparison between the decortication and microperforations (thickness variation) .....	82
4.16 Comparison of the initial displacement between the teeth (thickness variation)	83
4.17 Comparison of the initial teeth displacement among the different microperforation modalities (thickness variation).....	83
4.18 Pairwise comparison for displacement between each microperforation modality (thickness variation) .....	84
4.19 Displacement comparison with decortication (thickness variation) .....	84
4.20 Correlation between total stress and displacement (stiffness variation) .....	84
4.21 Correlation between stress at each PDL surface and displacement (stiffness variation) .....	85

4.22	Correlation between total stress and displacement (thickness variation) .....	86
4.23	Correlation between stress at each PDL surface and displacement (thickness variation) .....	86
4.24	Correlation between canine stress and cortical bone stiffness .....	87
4.25	Correlation between 1 <sup>st</sup> premolar stress and cortical bone stiffness .....	88
4.26	Correlation between trabecular bone stress and cortical bone stiffness .....	88
4.27	Correlation between canine stress and cortical bone thickness .....	89
4.28	Correlation between 1 <sup>st</sup> premolar stress and cortical bone thickness .....	89
4.29	Correlation between trabecular bone stress and cortical bone thickness .....	90
4.30	Correlation between canine displacement and cortical bone stiffness .....	90
4.31	Correlation between 1 <sup>st</sup> premolar displacement and cortical bone stiffness ...	91
4.32	Correlation between canine displacement and cortical bone thickness .....	91
4.33	Correlation between 1 <sup>st</sup> premolar displacement and cortical bone thickness ..	92
4.34	Descriptive statistics for the volume of bone removed in each modality .....	92
4.35	Correlation between volume of bone removed and stress (stiffness variation) .....	93
4.36	Correlation between volume of bone removed and stress in all the modalities except decortication (stiffness variation) .....	94
4.37	Correlation between volume of bone removed and stress (thickness variation) .....	94
4.38	Correlation between volume of bone removed and stress in all the modalities except decortication (thickness variation) .....	94
5.1	Cortical bone impact on PDL stress and crown displacement based on the correlations results .....	114
5.2	Cortical bone impact on trabecular bone stress based on the correlations results .....	117

## ABBREVIATIONS

<b>CONT</b>	Control
<b>MOP</b>	Microperforations
<b>DEC</b>	Decortication
<b>1<sup>st</sup> PM</b>	First premolar
<b>3</b>	Canine
<b>4</b>	First premolar
<b>TB</b>	Trabecular bone
<b>U</b>	Displacement
<b>S</b>	Total stress in the stiffness variation
<b>T</b>	Total stress in the thickness variation
<b>a</b>	Apical
<b>m</b>	Middle
<b>c</b>	Cervical
<b>SB</b>	Stress at the buccal PDL surface (stiffness variation)
<b>SD</b>	Stress at the distal PDL surface (stiffness variation)
<b>SM</b>	Stress at the mesial PDL surface (stiffness variation)
<b>SP</b>	Stress at the palatal PDL surface (stiffness variation)
<b>TB</b>	Stress at the buccal PDL surface (thickness variation)
<b>TD</b>	Stress at the distal PDL surface (thickness variation)
<b>TM</b>	Stress at the mesial PDL surface (thickness variation)
<b>TP</b>	Stress at the palatal PDL surface (thickness variation)

## CANINE

<b>Stiffness</b>		<b>Thickness</b>	
<b>SB3</b>	Stress at the buccal PDL surface	<b>TB3</b>	Stress at the buccal PDL surface
<b>SD3</b>	Stress at the distal PDL surface	<b>TD3</b>	Stress at the distal PDL surface
<b>SM3</b>	Stress at the mesial PDL surface	<b>TM3</b>	Stress at the mesial PDL surface
<b>SP3</b>	Stress at the palatal PDL surface	<b>TP3</b>	Stress at the palatal PDL surface
<b>SU3</b>	Canine displacement	<b>TU3</b>	Canine displacement

## FIRST PREMOLAR

<b>Stiffness</b>		<b>Thickness</b>	
<b>SB4</b>	Stress at the buccal PDL surface	<b>TB4</b>	Stress at the buccal PDL surface
<b>SD4</b>	Stress at the distal PDL surface	<b>TD4</b>	Stress at the distal PDL surface
<b>SM4</b>	Stress at the mesial PDL surface	<b>TM4</b>	Stress at the mesial PDL surface
<b>SP4</b>	Stress at the palatal PDL surface	<b>TP4</b>	Stress at the palatal PDL surface
<b>SU4</b>	1 <sup>st</sup> premolar displacement	<b>TU4</b>	1 <sup>st</sup> premolar displacement

<b>FEM</b>	Finite Element Method	<b>FEA</b>	Finite Element Analysis
<b>FE</b>	Finite Element	<b>OTM</b>	Orthodontic Tooth Movement
<b>PDL</b>	Periodontal Ligament	<b>RAP</b>	Regional Acceleratory Phenomenon
<b>3D</b>	Three Dimensional	<b>2D</b>	Two Dimensional
<b>CT</b>	Computed Tomography	<b>CBCT</b>	Cone Beam Computed Tomography
<b>RCT</b>	Randomized Clinical trials	<b>CAD/CAM</b>	Computer Aided Design/ Computer Aided Manufacturing
<b>TAD</b>	Temporary Anchorage Device	<b>MRI</b>	Magnetic Resonance Imaging
<b>HU</b>	Hounsfield Unit	<b>NiTi</b>	Nickel Titanium
<b>inp</b>	Input	<b>STL</b>	Stereolithography

# CHAPTER 1

## INTRODUCTION

The process of tooth movement can either be part of a normal physiologic process or secondary to orthodontic manipulation. This requires both periodontal and alveolar bone changes, in a coupled process of resorption and formation (Frost, 1989). Orthodontic tooth movement is described as the movement of teeth through alveolar bone using externally applied forces, and resulting in a biological reaction within the dentoalveolar tissues (Ren et al., 2004). Therefore, orthodontics is the biomechanical manipulation of bone.

The remodeling of bone following an injury involves a complex array of processes that ultimately determine the rate of tooth movement. Hence, there is a limitation to the rapidity at which orthodontic treatment can be completed without adverse effects (Roberts, 2011). Prolonged treatment duration has been associated with various sequelae such as pain, caries, white spot lesions, periodontal problems (Bishara et. al 2008). It is well documented that the longer the duration of tooth movement, the greater the risk of root resorption (Sameshima et al., 2001; Mohandesan et al., 2007; Gonzales et al., 2008). In addition, long treatment duration adversely affects patients' compliance during treatment, and their satisfaction with the outcome (Uribe et al., 2014; Pachêco-Pereira et al., 2015).

In line with the goal of orthodontic treatment targeting improvement of the patient's life through enhancement of dentofacial functions and esthetics, and with the myriad of complications associated with long treatments, reducing orthodontic treatment duration has become an issue of importance, particularly for adults. Limitations of conventional

orthodontic treatment along with the length of treatment duration often result in difficulties for clinicians and create barriers to patient willingness to accept treatment.

During the last decades, the number of patients with esthetic concerns and time limitations has increased significantly. Simultaneously, substantial advancements in the orthodontic field have broadened the range of potential tooth movement. In this regard, investigation of new approaches to boost treatment efficiency by accelerating tooth movement, and facilitating a therapeutic process without foregoing the optimal results, has become a goal for orthodontists (Oliveira et al., 2010). The findings that cells can respond to physical, chemical or surgical signals have created an insight that accelerated tooth movement can become a clinical reality. Accordingly, several techniques have been advocated in conjunction with orthodontic treatment, in order to accelerate tooth movement, including bone manipulation via surgical intervention.

Corticotomy-facilitated orthodontic therapy has been present in the literature since the mid-twentieth century; It is a surgical procedure consisting of alteration of the cortical bone, to accelerate tooth movement, by increasing cellular activity and reducing bone resistance (Buschang et al., 2012). Various modifications to the technique have been proposed in the literature in an attempt to increase its effectiveness and reduce its invasiveness, from Wilcko's decortications, to more recently, micro-osteoperforations (MOPs).

The acceleration rate of tooth movement in human patients varies depending on the choice of the corticotomy technique, force magnitude and duration of activation, type of tooth movement, quality and type of bone, and individual variations (Patterson et al., 2016; Chandran et al., 2018). Due to a lack of comparative data and full understanding of the

physiologic and biomechanical processes of tooth movement through corticotomies, it is unclear which surgical protocol is preferable regarding treatment efficiency (Hoogveen et al., 2014).

To date, studies have evaluated the effect of a corticotomy by using cone-beam tomography (Wang et al., 2014), microtomography (Lee et al., 2008; Baloul et al., 2011), radiography and histological sections of animals (Lino et al., 2007). With the development of engineering in the field of medicine, it has become quite established in the field of dentistry, especially orthodontics. Modern medical imaging, modeling and finite element analysis (FEA) solutions can provide powerful tools for optimizing three-dimensional (3D) morphology from radiographic scans and determining stress and deflection distributions for complex anatomic geometries such as teeth and bone (Ammar et al., 2011).

Orthodontic tooth movement is a force-related process that occurs in response to a mechanical stimulus. The effect and distribution of this mechanical stimulus can be denoted with stress and strain, rather than with orthodontic force (Viecilli et al., 2013). After a corticotomy, the continuity of the cortical bone is disrupted, which causes a change in the stress and strain of the dentoalveolar structure (Xue et al., 2013). This change can be calculated using three-dimensional (3D) finite element method.

Orthodontic treatment relies on mechanical stress leading to tissue strain and the resultant change in the parodontal tissues. Stress in the periodontal ligament (PDL) can be used as a factor to stimulate changes in the behavior of cells responsible for bone remodeling in orthodontic tooth movement (Field et al., 2009). Knowing the relationship between the change in the induced mechanical strain fields and the corresponding biologic reaction is crucial. At present, little research regarding the biomechanical effects of

corticotomy approaches on dentoalveolar structures has been done, and studies are lacking comparing corticotomy techniques for acceleration of tooth movement on finite element modeling, more specifically studies comparing decortications and micro-osteoperforations. A better understanding of the mechanical process behind these procedures will allow the clinician to make better clinical judgments and lead to evidence-based practice.



## CHAPTER 2

### LITERATURE REVIEW

#### **2.1. Alveolar bone**

The alveolar bone, also known as the alveolar process, is responsible for tooth support and protection. With regard to its composition, it is similar to other bone tissues, being a mineralized connective tissue consisting of 60 % inorganic material (mineral tissue), 25% organic matrix which is mostly collagen, and 15% water (Moss, 1997). Although the bulk of the alveolar bone is trabecular bone, it contains a plate of compact bone adjacent to the periodontal ligament called the lamina dura. The inner and outer cortical plates are also composed of cortical bone (Andrei et al., 2018).

Bone is a metabolically active tissue capable of responding to changes in mechanical stimuli, adapting its internal architecture, and repairing structural damage. The processes of bone formation and resorption are regulated through the actions of the bone cells: the osteoblast and osteoclast. The formation of the organic matrix of bone is executed by the osteoblast. This extracellular matrix becomes calcified through the precipitation of calcium phosphate crystals within the matrix. During this process, the osteoblast becomes entombed in the deposited matrix, transforming into an osteocyte. The osteocytes, which are no longer involved in new bone-forming duties, are responsible for maintaining the bone tissue and participate in the calcium exchange between bone and blood. Osteoclasts are responsible for bone resorption and are regulated by osteoblasts through a signaling axis that controls osteoclast generation and activity (Sherwood, 2015).

## **2.2. Orthodontic tooth movement**

Orthodontic tooth movement is the “result of a biological response to an interference in the physiological equilibrium of the dentofacial complex by an externally applied force” (Proffit, 2007). A mechanical stimulus which is transmitted to the PDL and then to the alveolar bone producing a mechanical change of the dentoalveolar structures, which triggers a series of biological processes including a temporary regulation of bone apposition or resorption, thereby allowing tooth movement (Henneman et al., 2008). The site-specific remodeling of the periodontal tissues is mediated by physical, cellular, biochemical, and molecular reactions (Krishnan and Davidovitch, 2006).

### ***2.2.1. Theories of orthodontic mechanism: Pressure-tension theory***

Once explained mainly by the piezoelectric activity which postulates that bone bending releases electric signals responsible for tooth movement, orthodontic tooth movement is better described by the pressure-tension theory that relates tooth movement to cellular changes produced by chemical messengers be generated by alterations in blood flow through the PDL. Thus, under prolonged light pressure on the teeth, the stress-strain distribution in the PDL is altered and tension and compression sites develop, which results in changes in blood flow (Graber et al., 2016). This will trigger the release of chemical messengers involved in both the osteoclastic and osteoblastic activity. The pressure side, located in the direction of tooth movement, will display disorganization and diminution of fiber production. Conversely, on the tension side, there is an increase in cell replication and fiber production (Busse et al., 2009). The result is tooth movement through resorption of bone on the pressure side and deposition of bone on the tension side (Lee et al., 2008).

### ***2.2.2. Phases of tooth movement***

In 1962, Burstone suggested that, if the rates of tooth movement were plotted against time, there would be 3 phases of tooth movement:

1. The initial phase (1-2 days): characterized by rapid movement immediately after force application, largely attributed to the displacement of the tooth in the PDL space.
2. The lag phase (20-30 days): Immediately after, with relatively low rates of tooth displacement or no displacement, due to PDL hyalinization in areas of compression.
3. The post-lag phase: follows the lag period, during which the rate of movement gradually or suddenly increases after complete removal of the necrotic tissue.

### ***2.2.3. Biology of tooth movement***

Orthodontic tooth movement is an aseptic and acute inflammatory process (Alansari et al., 2018). Within hours of force application, the induced tissue strain produces local alterations in vascularity, as well as cellular and extracellular matrix reorganization, leading to the synthesis and release of various neurotransmitters, chemokines, cytokines, growth factors and enzymes that act as secondary messengers on signal transduction pathways. Consequently, an inflammatory process is launched leading to a cascade of events encompassing cellular differentiation and recruitment. Through the RANK/RANKL pathway, where the RANKL receptor activator expressed on the osteoblasts surface binds to its receptor, RANK, on the surface of osteoclasts and their precursors, the differentiation and activation of the osteoclasts is regulated. In the next 48 hours, osteoclasts appear within the compressed PDL and engage in the “frontal resorption” of the adjacent bone indicating

the beginning of movement (Fig. 2.1). Soon after, osteoblasts appear in the enlarged PDL at the tension side and initiate bone formation (Krishnan and Davidovitch, 2006).

However, the forces applied to the tooth are not uniform and the tissue remodeling response is variable (Andrade et al., 2012). In the presence of heavy forces, blood supply is cut in the compression area, ensued by the propagation of a sterile necrosis in the PDL producing a hyalinized tissue. Several days later, osteoclasts appear within the adjacent bone marrow spaces and promote the “undermining resorption”, a process of removal of necrotic tissue and resorption from within the bone that progresses to the surface, resulting in further delay of tooth movement (Proffit et al., 2012).

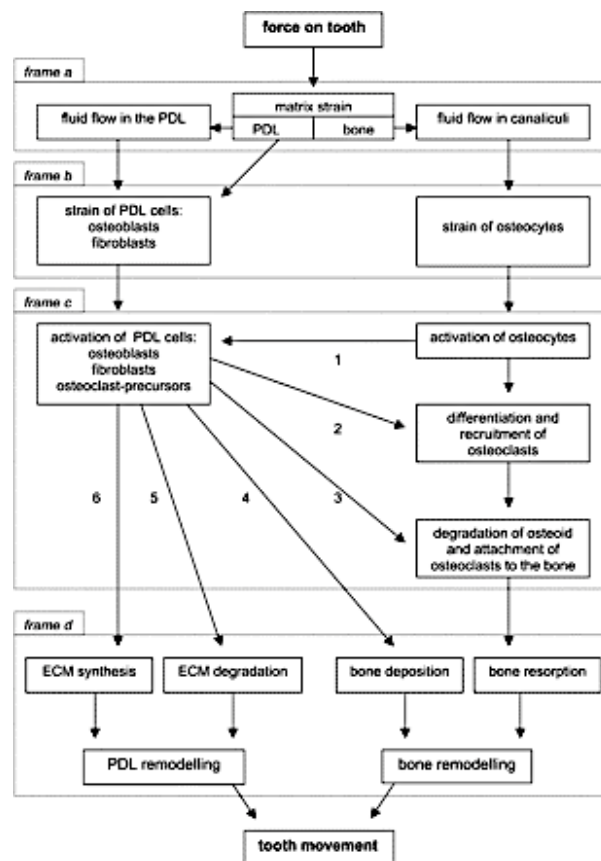


**Fig. 2.1:** A theoretical model describing the 4 stages of tooth movement: (a) matrix strain and fluid flow, (b) cell strain, (c) cell activation and differentiation, and (d) remodeling of PDL and bone (Adapted from Henneman et al., 2008).

#### 2.2.4. Bone modeling and remodeling

Bone modeling is the uncoupled process of resorption or formation on bone surfaces, resulting in the change of shape, size, or position of the bone. Bone remodeling or turnover, on the other hand, is a coupled local process, which starts with bone resorption, followed by reversal and bone formation, resulting in the replacement of old bone with new bone (Fig. 2.2). According to “Wolff’s law”, bone can modify its internal architecture to provide optimal support in response to alteration in applied mechanical loads.

Both bone modeling and remodeling are determinants for the rate of orthodontic tooth movement (Huang et al., 2014). Bone modeling during orthodontic tooth movement is an inflammatory process, and the rate-limiting factor for tooth movement is bone resorption at the bone and PDL interface (Roberts et al., 2004). Even though bone remodeling renews the internal content of bone without changing the size or shape of the bone under physiologic conditions, it also affects the rate of OTM (Verna et al., 2000).

Whether tooth movement occurs with or through bone depends on the stress/strain distribution in the PDL. The latter is determined by the following factors: force magnitude, bone area, and force distribution, depending on the type of tooth movement. In tipping movements, the forces are concentrated in the marginal and apical parts of the alveolus, whereas translation results in more uniform force distribution (Melsen, 1999).

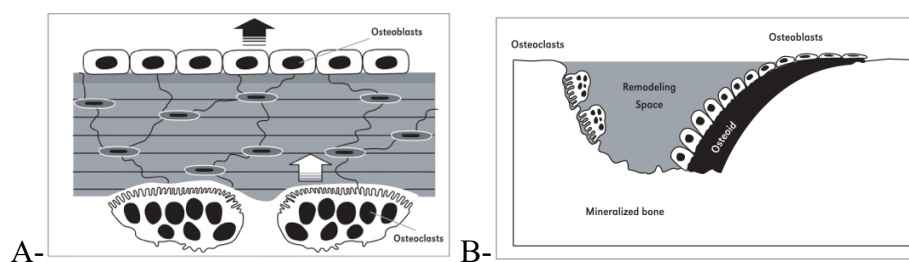


Fig. 2.2: A: Modeling; B: Remodeling processes (adapted from Office of the Surgeon US., 2004).

## **2.3. Regional acceleratory phenomenon (RAP)**

### ***2.3.1. Definition***

The regional acceleratory phenomenon (RAP) is another example illustrating the biologic process of orthodontic tooth movement. RAP was first suggested by Frost in 1983, and refers to a situation in which an injury (noxious stimuli) results in a local acceleration of tissue healing processes (2-10 times faster than physiologic healing (Frost, 1983).

### ***2.3.2. Nature***

The RAP is by definition a local reaction and it has been seen in a thorough histological animal study that it rarely extends more than a one tooth distance (Sebaoun et al., 2008). This phenomenon is typical of not only hard tissues such as bone and cartilage, but also of soft tissues, and both the stimulated area and the surrounding tissues are affected. These tissues responses vary depending on the duration, strength and size of the harmful stimulus, with an individual variation in the degree of response. RAP does not seem to provide new processes, but rather increases the rapidity of healing through the post-fracture stages, including modeling and remodeling, which means that additional cycles of resorption followed by formation are activated (Frost, 1989).

When bone is surgically irritated, a wound is created, which initiates a localized inflammatory response catalyzing the recruitment of inflammatory markers (chemokines, prostaglandin, RANK/RANKL pathway) and cellular differentiation. In the alveolar bone, RAP is characterized, at a cellular level, by increased activation of the basic multicellular units (BMUs), thereby increasing the remodeling space. At a tissue level, it is characterized by the production of woven bone, that will later be reorganized into lamellar bone. This

process is followed by a period of predominant resorption, with a radiographically detected decrease in bone density. It is postulated that osteoclast and osteoblast cell populations shift in number, resulting in a state of “osteopenia” (Bogoch et al., 1993).

### ***2.3.3. Contributing factors***

In addition to trauma, RAP can be caused by several stimuli including vitamin D, thyroxine and electrical stimuli. In the maxilla and mandible, RAP typically occurs in the healing processes of the alveolar sockets after tooth extraction, fractures, in periodontal disease, implant placement, and during orthodontic treatment. In relation to orthodontic tooth movement, RAP can be seen as a tissue response to the mechanical cyclic perturbation that induces the formation of microdamage that has to be removed to avoid their accumulation and the following bone failure. The adaptation to the new orthodontically induced mechanical environment is ensured by an increased activation of the BMU that return to normal levels after few months (Verna et al., 2016).

### ***2.3.4. Duration***

Frost estimated the total duration required for activation, resorption, and formation (ARF) to be 12 weeks. RAP is suggested to begin within a few days of surgery, typically peaking at 1-2 months, and may take 6 to more than 24 months to subside (Murphy et al., 2009). In other words, it may take at least one formation period of the remodeling cycle (lasting 3-4 months) after the last perturbation. Frost (1989) also stated that the duration and intensity of the RAP are proportional to the extent of injury and tissue involvement. Later studies showed that this effect is, however, temporary and lasts for about 4 months,

and the injury needs to be repeated in case faster tooth movement is still required (Mathews & Kokich, 2013).

## **2.4. Accelerating orthodontic tooth movement**

The average treatment duration extends from 21 to 27 months for non-extraction treatment and 25 to 35 months for extraction treatment (Buschang et al., 2012). Most tooth movements occur at a rate of  $\cong 1$  mm/ month (Iwasaki et al., 2000; Ren et al., 2004). The velocity of orthodontic tooth movement is influenced by bone turnover, bone density, and PDL hyalinization (Verna et al., 2000; Verna & Melsen, 2003).

Throughout history, orthodontic specialty has attempted numerous physical, chemical and surgical means to enhance the effect of applied mechanical forces through bone remodeling. The basic tenet of these approaches is substantially increasing catabolic and anabolic activity of tissues in the tooth-moving location (Chandran et al., 2018). Adjunct to the proper selection of brackets, wires, appliances, force levels, and anchorage systems, an array of novel techniques has been introduced to accelerate orthodontic tooth movement. These techniques can be briefly categorized as surgical and non-surgical.

### ***2.4.1. Non-surgical techniques***

#### **2.4.1.1. Low-intensity laser therapy (LLLT)**

Low level laser therapy has been introduced in orthodontic procedures with its initial purpose to alleviate pain after adjustments and to enhance healing of sore spots caused by appliance impingement (Kim et al., 2015). This technique has been suggested to



accelerate turnover of periodontal tissues through its bio-stimulatory effect by producing an upregulation of ATP production by mitochondrial cells and elevation of the metabolic activity (Yoshida et al., 2009). In addition, recent reports have shown that LLLT may stimulate the differentiation and proliferation of osteoblasts and osteoclasts, and enhance the velocity of tooth movement due to accelerated bone remodeling mediated by the RANK/RANKL/OPG system (Fujita et al., 2008) (Domínguez et al., 2015). The use of LLT in accelerating OTM was mostly studied in canine retraction cases with a marginal increase in the rate of retraction (0.42mm/month) over a period of 3-4.5 months (Sousa et al., 2011; Doshi-Mehta et al., 2012). However, results are contradictory due to the difference in the parameters used in each study regarding its design, application method, wavelength, dose of irradiation, and exposure time (Huang et al., 2014).

#### 2.4.1.2. Electric currents and electromagnetic fields

The application of electric currents and pulsed electromagnetic fields (PEMF) have demonstrated enhanced rates of tooth movement. Davidovitch et al. (1980) reported that when a force was applied simultaneously with electric currents (10-20 mA), teeth moved faster than with force application alone in a feline model. Increased levels of osteoclasts and subsequent increased rate of OTM was observed by Stark and Sinclair (1987) who described the use of PEMF in tooth movement in a rat model over a 10-day period. Changes in serological parameters related to protein metabolism and muscle activity were noted. Later studies supported these theories (Darendeliler et al., 2007; Showkatbakhsh et al., 2010), but the evidence is still inconclusive.

#### 2.4.1.3. Resonance vibration

Based on the piezoelectric theory, applied forces generate an electric charge that induces the osteogenic response. Since the charges are created only when stress is applied and released, it was suggested that orthodontic forces should not be continuous (Shapiro et al., 1979). Therefore, vibrational devices may be suitable for initiating stress-induced charges by rapidly applying an intermittent force (Aljabaa et al., 2018). This method is also recommended for pain reduction after orthodontic adjustments (Staud et al., 2011). An animal study by Nishimura et al., in 2008 found that secondary to mechanical strain, the vibration of bone enhances RANKL expression in the PDL. One of the commercially available vibrating devices is Acceleident (OrthoAccel Technologies, Texas). It has been marked as a safe non-invasive device consisting of an activator and a removable mouthpiece, and patients are instructed for 20 minutes of wear/day. However, recent systematic reviews reported that the evidence to confirm its efficacy is weak (El-Angbawi., 2015) (Jing et al., 2017).

#### 2.4.1.4. Pharmacological approaches

Several researchers have suggested that there might be ways to increase cellular activity with agents more potent than mechanical force alone. Considerable scientific interest has been focused on chemical stimuli in combination with mechanical forces for more rapid bone turnover and faster OTM. These studies used prostaglandins (PGs), cytokines, neuropeptides and leukotrienes, which are considered physiologic mediators between the applied force and the cellular response, to reduce tissue resistance during tooth movement (Cağlaroğlu et al., 2012). Despite the several reports on the association between

local injections of prostaglandin (PGE<sub>1</sub>) and (PGE<sub>2</sub>) and 1,25-dihydroxycholecalciferol (1,25-DHCC) which is the biologically active form of vitamin D, and the increase of the osteoblastic and osteoclastic activity (Kale et al., 2004), most studies are based on animal models, and applications of these agents on human did not gain much popularity (Bartzela et al., 2009). In addition, due to their rapid flush out by blood circulation, daily systemic administration or local injection is needed.

#### 2.4.1.5. Gene therapy

Selective gene therapy has been experimentally tested as an alternative method to accelerate OTM. A previous animal study demonstrated that the local transfer of RANKL gene to periodontal tissue activated osteoclastogenesis and accelerated OTM without producing any systemic effects (Kanzaki et al., 2004, 2006). Iglesias-Linares et al., 2011 found that maintaining transgenic expression of RANKL allowed OTM acceleration over time rather at the beginning of the therapy only, in contrast with corticotomy. Local osteoprotegerin (OPG) transfer has also been used to inhibit tooth movement, which might be, in the near future, an important tool to enforce the anchorage unite or increased the stability of the results (Zhao et al., 2012). Nonetheless, further research is needed to determine the safety and efficacy of these techniques.

#### **2.4.2. Surgical techniques**

The idea of surgically accelerated tooth movement although more than a century old has only gained momentum and interest recently (Murphy et al., 2012). Bone manipulation via surgical intervention, including orthognathic (total or segmental correction of

maxillofacial bones) and dentoalveolar (surgery limited to the dentoalveolar region, including a single tooth or a group of teeth and cortical and/or trabecular bone) surgery became a subject of interest based on the associated alteration in the bone biology of tooth movement (Oliveira et al., 2010). Theoretically, selective surgical alveolar bone reduction induces a localized increase in turnover of alveolar cancellous bone, suggesting a possible mechanism underlying the observed acceleration of tooth movement (Baloul et al., 2011). Another possible mechanism could be attributed to the removal of the hyaline zone formed soon after force application, which allows earlier bone resorption required for tooth movement (Kim et al., 2009). The surgical category includes distraction of the periodontal ligament, distraction of the dento-alveolus, and corticotomy (Uzuner et al., 2013) (Fig. 2.3).

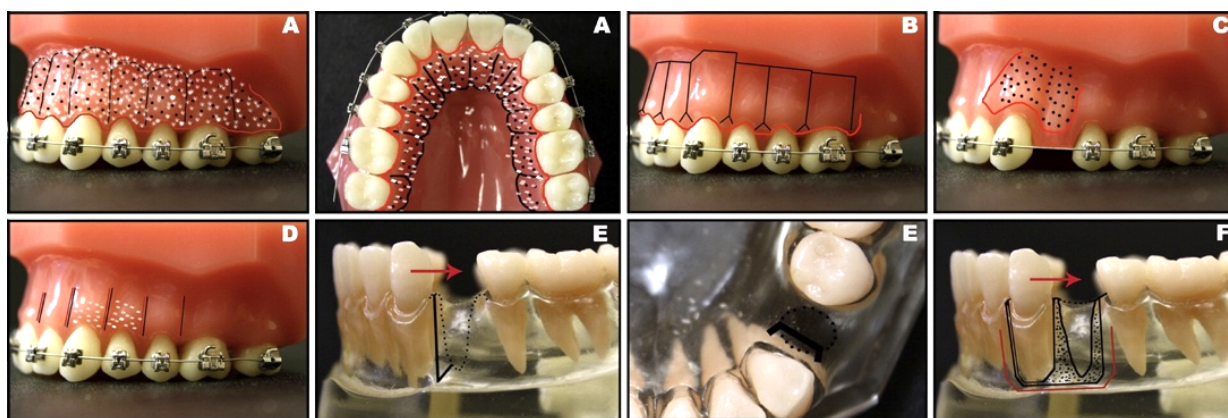


**Fig. 2.3:** Different surgical techniques: A- PAOO or Wilckodontics (buccal and palatal views); B- Monocortical piezosurgery; C- Monocortical perforations (black dots); D- Piezocision; E- PDL distraction (buccal and occlusal views); F- Dentoalveolar distraction. (Hoogeveen et al., 2014).

#### 2.4.2.1. Distraction of the periodontal ligament (PDL) and the dento-alveolus

The concept of distraction osteogenesis relies on the process of growing new bone by mechanical stretching of the pre-existing bone tissue. First described by Liou and Huang

in 1998, based on the concept of osteogenesis in the mid-palatal suture, distraction of the periodontal ligament is the surgical undermining of the inter-septal bone, which elicited rapid canine retraction (6-7 mm) in three weeks, when performed on the mesial aspect of the socket of an extracted first premolar. The surgical procedure consisted of buccal and lingual vertical osteotomies at the inter-septal bone site adjacent to the canine, which were connected with an oblique osteotomy extending toward the base of the interseptal bone to weaken the resistance (Fig. 2.4). A tooth-borne distractor was cemented in place to the canine and first molar after the surgery.

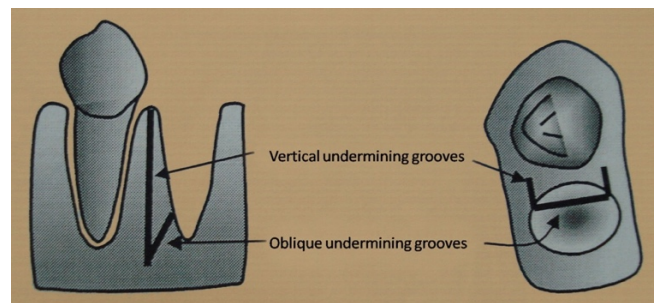


**Fig. 2.4:** Periodontal distraction technique (Kharkar et al., 2010).

On the other hand, dento-alveolar distraction, which was described by Iseri et al. (2002; 2005 and 2017) involves the separation of the dental segment from the jaw bone to allow distraction osteogenesis in the osteotomy site. In extraction cases, the buccal cortical bone of the extraction socket is removed, and osteotomies outlining the canine root are made to achieve rapid canine retraction (Fig. 2.5). In 2010, Kharkar et al. compared PDL distraction with dento-alveolar distraction. Clinical and radiographic means were used to assess the time required for retraction, canine tipping, anchorage loss and external root resorption. The dentoalveolar group was more effective with less root resorption.



**Fig. 2.5:** Surgical technique for dento-alveolar distraction (Adapted from Kharkar et al., 2010).

In both techniques, the distraction is executed at a rate of 0.5-1mm/day, with the objective to surgically reduce bony resistance, and minimal force was necessary for full mobilization of the bone segment which was kept passively for 12 weeks of consolidation. Proposed indications are: Canine retraction in extraction cases, with minimal posterior anchorage loss, class II division 1 malocclusion, bimaxillary protrusion, and anterior crowding (Fleming et al., 2015). Distraction procedures may expedite tooth movement by facilitating movement of teeth at a known rate, while other surgical procedures rely on triggering heightened osteoclastic activity by inducing regional accelerated phenomena (Wilcko et al., 2001). These cellular mechanisms result in a reduction in bone density, reducing the impediment to tooth movement (Teixeira et al., 2010).

#### 2.4.2.2. Corticotomy

A corticotomy *is* defined as a surgical procedure whereby only the cortical bone is cut, perforated, or mechanically altered while the medullary bone is preserved. This contrasts with an osteotomy, which is defined as a surgical cut through both the cortical and medullary bone (Lee et al., 2008) (Wang et al., 2009).

- The “bony block concept”

The use of surgical alveolar corticotomies in orthodontic treatment has been discussed in the literature for decades. Heinrich Köle's publication in 1959 was the first to introduce the use of corticotomies in the acceleration of orthodontic tooth movement. He believed that dense cortical bone was the main resistance to orthodontic tooth movement. His surgical technique involved reflection of full thickness mucoperiosteal flaps, followed by interproximal vertical corticotomy cuts on the buccal and lingual cortical alveolar bone of the teeth of interest, connected by supra-apical horizontal osteotomy cuts (Fig. 2.6). The cancellous bone was not involved in the corticotomy cuts. It was hypothesized that leaving intact cancellous bone allowed a continued supply of nutrition to the bone and teeth and the prevention of unwanted sequelae, such as root resorption, periodontal injury, and tooth devitalization.

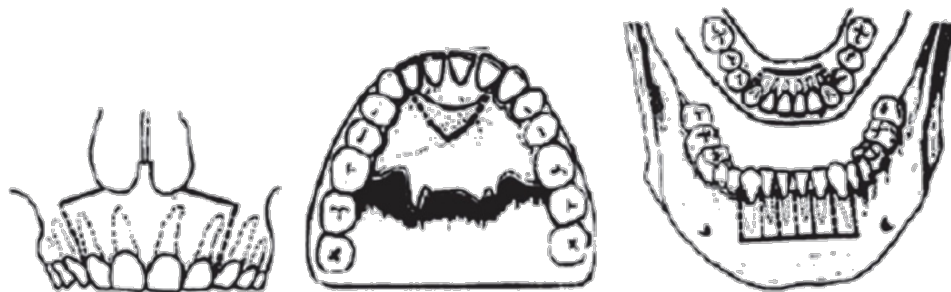


**Fig. 2.6:** Bony block osteotomies (Köle, 1959).

Furthermore, Köle explained that rapid tooth movement after corticotomy surgery is caused by what he referred to as the “bony block” concept: By disrupting the continuity of the cortical layer, this would create blocks of bone in which teeth are embedded, that could be moved rapidly and independently because they were connected by less dense intact medullary bone. Köle reported that the major active tooth movements were accomplished

in 6 to 12 weeks. This treatment approach never gained widespread acceptance. Soon after Köle's articles were published, many authors described variants of the technique where the subapical osteotomy cuts were replaced with corticotomy cuts to reduce the risk of periodontal damage and devitalization of the teeth and osseous segments because of inadequate blood supply (Düker et al., 1975) (Gantes et al., 1990) (Suya et al., 1991).

- Wilckodontics: Periodontally-Accelerated Osteogenic Orthodontics (PAOO)

In 2001, Wilcko et al. refined Köle's traditional technique. Their approach included buccal and lingual full thickness flaps, selective decortications of the cortical plate (SAD) with a round bur extending to the superficial aspect of the medullary bone, and concomitant bone grafting. The groove extended from a point 2 to 3 mm below the alveolar crest to a point 2 mm beyond the apex (Fig. 2.7). They termed their technique as "Accelerated Osteogenic Orthodontics (AOO) and, more recently, Periodontally-Accelerated Osteogenic Orthodontics (PAOO). Tooth movement is initiated within 1 to 2 weeks after surgery and the patient is seen every 2 weeks for adjustments (Wilcko et al., 2003).

The objective of bone grafting is to increase pre-treatment bone thickness and volume, and "sandwiching" the roots between intact buccal and lingual layers of bone while correcting the pre-existing alveolar dehiscences and fenestrations, and compensating for any corticotomy-related reduction in bone volume (Wilcko et al., 2008). This additional step is believed to be responsible for the increased post-treatment alveolar bone width, which may be responsible for enhanced long-term stability. The volume of the graft material is dictated by the direction and amount of tooth movement predicted, the pretreatment alveolar bone thickness and the need for labial support (Murphy et al., 2009).



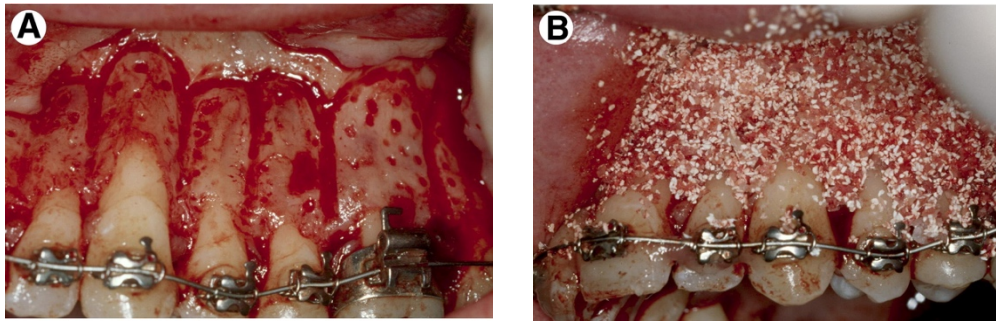


**Fig. 2.7:** A: After bone activation using circumscribing corticotomy cuts and intramarrow penetrations. B: Bone grafting mixture placed over the activated bone (Wilcko et al., 2009).

Case reports in which surface computed tomography (CT) scan evaluation of patients who underwent selective decortication showed that the rapid tooth movement was not the result of bony block movement as postulated by Köle, but rather a localized demineralization/remineralization process in the bony alveolar housing, resulting in a transient and localized state of osteopenia (Wilcko et al., 2009) consisted with first phase of the regional acceleratory phenomenon (RAP) characterized by an increased bone turnover and decreased bone density surrounding the surgical site due to a substantial increase in osteoclasts migration (Frost, 1989) (Fig. 2.8). The corticotomy surgery acts as a noxious stimulus to the area, causing the induction of the alveolar structures into a more pliable condition favoring rapid tooth movement.

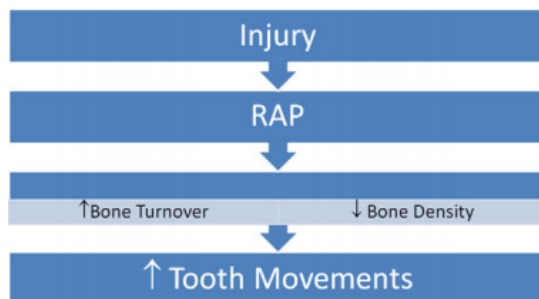


**Fig. 2.8:** The process by which corticotomies accelerate tooth movements (Bushang et al., 2012).

Wilcko et al. (2009) gave an objective account of the scenarios where the use of PAOO orthodontics should be avoided. These include the following:

1. Patients showing any sign of active periodontal disease
2. Inadequately treated endodontic problems
3. Prolonged use of corticosteroids
4. Use of medications that slow down bone metabolism, such as bisphosphonates and nonsteroidal anti-inflammatory drugs (NSAIDs)

The PAOO approach has been recommended for treatment of severe crowding without extractions (Wilcko et al., 2001) and arch expansion (Wilcko et al., 2003) (Fig.2.9-2.10), and it proved to accelerate the scope of treatment to one third the time of conventional treatment. According to Hajji et al. (2000), crowding in the mandibular arch was resolved 3-4 times faster with corticotomies compared to control patients. Animal studies have shown that teeth move approximately twice as fast when flaps and alveolar decortication are performed, and the effect is significant as early as the first week after force application (Cho et al., 2007) (Mostafa et al., 2009). Recent studies also reported evidence that supports this hypothesis (Lee et al., 2008) (Sebaoun et al., 2008).

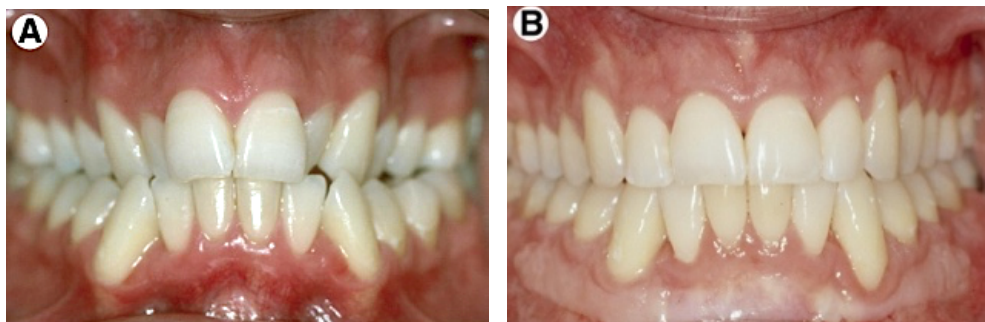


**Fig. 2.9:** Patient, male, age 23 years. A, Before treatment. B, After treatment, total treatment time 6 months 2 weeks (Wilcko et al., 2009).

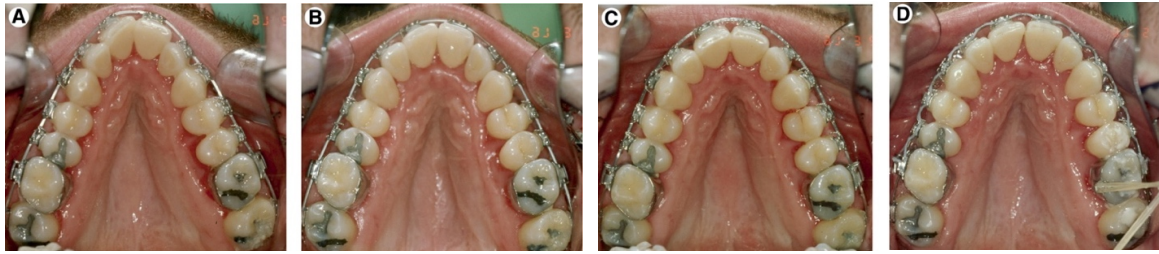


**Fig. 2.10:** 1 (A) 4, (B) 8, (C) 11, and (D) 16 weeks after AOO surgery (Wilcko et al., 2009).

However, others have shown greater experimental tooth movements as early as the first week but not after the fourth week (Lino et al., 2007; Ren et al., 2007). Sanjideh et al. (2008) demonstrated that a second corticotomy procedure initiated 4 weeks after the first surgical insult produced significantly greater overall tooth movement than performing one initial corticotomy, and maintained higher rates of tooth movement over a longer duration.

The invasive nature of this procedure, requiring extensive flap elevation, thus increasing the risk of complications such as root and nerve damage, infection, dehiscence, potential loss of alveolar bone height and postoperative discomfort, limited its acceptance among patients. In addition, some studies concluded that the acceleration was only in the first 3 to 4 months and it declined with time to the same level as the controls (Aboul-Ela et al., 2011). Therefore, less invasive corticotomy techniques were proposed.

- Corticision

Park et al. (2006), followed by Kim et al. (2009) introduced the corticision technique in which a scalpel and a mallet are used to separate the interproximal cortices transmucosally without flap reflection (Fig. 2.11). Authors advocated that these minimally invasive bone insults were enough to induce RAP and accelerate tooth movement. While decreasing the

duration of the surgery, this procedure does not provide the benefit of bone or soft tissue graft. In addition, transient dizziness and benign paroxysmal positional vertigo have been reported following the repeated hammering in the maxilla (Penarrocha-Diago et al., 2008).

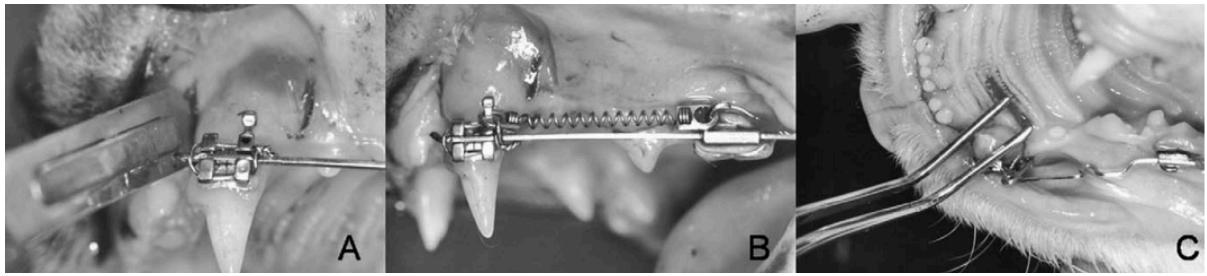


**Fig. 2.11:** Photographs of experimental canine (A) Corticision on the mesiobuccal side of the upper canine. (B) Orthodontic appliance in place. (C) Additional manipulation (Kim et al., 2009).

- Piezocision

In 2007, Vercelloti and Podesto proposed the use of piezosurgery in conjunction with the conventional flap elevation, instead of surgical burs and handpieces to minimize the surgical trauma, with more precise incisions, and less risk of osteonecrosis. A flapless piezosurgical decortication was later introduced by Dibart et al. in 2010 in what they called “Piezocision”. The technique starts with vertical inter-radicular gingival incisions buccally through which an ultrasonic piezosurgical knife, the Piezotome (Satelec, Acteongroup, Merignac, France), is used to decorticate the alveolar bone to a depth of 3 mm (Fig. 2.12). It allows hard and soft tissue grafting through selective tunneling, in areas of recessions, dehiscences or fenestrations. Due to its conservative nature, this procedure can be repeated more than once in the same area after 5-6 months (Dibart et al., 2015).

Piezocision™ can be used in a generalized, localized, or sequential manner if the correction of the malocclusion requires a “staged” approach, where selected areas or segments of the arch are being demineralized at different times during orthodontic treatment to help achieve specific results (Nelson and Dibart, 2014). Piezocision was reported successful in resolving class II (Dibart et al., 2010) (Aksakalli et al., 2015) and class III malocclusions (Keser and Dibart, 2013) in a duration ranging between 5 to 9 months. A recent RCT conducted by Charavet et al. (2019) demonstrated that overall treatment duration of decrowding was significantly reduced by 43% in the piezocision group compared with the control group.

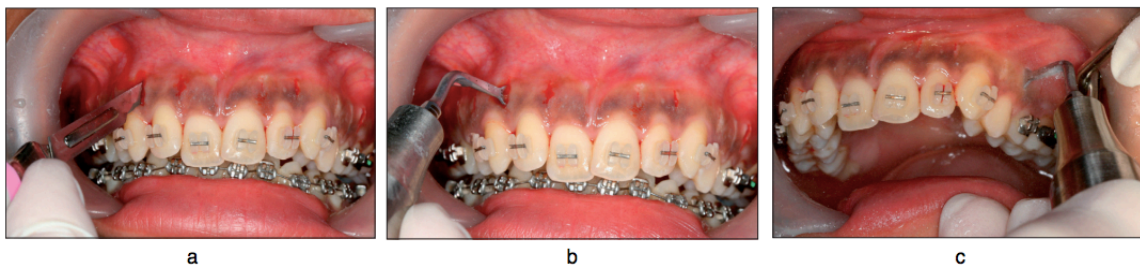


**Fig. 2.12:** (a) Micro-incisions are made through the attached gingiva. (b and c) Bone is decorticated using the ultrasonic insert (Piezotome, Satelec) to a depth of 3 mm (Sebaoun et al., 2011).

- Micro-osteoperforation (MOP)

Micro-osteoperforations (MOPs) are a new, minimally invasive method to accelerate tooth movement, where shallow perforations are made into the cortical bone through the gingiva, either with a round bur and handpiece (Safavi et al., 2012), through repeated insertion and withdrawal of orthodontic mini-implants (Cheung et al., 2016; Alkebsi et al., 2018; Sivarajan et al., 2019), or using the Propel device, (Alikhani et al., 2015; Attri et al.,

2018) which is an FDA-approved medical device with a stainless-steel tip that can be set to perforate the bone either 3, 5, or 7mm depending on the clinician's preference (Fig. 2.13). The perforations should be placed within a 10 mm radius of the tooth to be moved (propelorthodontics.com). The theory behind MOPs is very similar to that of alveolar decortication; However, it does not require the release of a flap.

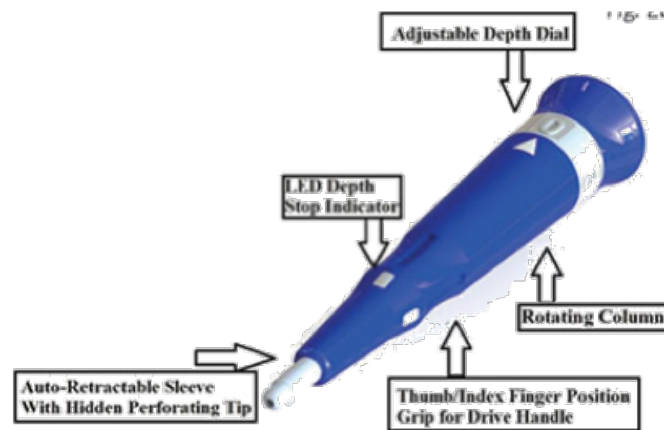


**Fig. 2.13:** Propel Excillator with depth limiter LED indicator (adapted from propelorthodontics.com).

A study performed by Teixeira et al. (2010) on rats had shown twice as much molar movement with flap surgery and 3MOPs than with a flap alone, with a 53% decrease in treatment duration, and with no side effects, suggesting that MOPs were sufficient to induce RAP. It was observed that the biologic mechanism behind these perforations is to increase the cytokine expression and to trigger bone remodeling changes which leads to increased bone resorption, thus a faster tooth movement (Fig. 2.14). A similar rat study reported enhanced tooth movement initially, but no significant difference in overall tooth movement after 42 days (Baloul et al., 2011).

Nevertheless, studying rates of tooth movements in rodents is problematic because their teeth are 40-50 times smaller than human teeth, making it difficult to appropriately calibrate appliances and maintain forces within acceptable ranges (Ren et al., 2004). The suitability of any animal model for evaluating the effects of corticotomies on tooth movement is directly related to the similarities in bone composition, density and quality, as well as bone turnover compared with humans. Several reports concluded that dogs have the most similar bone structures to humans (Egermann et al., 2005; Pearce et al., 2007).

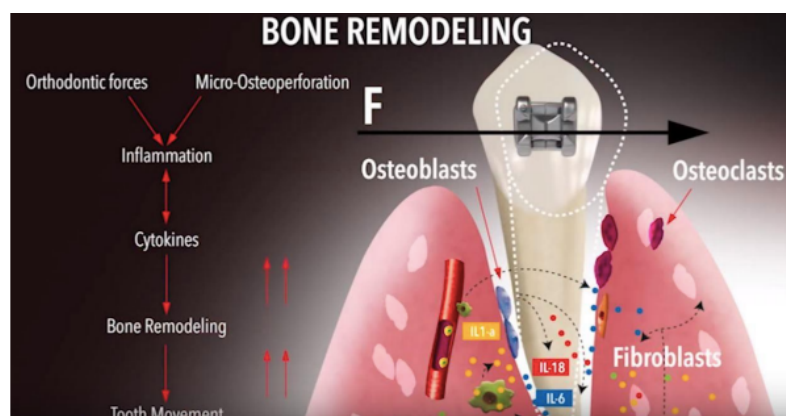


**Fig. 2.14:** Role of micro-osteoperforations on bone remodeling (propelorthodontics.com).

Later, a human clinical trial conducted by Alikhani et al. in 2013 based on the positive results of the study by Teixeira, where 3 MOPs were placed in a premolar extraction site using a Propel device, reported a 2.3-fold increase in the rate of OTM over the first 28 days of canine retraction, and a 62% reduction in treatment time (Fig. 2.15). Later animal studies (Tsai et al., 2015) and (Cheung et al., 2016) also showed 1.49 and 1.86 faster tooth movement with MOP respectively. Other human studies (Fischer, 2007; Aboul-Ela et al. 2011) also supported the claim that MOPs promote faster OTM.



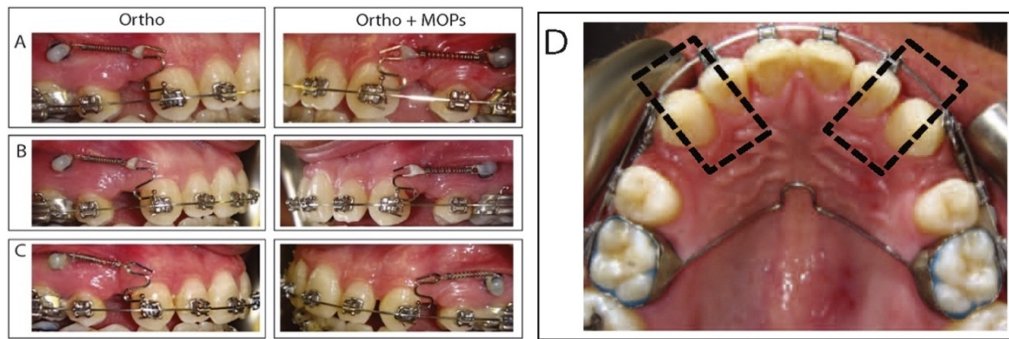


**Fig. 2.15:** A. After application of MOPs and initiating canine retraction; B. After 24 hours, complete healing of the sites of MOPs; C and D. 28 days after, canine retraction on the MOPs side (right) is greater than on the control side (left) (Alikhani et al., 2013).

Nonetheless, several reports found no clinically significant acceleration in OTM. Swapp et al. (2015) believed that flapless perforations produced no significant differences in either tooth movement or the bone surrounding the tooth that was moved, because the cortical bone only was perforated, and the medullary bone was not affected. Cramer et al. (2019) concluded in their study on beagle dogs that MOPs may produce a slight, early and temporary increase in tooth movement during the first 2 weeks, but the effects are small, of limited duration and clinically insignificant. Several recent RCTs (Alkebsi et al., 2018; Sivarajan et al., 2019; Alqadasi et al. 2019) evaluating the effect of MOPs on mini-implant supported canine retraction found that 3 MOPs did not accelerate tooth movement (Fig. 2.16). Another split mouth study conducted by Aboalnaga et al. (2019) reported same results but stated that 3 MOPs did in fact facilitate canine root movement. Van Gemert et al. (2019) evaluated the effect of MOPs after 2 and 4 weeks and concluded that MOPs in cortical and trabecular bone produce acellular bone adjacent to placement site, and that the demineralization effects are transient, and not evident after 4 weeks. Although bone density is decreased up to 4.2 mm, the principal effects do not extend more than 1.5mm from MOP.



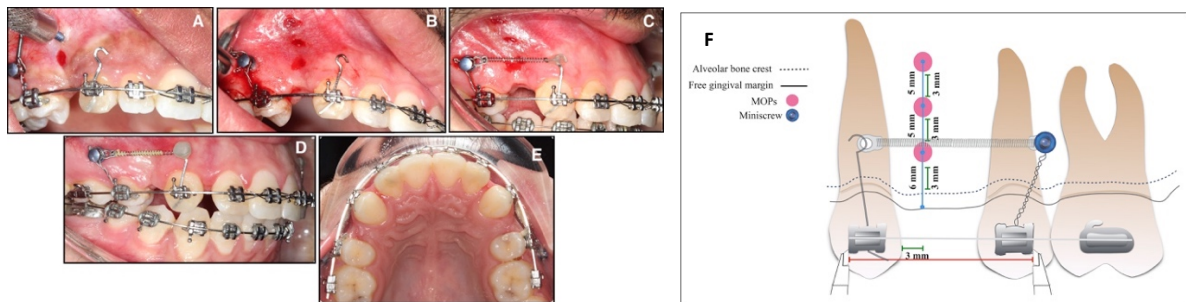


**Fig. 2.16:** A and B: MOPs application distal to canines on the right; C, canine retraction by NiTi closed coil spring; D and E, occlusal view of canine movement during treatment; F: MOP protocol (Alkebsi et al., 2018).

However, in recent RCT study by Bansal et al., (2019), where 6 MOPs were performed using a mini-implant on the buccal side of mandibular anterior teeth, results showed a significant difference in the total treatment duration for complete alignment of the mandibular incisors (44% faster than the control group) (Fig. 2.17). Blasi and Pavlin (2017) suggested that repeated use of MOP can maintain higher levels of inflammatory markers leading to a higher rate of tooth movement.

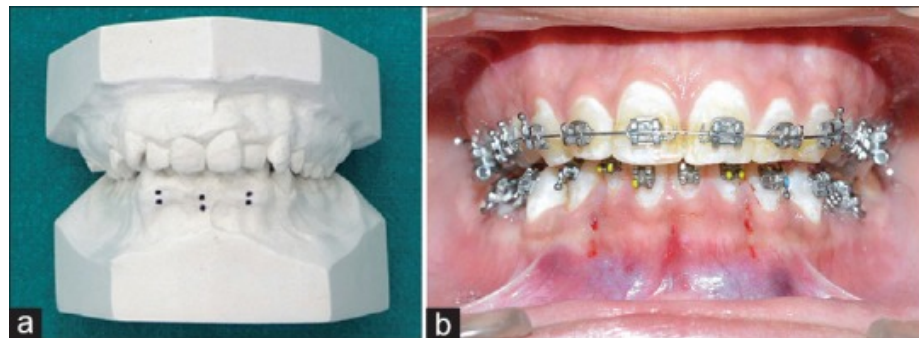


**Fig. 2.17:** (a) MOP sites shown on the study model. (b) MOP sites shown clinically (Bansal et al., 2019).

Due to the contradictory results, questions regarding the frequency of microperforations (how often should they be repeated) and the number of microperforations

(how many times should they be repeated and should the rate be variable in different patients) to obtain effective acceleration in OTM remain unanswered (Ghafari, 2015). More high-quality studies are needed to evaluate the effects of MOP (Shahabee et al., 2019).

- Comparison between different techniques

Alveolar cortectomies can be used to accelerate orthodontic treatment, to facilitate the implementation of mechanically challenging orthodontic movements, and to enhance the correction of moderate to severe malocclusion. Corticotomy has been described in conjunction with several orthodontic treatments: non extraction treatment of crowding (Wilcko et al., 2001, 2008), arch expansion (Ferguson et al. 2015), borderline orthognathic surgery (Vercellotti et Podesta, 2007), intrusion of posterior teeth to correct anterior open bites (Akay et al., 2009), canine retraction into extraction spaces (Aboul-Ela et al., 2011; Chandran et al., 2018), and impacted canines (Fischer, 2007), and it appears to be a promising mean of accelerating tooth movement (Long et al., 2012), especially for adult patients in whom tooth movement is slower due to a decreased metabolism of the periodontal ligament and alveolar bone (Verna & Melsen 2003).

According to Wilcko et al. (2008), “it is not the design of the decortication that is responsible for the accelerated tooth movement, but rather the degree of tissue metabolic perturbation per se”. The extent of injury has been suggested to be correlated to the duration and effect of RAP (Frost, 1989; Melsen, 1999). Cohen et al. (2010) also found that the magnitude of the RAP is proportional to the magnitude of the surgical trauma, which leads to the assumption that flapless alveolar decortications where the magnitude of the surgical insult is less due to the lack of the full thickness flap might not be as effective as

the traditional alveolar decortication. Similarly, McBride et al. (2014) suggested that with greater surgical insult, bone volume and density decreased and the rate of OTM increased.

Current surgical adjuncts to accelerate tooth movement vary in invasiveness, ranging from flapless microperforations to more traumatic approaches such as decortication. There is a paucity of evidence to evaluate the balance between maximizing the effect of RAP while minimizing the extent of trauma. A study by Abbas et al. (2016) that compared the effects of corticotomy and piezocision in rapid canine retraction found that corticotomy produced more rapid canine movement. Another study by Alfawal et al. (2018) which compared flapless corticotomy with piezocision found no significant difference in rate of canine retraction over the 4-month period. Tsai et al. (2015) found no difference in flapless micro-osteoperforation and corticision during tooth movement in rats. A recent systematic review on alveolar corticotomies by Gil et al. (2018) concluded that the design of the corticotomy cuts seems to be irrelevant, but it seems clear they must cut the cortical layer of bone and extend into the superficial aspect of the medullary bone.

Overall, the available evidence concerning the effectiveness of the various corticotomy techniques is limited to case reports, case series and a limited number of randomized controlled trials, and the majority is carried out on animal models. Its routine use is still controversial. These drawbacks signify the need for conducting high quality randomized clinical trials. Further research is needed to draw valid conclusions in the field of corticotomy-accelerated orthodontics (Long et al., 2012; Gkanditis et al., 2014; Hoogveen et al., 2014; Fleming et al., 2015; Liem et al., 2015; Patterson et al., 2016; Yi et al., 2017).

## **2.5. Finite Element Analysis (FEA)**

The optimal application of orthodontic forces enables maximum movement of teeth with minimal irreversible damage of the PDL, alveolar bone and teeth (Ren et al., 2004). A previous study suggested that the stress field during initial loading is the primary implication to trigger bone remodeling and determine OTM (Middleton et al., 1996). This confirms Wolff's law, which is the basis for analysis of the remodeling of bone after orthopedic procedures. Excessive stresses during orthodontic loading can lead to substantial degradation of tooth tissue and reduced functionality. For this reason, the biomechanics of orthodontic tooth movement has been an increasing area of investigation in the orthodontic research field in an effort to improve clinical efficiency and treatment outcome (Jones et al., 2001).

Whenever load is applied to a structure, deformation of the structure and stresses are generated, which cannot be measured directly. However, due to the anatomic and material complexity of tooth supporting apparatus (alveolar bone, PDL and root cementum), it is difficult to quantitatively determine mechanical responses to orthodontic loads without developing a realistic biomechanical model. Changes in the stress and strain distribution are the triggers for bone modeling that allows the teeth to move when an orthodontic loading system is applied. A precise quantification of the stress-strain response to orthodontic loading cannot be achieved without a biomechanical model able to capture the anatomic complexity and biologic variability of the dentoalveolar structures. Several methodologies have been developed with the aim to improve our understanding of the distribution of forces in the stomatognathic system, and aid in the planning and prediction of orthodontic treatment, such as the finite element analysis method (FEA) (Singh, 2016).

### ***2.5.1. Definition***

First developed in 1943 by R. Courant, FEA is a modern engineering tool for an accurate three-dimensional representation of complex physical systems and for numerical stress analysis that approximates these models into numerical mathematical equations (Tanne, Sakuda, & Burstone, 1987). In FEA, the behavior of a particular physical system is simulated. The analysis involves, first discretization of the structure into its components called “finite elements” connected to each other by nodes with well-defined physical properties (e.g. stiffness, elasticity). Then, a quantitative analysis is conducted where each of these elements is described by differential equations and solved using mathematical models selected according to the data under investigation (Vasudeva, 2009). Equations from all the elements need to be solved simultaneously, a task that can only be performed by computers. Engineering phenomena such as deflection, stress, strains, vibration, energy storage and many other can be calculated. The steps followed are generally constructing a finite element model, followed by specifying appropriate material properties, loading and boundary conditions. Various engineering softwares are available to model and simulate the structure of interest.

FEA allows the creation of models for complex structures, reproducing the irregular geometries of either natural or artificial tissues. In addition, it allows to modify the parameters of those geometries, which makes it possible to apply a force or a system of forces (external forces, pressure, thermal changes...) to any point and/or in any direction, thereby providing information on movement and on the degree of tension and compression caused by these loads (Wakabayashi et al., 2008).

### ***2.5.2. Development of FEA in dentistry***

FEA was first used in dentistry by Ledley and Huang in 1968 when they developed a linear model of a tooth based on linear displacement force analysis. Stress analysis studies of inlays, crowns, fixed bridges, complete dentures, partial dentures and endodontic posts have been reported, as well as studies of teeth, bone, and oral tissues. FEA has also been employed to model and predict the biomechanical performance of various implant designs used in dentistry and medicine (Gačnik et al., 2014).

Since its introduction to dental research, the FE method has improved significantly. Early dental models were two dimensional (2D) and analyses were not computerized. With the advancement in imaging technologies, 3D modeling was introduced to dentistry. Computer tomography (CT) data provided stacks of sectional geometries of human jaws that could be digitized and reconstructed into 3D models. However, the element size was relatively large due to the immature meshing techniques at that time, which made models time consuming to build. As computer and FE solvers capability was evolving, and with the use of anatomical records with better resolution (microCT images), more complex 3D anatomic structures (e.g. occlusal surfaces, pulp, dentin, enamel) were simulated. The outburst of computer-aided-design (CAD) has allowed accurate rendition of dental anatomy and prosthetic components such as implant configuration and veneer crowns (Fig 2.18). CAD softwares such as SolidWorks© (Waltham, MA, USA) have been adapted to construct models from datasets of computer tomography (CT) images, microCT images, or magnetic resonance images (MRI) that are then converted to FE programs (e.g., Abaqus, Ansys, Mimics) for meshing and solving (Ko et al., 2012).

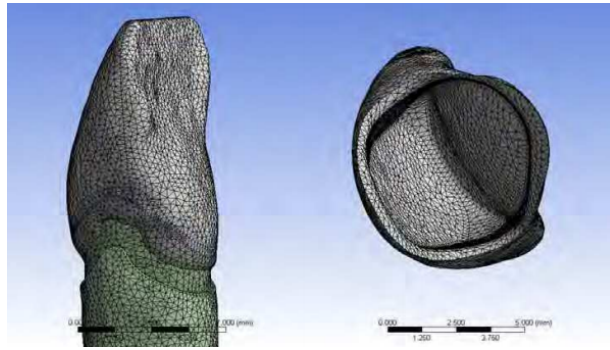


**Fig. 2.18:** Fine finite element mesh generated for ceramics veneer simulation (Ko et al., 2012).

### ***2.5.3. FEA in Orthodontics***

Finite element analysis (FEA) has not only taken medicine and dentistry to new heights, but is also a promising tool in the orthodontic research field. The method is a non-invasive numeric tool for an accurate three-dimensional (3D) representation of complex physical systems such as teeth, alveolar bone and periodontal ligament (Ammar, 2011). It provides the ability to simulate various clinical scenarios of orthodontic forces application, and to compare their effects by obtaining a quantitative detailed prediction regarding physiologic responses such as stress, strain and displacement of the dentoalveolar response to the mechanical loads (Yang et al., 2015). Moreover, it allows for the possibility to study a homogenous sample while controlling all study variables and to anticipate the tissue responses to the orthodontic mechanics applied.

The role of FEA in treatment planning, bone remodeling, determining the center of resistance and rotation, and retraction has helped in understanding the biomechanics of tooth movement, without increasing the numbers of patients or animals in the sample, unlike clinical or animal investigations. Newer ideas can be easily implied using FEA (Singh, 2016).

Tanne et al. (1987) were the first to introduce FEA into orthodontics (Fig. 2.19). Earlier studies reported stress levels following the application of a force on a single tooth system that was constructed on the basis of average anatomic morphology (Cobo et al. 1993). With advances in softwares and introduction of 3D radiography in dentistry, more sophisticated models were generated to evaluate stresses in a group of teeth (Liu et al., 2015).

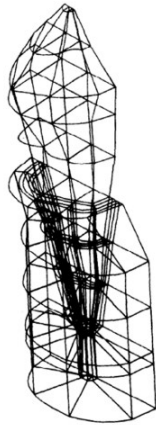


**Fig. 2.19:** Three-dimensional finite element model of the lower first premolar. The model consists of 240 isoparametric elements and comprises the tooth, PDL and alveolar bone (Tanne et al., 1987).

In the last two decades, FEA was extensively used in orthodontic research, underlining several variables involved in orthodontic mechanics, such as:

1. Stress distribution areas in the periodontal ligament (PDL) and alveolar bone during different types of tooth movements: canine and incisors retraction (Lombardo et al., 2014; S.-J. Sung et al., 2010) ; molar and incisors intrusion (Çifter & Saraç, 2011); torque expression (Liang et al., 2009); distalization (E.-H. Sung et al., 2015); molar protraction (Kojima & Fukui, 2008); maxillary expansion (Han et al., 2009; Lee et al., 2012); alignment of impacted canines (Wang et al., 2014); maxillary protraction (Kim et al., 2015; Yan et al., 2013).
2. Stress distribution on orthodontic components such as archwires and TADs: (Ammar et al., 2011; Holberg et al., 2014; Suzuki et al., 2011; Techalertpaisarn & Versluis, 2013)



3. Direction and amount of tooth displacement during different types of movements:  
Molar protraction (Kojima & Fukui, 2008; Liang et al., 2009; Nihara et al., 2015); distalization (Yu et al., 2014; E.-H. Sung et al., 2015); molar intrusion (Çifter & Saraç, 2011); torque expression (Liang et al., 2009); expansion (Han et al., 2009; Lee et al., 2012); aligner treatment (Gomez et al., 2014); maxillary protraction (Yan et al., 2013; Kim et al., 2015) and incisors retraction (S.-J. Sung et al., 2010; Lombardo et al., 2014).
4. Strain distribution in the bone and PDL: (Holberg et al., 2014) (Cattaneo et al., 2009)
5. Areas most prone to root resorption: (Kamble et al., 2012)
6. Ideal position of orthodontic appliances during specific mechanics: (Kojima et al., 2012; Tominaga et al., 2014; Nihara et al., 2015)

#### **2.5.4. Limitations**

FEA has proved to be a valid a reliable technique for the calculation of the local state of deformation and loading of complex structures. It has various advantages compared with studies on real models. The experiments are repeatable, there are no ethical considerations and the study design may be modified as per the requirement. However, there are certain limitations too:

##### 2.5.4.1. Sensitivity of the meshing process

Every finite element is based on an assumed shape function expressing internal displacements as functions of nodal displacements. A certain element may give accurate answers for a particular type and location of loading, but inaccurate answers for another type and location. Even with "well-behaved" elements, the solution is heavily dependent on

the mesh, not only on the number of elements into which the region is divided, but also on their shape and arrangement (Van Staden et al., 2006). In fact, constructing accurate and suitable FE meshes of the studied geometry is essential since FE simulations results are highly sensitive to geometric modelling assumptions (Hohmann et al., 2011).

#### 2.5.4.2. Inaccurate assumptions

In FEA, the results obtained are only “as good as the initial data used to set the parameters of tissue response” (Middleton et al. 1996). Unlike engineering structures, there is no definitive knowledge of the mechanical behavior of biologic tissues. This shortcoming is mainly related to the complex anatomy, lack of experimental studies, and absence of modern technologies to measure the properties of the oral tissues. The validity of the results of FE-analyzes is dependent on the ability to model the complexity of morphology and material properties of the structures analyzed. When mathematical models are used to mimic these structures, it is understood that some simplifications have to be introduced; As a result, certain assumptions are accepted in the FEA studies applied in orthodontics (Qian, Chen, & Katona, 2001). however, these should not be detrimental to the correctness of the results (Cattaneo et al., 2005; Vecilli et al., 2008).

Tooth movement is a periodontally-driven mechanism, thus the importance of the material property definition of the PDL. The results of a systematic review about the mechanical assumptions of PDL in FEA studies indicated the use of a myriad of modelling approaches encompassing linear-elastic, viscoelastic, hyperelastic and multiphase approaches (Fill et al.,2012). An affinity for using simplified approaches/assumptions (linear-elastic) may have inadequately represented the PDL because it prevents full

characterization of its time-dependent behavior. Most virtual models shared the assumption that the PDL is homogenous and isotropic, but histologic studies clearly demonstrated that the PDL is a fiber-reinforced structure. Presumably, the principal fibers resist tensile forces, whereas the other components resist compressive forces (Qian, Chen, & Katona, 2001).

Wrong assumptions were not only limited to the PDL. The utmost majority of the studies have judged the cortical and cancellous bone to be isotropic (material properties do not vary by direction), homogeneous, and linearly plastic (linear relationship between stress and strain is invariant with changes in time and frequency of loading). Schwartz-Dabney et al. (2003) showed variations in material anisotropy (material properties differ by direction) and direction of maximum stiffness in different areas of 10 dentate mandibles. Local anisotropy and regional variations in skeletal material properties can have drastic effects on the relationship between stress and strain (Cowin & Hart, 1990).

As a consequence of using different material properties assumptions in studies involving tooth movement, various ranges of results are obtained preventing comprehensive comparisons even between two papers. The resulting quantitative data have hypothetical value and not major clinical relevance.

#### 2.5.4.3. 3D modeling of human tissues:

One inherent shortcoming in utilizing FEA simulation is the difficulty to model the actual anatomy of human hard and soft-tissues. The considerable time and effort required to generate a realistic model is a significant problem. Despite the enormous progress made in the 3D modeling softwares, manual segmentation still dominates the segmentation process. Creating an accurate maxillary or mandibular arch, complete with enamel, dentin, pulp and

PDL for each tooth, as well as lamina dura and distinct cortical and trabecular bones may take hundreds of hours (Pollei, 2009).

Owing to the small space they occupy, the PDL tissue and the trabeculae of the spongy bone are difficult to visualize using normal resolution CT and CBCT scans, posing a critical issue during FE model construction. Several protocols are used to create a layer between the teeth and the bone representing the PDL. However, the layer thickness depends on the highest resolution the 3D modeling software can read. This interaction led to the adoption of various PDL thicknesses in different investigations (Fill et al., 2012).

#### 2.5.4.4. Tooth movement simulation over time

The difficulty to model the mechanical behavior of human tissues and their response to mechanical forces over time reflects another shortcoming of FEA simulations. Most FEA studies provide a “snap-shot” view of the initial conditions within the model; they do not depict changes over time, such as bone remodeling, healing, and friction (Pollei, 2009).

To date, simulation of long-term orthodontic tooth movement (OTM) quantitatively and accurately has not been possible with FEA because the physiologic and biomechanical processes of OTM are not fully understood and represented mathematically (Ammar et al. 2011). Middleton et al. (1996) were the first to introduce a time-dependent (continuous/dynamic) finite element model for tooth movement. Aiming to validate that OTM is a “periodontally mediated phenomenon”, all tissues were assigned with linear elastic material properties (therefore do not exhibit time dependent behavior), except for the PDL where a viscoelastic material property was incorporated using an overlay model. They found that only the periodontal ligament experienced a strain above the threshold (= 0.02) necessary to

initiate a bone remodeling process, a finding that confirmed their hypothesis. Cheng et al. (2004) proposed a soft-tissue driven bone remodeling model for simulating OTM in a time-dependent manner. To determine the remodeling parameters, the FEA simulation used clinical data from an in vivo study conducted for this purpose.

The addition of a time dependent feature would be a novel approach allowing for all treatment mechanics to be simulated in silico (on virtual computer simulations) and observe the results before applying them clinically, thus avoiding side effects and complications.

#### 2.5.4.5. Applicability of results

The majority of FEA studies measure stresses (Von Mises and principal), findings that do not have a known direct clinical implication. Does increased stress values reflect increase of tooth movement, more pain, more hyalinization (therefore slower tooth movement), or more root resorption? Thus, the need for studies that link stress values to clinical measures (ex: pain, resorption, speed of tooth movement). This type of research would be revolutionary because it would translate FEA studies into strong contributions to dental knowledge by answering questions that experimental studies cannot answer because of ethical or logistical limitations. To date, increased stress units (Von Mises) at the PDL was correlated with increased tooth movement (displacement) in most studies using FEA (Cai et al., 2015; Kang et al., 2016; Vasudeva, 2009).

#### 2.5.4.6. Generalizability of results

By definition, generalizability is the extent to which findings from a study can be generalized (or extended) to the natural settings (i.e., outside the lab). FEA allows

inferences and readings to be made from a single mathematical solution for one single set up or scenario.

In the engineering field a single problem with predetermined initial settings and properties allows for a single solution or result. However, in the medical and dental fields' individual variations lead to different results for a similar clinical problem. Thus, clinical trials are needed that include samples representing the variations present in the population, following well-defined research protocols with proper statistical analyses to test the validity and significance of the results. Unfortunately, most of the dental FEA studies followed the "single-model" engineering method, leading to question the clinical significance of their results. Future studies must account for variations between real patients, thereby creating a closer link between the virtual finite element models and actual clinical situations.

In summary, FEA is a computerized in vitro study in which clinical condition may not be completely replicated. Stress analysis is usually conducted under static loading, and mechanical properties of materials are set as isotropic and linearly elastic, although it is not so in reality. Therefore, results may only be acknowledged qualitatively. Keeping in mind these limitations, further FEA research should be supplemented with clinical evaluation and inclusion of individual variations generated from several patients.

## **2.6. Progress in bone modeling**

In the human body, there are individual variations with respect to bone quality, quantity and shape. Recently with the advances of digital imaging systems (CT and MRI), it has become possible to extrapolate the individual specific data of bone geometry and property to an FEA model (Lu et al., 2013). CT and MRI represent bone in the three

dimensions of space. These patient-specific “biological data based FEA” are unique to that patient as bone morphology and quality vary among individuals. Thus, accurate anatomical models can be created which in turn provides reliable results.

Nowadays, computer-tomography (CT) is the most widely used technique for determining bone density. CT scan data are used to define the Hounsfield unit [HU] of bone density and the Hounsfield units can be directly related to bone density classifications. Specific preprocessing software’s superimpose the 3D model and the actual scan, then automatically assign for each element a material property that correlates to the HU value of the same voxel in the scan (Gačnik et al., 2014).

Information pertaining to individual patients is incorporated in the FEA to personalize the biomechanical models of bone. This approach, called “Bone Mapping”, implies that the mechanical properties of bone significantly correlate with bone mineral density and HU values obtained from CT scans (Wachter et al., 2002). A series of patient CT image data is binarized to build model geometry consisting of both cortical and cancellous bone. Then apparent density or porosity is appraised using different correlations to model the heterogenous distribution of mechanical properties (Trivedi, 2014).

## **2.7. Significance**

Upon an extensive review of the literature, there still is an apparent need for further research on the biomechanical processes related to different corticotomy techniques. A better understanding of the mechanisms behind bone manipulation and the resulting changes in the dental and paradental tissues will allow the clinician to make better clinical judgments and lead to evidence-based practice.

At present, there is no study comparing decortications and micro-osteoperforations, two different corticotomy techniques, on finite element analysis. By testing the effects of different numbers of microperforations and comparing them to the decortication, we will be able to explore how the extent of the surgical cut affects the response of the surrounding structures, thus determine the number of MOPs needed to accelerate tooth movement. The outcome of this study is expected to widen the scope of FEA application in orthodontics, which is the only non-invasive method that can produce both quantitative and qualitative data. Although FEA may not simulate the reality of tooth movement, but by discretizing the geometry into elements and validating the assumptions given to these elements from clinical data, results should come close to clinical reality.

Furthermore, by introducing individual variation drawn from actual human data of real patients, this study will constitute a landmark attempt to study the variability of response, a concept that no FEA study to date has approached. Defining bone properties is crucial when a FE analysis of a bony structure is contemplated. In this research, unlike previous FEA researches, variations in cortical bone stiffness and thickness, two factors that can drastically affect the results of orthodontic procedures, are accounted for. This contribution will thereby help creating a closer link between finite element simulations and actual clinical situations.

In this context, the importance of deciphering the material properties of specifically the compact bone must be noted. The reason for this focus is the fact that trabecular bone usually does not hamper tooth movement. The role of cortical bone in hindering or actually aiding (Ten Hove and Mulie, 1977) tooth movement has been shown as a general determining factor. We will investigate how decreasing cortical bone resistance affects



tooth movement by analyzing the effect of stiffness (related to bone density) and thickness of the cortex. Accordingly, the results should underline which of the variables, stiffness, thickness, or both impact the initial stress and displacement following the application of different corticotomy techniques. The fact that this displacement will be anchored against mini-implants eliminates the confounding effect of the movement of an anchoring unit.

This landmark attempt shall be followed by much research to explore not only stresses and initial displacement but also real time displacement, all toward the eventual development of the science to a point when mechanotherapy may be planned with controlled personalized tooth movements that also would minimize side effects.

Until further tools are developed to simulate human anatomy, FEA offers a valuable opportunity, albeit somewhat cumbersome and demanding, to explore body response in a non-invasive way, based on records taken for regular diagnostic and therapeutic reasons, and not for research purposes exclusively. The ultimate achievement would require coupling the mechanical study with the biologic response to tooth movement in future investigations. We expect and hope that the present study shall lay additional foundations toward that objective.

## **2.8. Specific aims**

1. Compare the stresses and displacements generated by canine distalization against orthodontic miniscrews with and without decortication and micro-perforations.
2. Determine the conditions under which both techniques lead to similar effects.
3. Test the influence of individual variation in cortical bone properties through thickness and stiffness.

## **2.9. Hypothesis**

The following hypotheses were proposed:

- Corticotomy significantly affects the mechanical response of the surrounding dentoalveolar structures.
- Increasing the extent of the corticotomy cut leads to higher stresses and initial displacements.
- An effective acceleration of maxillary canine distalization requires more than the currently advocated three microperforations.
- Cortical bone thickness and stiffness influence stress generation.

## CHAPTER 3

### MATERIAL AND METHODS

#### **3.1. Material**

##### ***3.1.1. Anatomical record***

A 3D model of the maxillary arch previously created for a study entitled “Two distalization methods compared in a novel patient-specific finite element analysis” by Ammoury et al. (2019) was generated from a pre-treatment cranial CT scan of an adult patient seeking radiologic assessment (at the Department of Radiology at the American University of Beirut Medical Center). The CT scan was taken with a full head field of view with a resolution of  $0.3 \times 0.3 \times 0.4$  mm and high contrast. The scan disclosed a well-aligned complete dentition, parallel roots, and a Class I occlusion with the midlines on, suggesting a normal occlusion and possibly a previous orthodontic treatment. All permanent teeth were present except the third molars. A CT scan was opted for rather than a CBCT because of its higher contrast enabling the differentiation between cortical and trabecular bone.

##### ***3.1.2. Individual data acquisition***

Data from a study by Peterson et al. (2006) on the thickness and stiffness of cortical and inter-radicular maxillary cortical bone of 15 cadavers were integrated into the model. The authors of this study entitled “Material Properties of the Dentate Maxilla” aimed to explore the variability in the characteristics of the cortical bone at different regions of the maxilla. Cortical bone specimens were harvested from 15 maxillary sites located in three

regions: the palate (four sites), alveolar bone (four sites), and the body of the maxilla (seven sites) (Fig. 3.1). Thickness and density were calculated, as well as mechanical properties such as elastic modulus (E), shear modulus (G) and Poisson's ratio ( $\nu$ ).

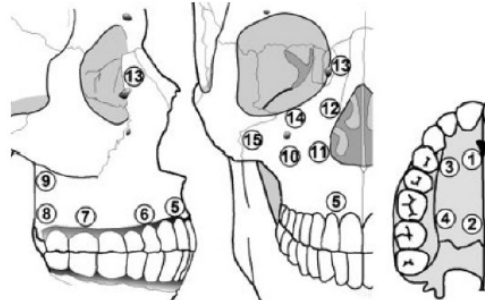


Fig. 3.1: Cortical bone sites in the maxilla (numbered for reference) (Peterson et al., 2006).

The results showed significant differences between sites in thickness and density of the outlined regions of the maxilla. Overall, where cortical bone was thin, its density was high. Cortical bone near the incisors and canines (sites 3, 5, and 6) had greater thickness than at other maxillary alveolar sites, but its density and stiffness were intermediate. Palatal cortical bone areas had relatively higher stiffness than buccal areas (Table 3.1).

Table 3.1: Density ( $\text{mg}/\text{cm}^3$ ), cortical thickness (mm) and ash weight (Peterson et al., 2006).

Site	N	Density		Thickness		Ash weight	
		Mean	SD	Mean	Mean	%	Mean
1	12	1.65	0.17	1.7	0.5	56	5
2	10	1.75	0.14	1.8	0.9	55	9
3	11	1.75	0.18	2.3	1.1	57	5
4	10	1.70	0.16	2.0	1.0	53	7
5	14	1.65	0.15	2.2	1.3	57	5
6	8	1.64	0.19	2.4	1.6	58	9
7	11	1.72	0.20	2.1	0.9	54	11
8	6	1.61	0.14	1.2	0.6	54	15
9	6	1.77	0.16	1.0	0.3	53	15
10	10	1.75	0.16	1.2	0.5	56	8
11	9	1.69	0.15	1.7	0.7	54	11
12	11	1.82	0.12	1.5	0.4	53	12
13	11	1.83	0.17	1.4	0.3	50	13
14	11	1.81	0.11	1.5	0.6	55	7
15	7	1.90	0.12	1.1	0.3	61	5
Grand mean		1.75	0.16	1.9	0.9	56	9
ANOVA		F	F	P	F	P	F
Sites		4.7	0.001	5.4	0.002	NS	NS

## 3.2. Methods

### 3.2.1. 3D Model

#### 3.2.1.1. Model construction

The CT scan was imported to ScanIP™ 7.0 software (Simpleware, Synopsys, Mountain View, CA, USA), in which it was processed and segmented, and a model of the Hemi maxilla was reconstructed to represent the region of interest. Masks of teeth, PDL, cortical and trabecular bone were created using manual and automated tools, depending on their respective Hounsfield unit (HU), which is proportional to the degree of x-ray attenuation and is allocated to each pixel to show the image representing the density of the tissue (Fig. 3.2). Because the PDL cannot be detected on a CT scan, its mask was created with a thickness assumption of 0.25mm, commonly used in FEA studies (Bowers, 1963). Smoothing of the masks was then performed (Fig. 3.3).

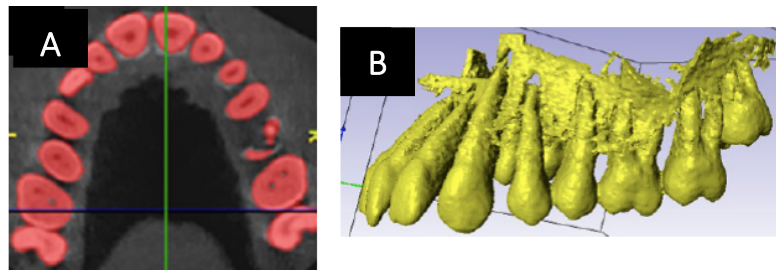


**Fig. 3.2:** Teeth mask captured according to the grayscale value using the Segmentation with Threshold tool: A- 2D axial cut; B- 3D view.

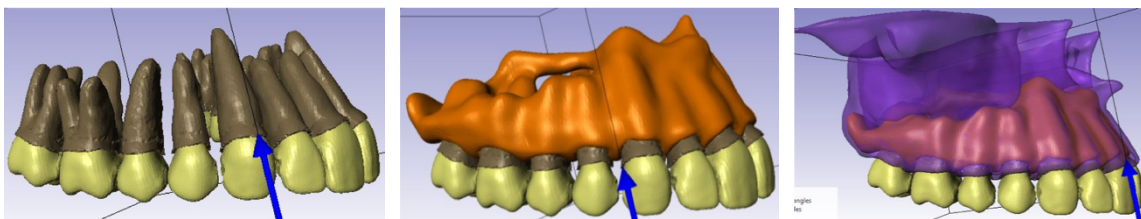


**Fig. 3.3:** A- Smoothed teeth and PDL masks; B- Smoothed trabecular bone mask; C- Smoothed cortical bone mask.

### 3.2.1.2. CAD processing

The brackets and miniscrew were sketched in the Autodesk® 3ds Max® Design software as CAD objects reproducing commercially available brackets (Mini-Twin bracket Orthos, SDS Ormco) and miniscrew (OSAS - DEWIMED - Tuttlingen, Baden Württemberg, Germany), then added to the 3D model using +CAD. The miniscrew, 6 mm in length and 1.5 mm in diameter, was inserted in the interradicular bone between the second premolar and the first molar 5 mm apical to the cemento-enamel junction, at an angle of 30° relative to the surface of the cortical bone with the neck/thread interface coincident with the external contour of the cortical bone (Deguchi et al., 2006). The maxillary right canine bracket was placed in the middle of the crown following its long axis simulating clinical practice, also facilitating the definition of the point of application and direction of load (Fig. 3.4).

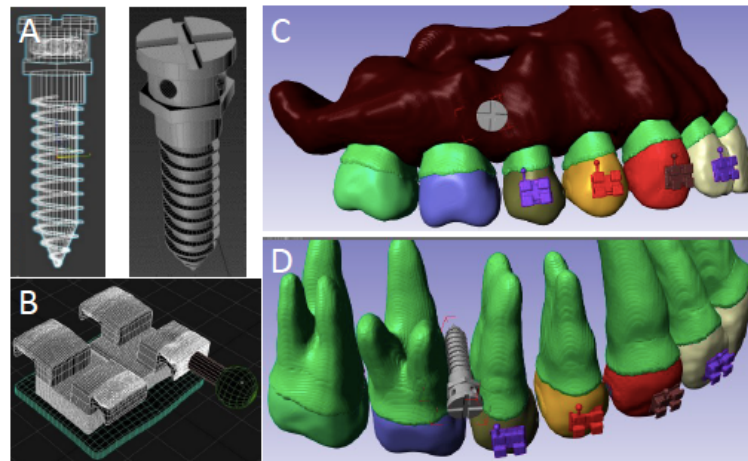


**Fig. 3.4:** CAD sketched in Autodesk® 3ds Max® Design software: **A-** TAD; **B-** Bracket; **C- D** Placement of the CAD objects in the model using the +CAD add-on module (Simpleware Ltd).

Brackets were also placed on the remaining teeth of the right hemimaxilla. The brackets and miniscrew were imported on Simpleware as STL files, fixed on the underlying surface then added to the model (Fig. 3.5).

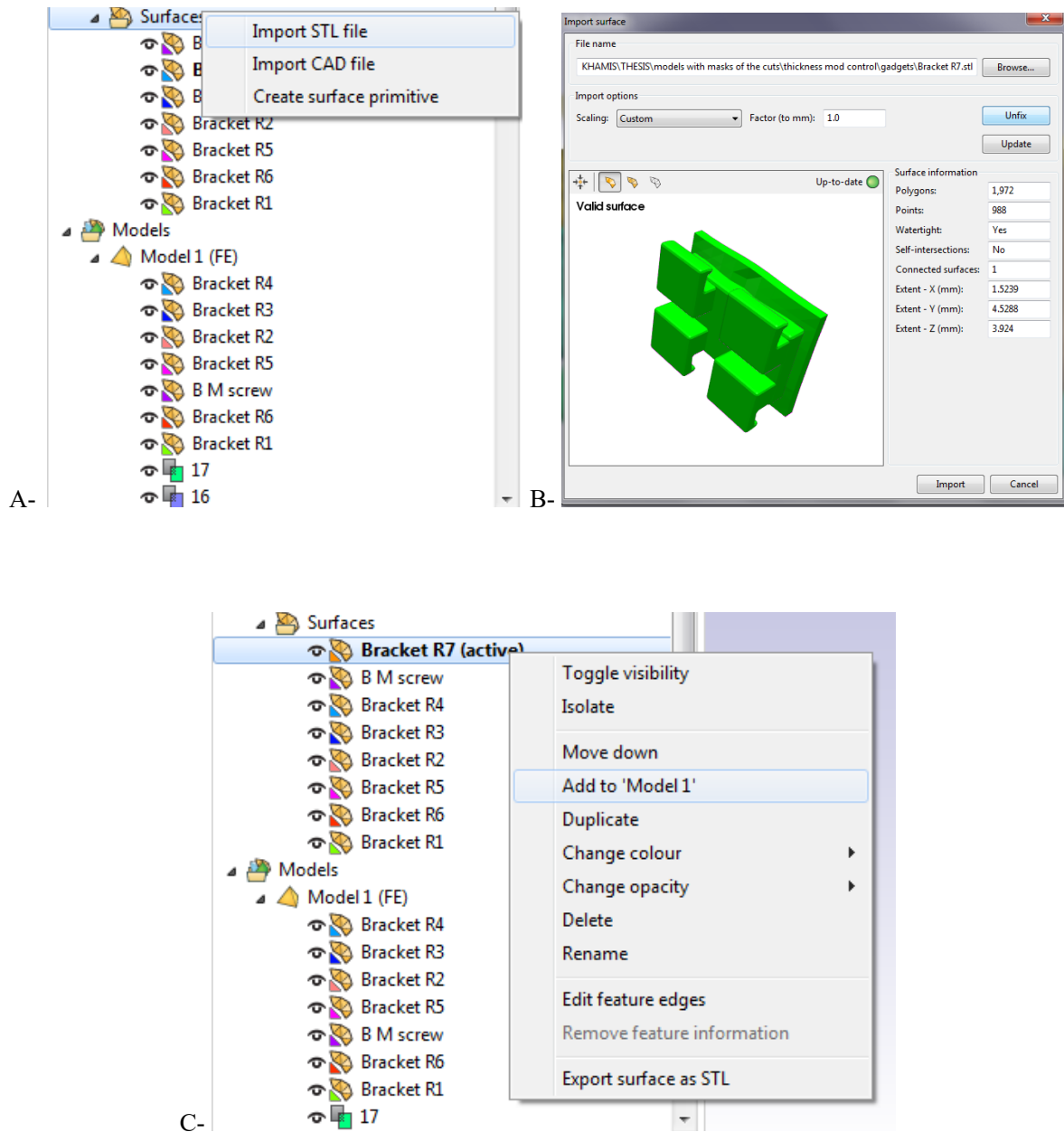


**Fig. 3.5:** A- Bracket imported as STL file; B- Bracket fixed on the crown surface; C- Bracket added to the model.

### 3.2.1.3 Individual variations

The unpublished individual data from 15 cadavers obtained from Peterson et al. (2006) were incorporated in the 3D models to replicate anatomical variations of the stiffness and thickness of cortical bone at different maxillary regions.

- Stiffness variation

The cortical bone mask was divided into 7 areas (4 buccal and 3 palatal) as described by Peterson et al. (2006). In ScanIP™, a new mask was created for each part. Then, each part was assigned a material property from the individual values provided at the different maxillary sites (Fig. 3.6).

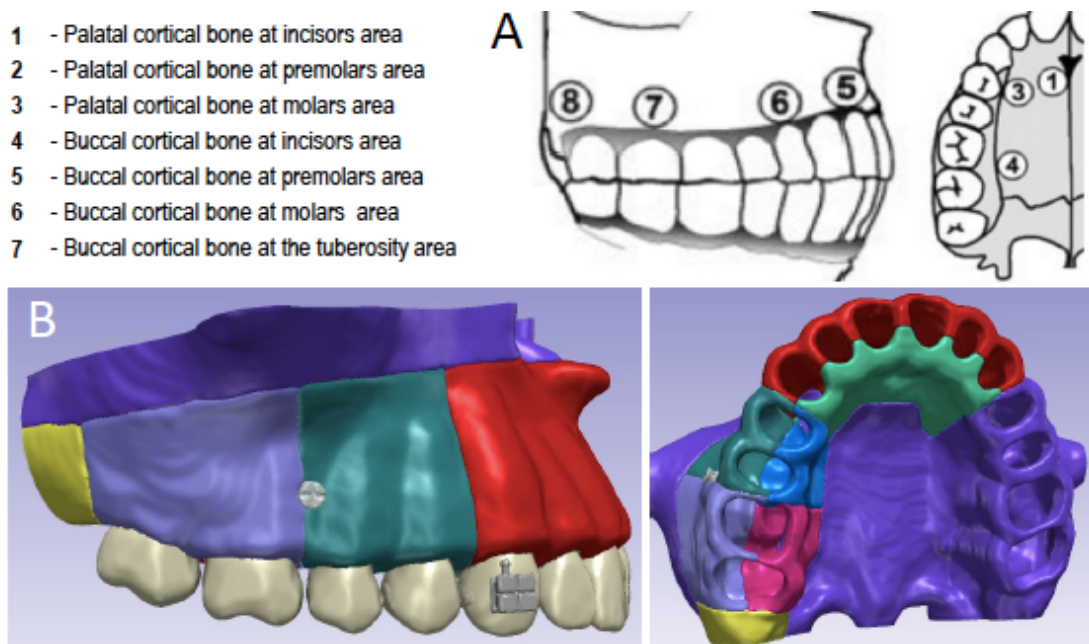


**Fig. 3.6:** A- Areas of the dentate maxilla (right) with corresponding definitions (After Peterson et al, 2006); B- 3D Model after cortical bone division.



- Thickness variation

The thickness values provided were replicated in the 7 areas of the template model, to generate separate models, each belonging to a single cadaver. Three of the cadavers were excluded from the sample for having three or more missing values. On the 12 remaining models, thickness variation was implemented depending on the need for expansion or reduction (using morphological dilate/ erode tools) at the expense of the trabecular bone to avoid changing of the outer contour of the model (Fig 3.7).

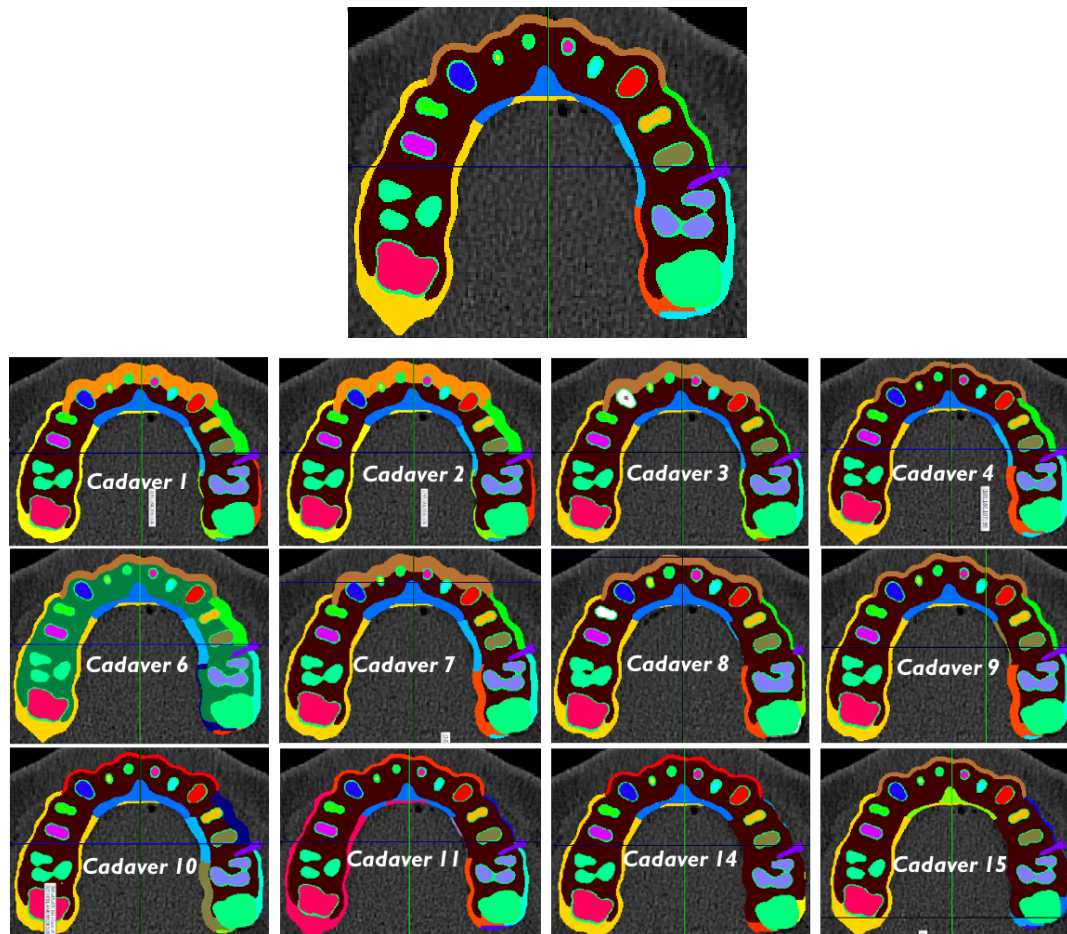


**Fig. 3.7:** A- TAD level axial cut of the original template model; B- Similar cuts individualized models corresponding to 12 cadavers with modified cortical bone thickness.

Eventually, 13 models (one template model on which stiffness was varied and twelve models with thickness variation) were obtained (Fig 3.8).

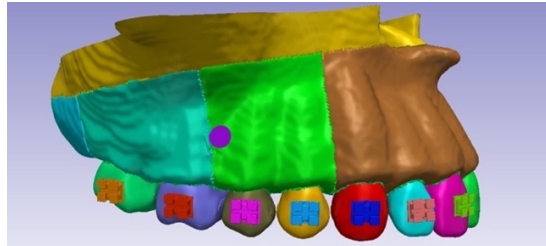


**Fig. 3.8:** The template model.

#### 3.2.1.4. Decortications and microperforations

Decortications and microperforations were designed and introduced distal to the canine. To create the corticotomy, a 3D editing tool in the image processing section was used followed by choosing the buccal incisal cortical bone as the targeted mask. Then, a region of interest was created representing the removed bone volume, using the rectangular shape for the decortication, and the cylindrical shape for the microperforation (Fig. 3.9).

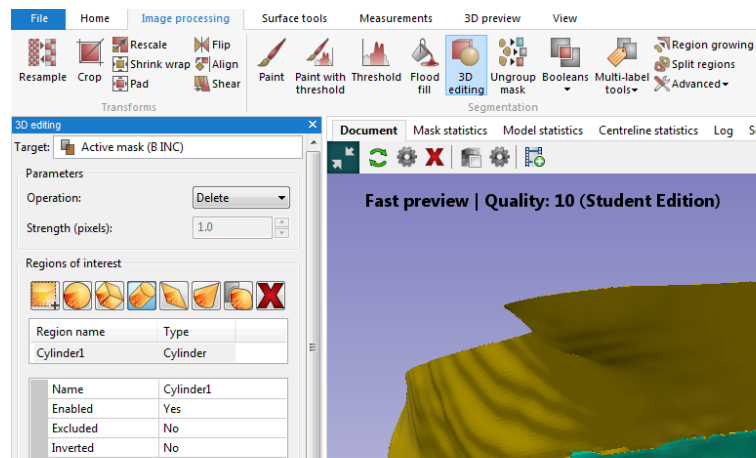


**Fig. 3.9:** Corticotomy created using 3d editing tool and selecting the targeted mask and the type of region of interest.

Once the modification was created, the shape was manually positioned on the maxillary model distal to the right canine and perpendicular to the cortical bone using a coordinate system formed by the three planes of space. Next, the dimensions were adjusted as reported in the literature to simulate the clinical situation. For the decortication, the dimensions of the created shear band followed the technique of Wilco et al. (2003), whereby the vertical cut extends from a point 2 to 3 mm above the alveolar crest to a point 2 mm beyond the apex, with a width of 1.5 mm and the depth comprising the full thickness of the cortical bone mask, leaving the trabecular bone intact.

The circular-shaped corticotomy performed by the Propel device (Propel®, Ossining, New York 10562, US) was applied for the microperforation. The same width as the decortication cut (1.5 mm) and the same depth were applied (Fig. 3.10). Both corticotomy designs were positioned at the same location relative to the canine to eliminate the distance from the tooth as an additional variable.

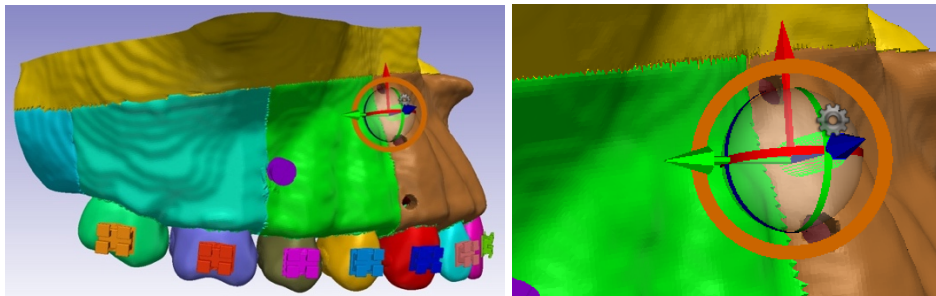


**Fig. 3.10:** Cylindrical shaped object positioned on the cortical bone mask.

After adjusting the position and dimensions of the corticotomy, the operation “delete” was selected to subtract the region of interest from the cortical bone mask, simulating the act of bone removal (Fig. 3.11).

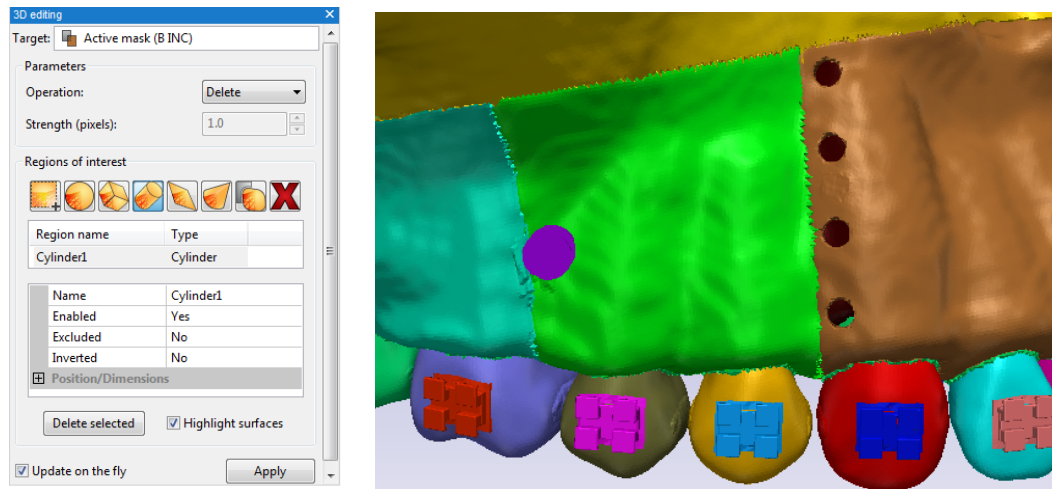


**Fig. 3.11:** The operation “Delete” performed to subtract the region of interest from the cortical bone.

Conforming to the research objective, to determine the number of microperforations needed to simulate the effect of decortication, different models with variation in the number of microperforations were created, spaced at an equal distance and aligned vertically with a specific volume of bone removed (Table 3.2). Eventually, six template models were generated representing the different clinical scenarios: control unaltered model, decortication model (DEC), and 4 microperforation (MOP) models with 3, 4, 5 and 6 perforations (Fig. 3.12).

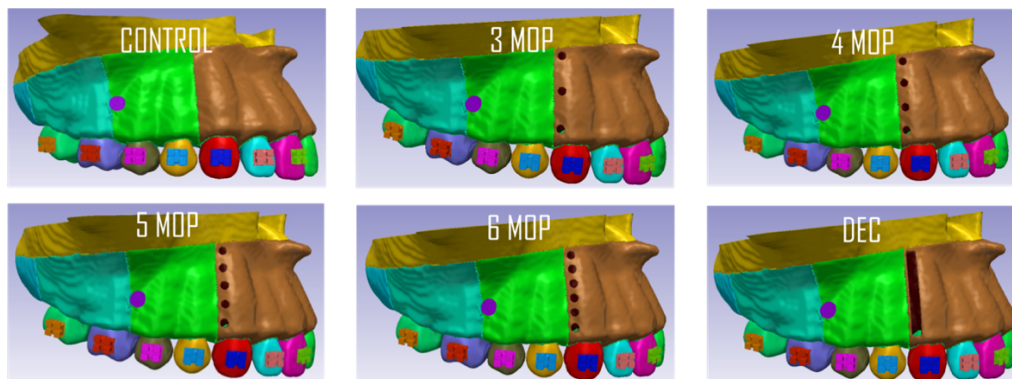


**Fig. 3.12:** The six generated models representing the different clinical scenarios.

**Table 3.2: Calculated volume of bone removed (mm<sup>3</sup>) in each modality**

	Control	3MOP	4MOP	5MOP	6MOP	DEC
Volume of bone removed (mm <sup>3</sup> )	0	7.32	9.76	11.30	14.64	30.85

In each of the twelve thickness models, the brackets were added as detailed previously, and each corticotomy was introduced by importing the cut as a mask. To obtain a mask of the corticotomy, the buccal cortical bone mask of the incisor and canine region was duplicated. Then, after creating the cut, the duplicated intact bone mask was subtracted from the decorticated bone mask creating a mask limited to the region of the cut (decortication and microperforations), and its visibility was turned off to mimic bone removal.

In the end, a total of  $6 \times 12 = 72$  thickness models (60 corticotomy models and 12 control models) were created. As for the stiffness, the data of 11 cadavers were incorporated in each of the template models in the mechanical modeling step (refer to section 3.2.2.1).

#### 3.2.1.5. Meshing

All the 3D models underwent the process of meshing, which is the discretization of models into elements, in preparation for the finite element analysis (Fig. 3.13). The size of the mesh was set at 0.604 mm following a convergence testing to determine the least number of elements that provide the most accurate solution (Ammoury et al., 2019). Models were then exported from ScanIP as inp. file format.

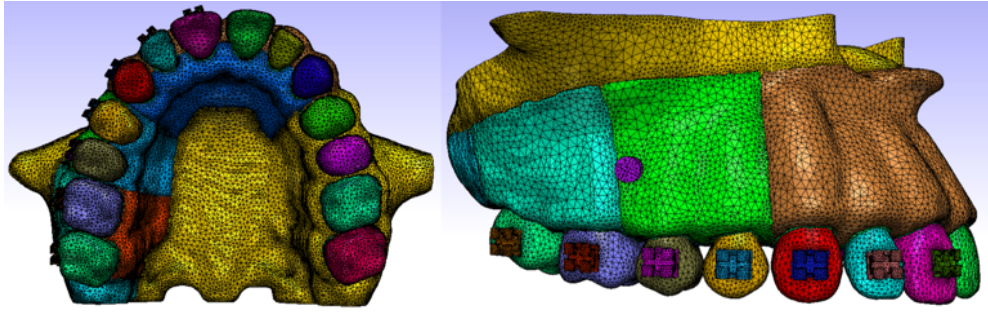


**Fig. 3.13:** The meshed template model.

### ***3.2.2. Finite Element Analysis (FEA)***

The meshed models in the input file format were imported into Abaqus 6.13 (Dassault Systèmes®, Vélizy-Villacoublay, France), a different engineering software (Fig. 3.14). The entire process from beginning to end is detailed in the following section:

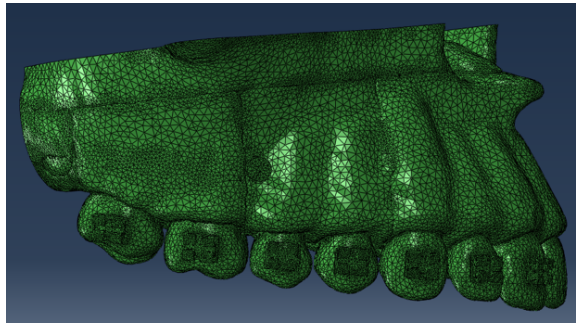


**Fig. 3.14:** The 3D model imported into Abaqus.

#### **3.2.2.1. Definition of material properties**

FEA results are only as good as the initial data used to set the parameters of tissue response (Middleton et al. 1996). Assumptions on the various skeletal elements are made based on scientific computations commonly used in FEA applications in orthodontics. The material properties (Young's Modulus of Elasticity and Poisson's ratios) of trabecular bone,

teeth, brackets and miniscrew were defined from data available in the literature (Table 3.3). The material property of the PDL was assigned based on the work of Kojima and Fukui (2012). Except for the cortical bone, all materials used were homogeneous, isotropic, and linearly elastic (Field et al., 2009; Lim et al., 2003; Tanne et al., 1987).

**Table 3.3: Material properties of anatomical components used in orthodontic FEA studies\*.**

	Young's modulus (MPa)	Poisson's ratio
Teeth	20000	0.3
Periodontal ligament (PDL)	0.68	0.45
Trabecular bone	1500	0.33
Cortical bone	Variable	0.33
Brackets and Miniscrew	200000	0.3
<i>*Field et al., 2009; Kojima et al., 2012; Lim et al., 2003; Tanne et al., 1987</i>		

Cortical bone stiffness was modified according to Peterson et al. (2006) to replicate bone qualities found in real subjects. The individual material properties provided at the maxillary sites 1, 3, 4, 5, 6, 7 and 8 (locations of interest directly related to our mechanical model) were incorporated into the template FE model. For stiffness variation, unlike other elements of the model, the cortical bone parts were assigned orthotropic material properties providing more detailed information about its behavior under different loads.

In material science and solid mechanics, material properties of an orthotropic material differ when measured from different directions. Therefore, engineering constants of Young's elasticity modulus:  $E_1$ ,  $E_2$ ,  $E_3$ , Shear Modulus of elasticity  $G_{12}$ ,  $G_{31}$ ,  $G_{32}$  and Poisson's ratio  $\nu_{12}$ ,  $\nu_{13}$ ,  $\nu_{23}$  were all incorporated into each cortical bone part (Table 3.4).



**Table 3.4: Orthotropic material properties at the site of “buccal cortical bone at incisors area (5)” in the 15 cadavers.**

	Site 5 (buccal incisors)								
	E1	E2	E3	v12	v13	v32	G12	G31	G23
<b>Patient 1</b>	17140	16918	21567	0.327	0.368	0.123	6603	6889	7175
<b>Patient 2</b>	6762	9888	12219	0.261	0.277	0.489	2879	2667	2455
<b>Patient 3</b>	11380	10731	16861	0.397	0.2	0.357	3990	5426	6862
<b>Patient 4</b>	8343	10246	14033	0.477	0.413	0.116	3229	3701	4173
<b>Patient 6</b>	10825	10006	13323	0.52	0.307	0.265	3453	4626	5799
<b>Patient 7</b>	17129	17209	21765	0.341	0.385	0.365	6411	6594	6777
<b>Patient 9</b>	9188	9143	11113	0.445	0.454	0.227	3198	3443	3688
<b>Patient 10</b>	8301	9263	12943	0.485	0.467	0.066	3098	3490	3882
<b>Patient 11</b>	8993	10380	16675	0.493	0.366	0.176	3293	4141	4990
<b>Patient 14</b>	7129	9636	10967	0.237	0.175	0.44	3114	3362	3610
<b>Patient 15</b>	8550	9582	10798	0.307	0.22	0.343	3395	3792	4198

Each stiffness element was defined in 3 dimensions: 1: through the thickness of the cortical plate; 2: within the plane of the cortical plate; 3: Parallel to the long axis of the three-pillars of the maxilla. To rule out the effect of stiffness, the same isotropic properties were assigned to all cortical bone parts when the thickness was tested (72 models).

### 3.2.2.2. Analysis type definition

After defining the material properties, a step was initiated and the analysis type was defined as linear static. Next, the study variables and components (Von Mises stresses and displacement in all three planes of space) were selected in the “Field output” section and later viewed and plotted in the final loaded state.

### 3.2.2.3. Interactions

The majority of FEA studies in orthodontics addressed vertical (intrusion) and transverse (expansion) movements of teeth or investigated movements into edentulous



areas in the maxilla and mandible (such as canine retraction, incisors retraction and molar protraction into extraction spaces). Unlike distalization, these movements do not require the definition of interaction settings to aid in load transmission between adjacent teeth, thus the insufficient literature about this topic.

To accurately represent the transmission of load through the contact point surface, ScanIP was used to separate the teeth by a “dental floss” distance equal to 0.2 to 0.4 mm. Afterward, ellipsoid shaped mesial and distal surfaces of each tooth were created using the 3D edit tool and then exported as surfaces in the inp. format file (Fig. 3.15).

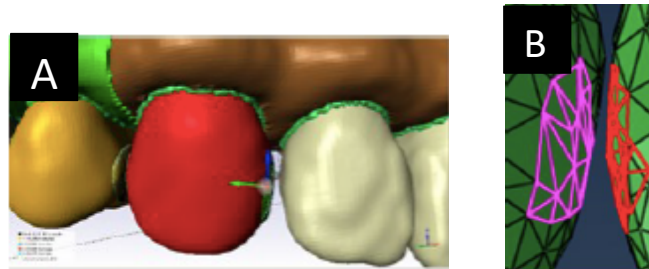


**Fig. 3.15:** A- Creation/positioning of ellipsoid shaped surface at the mesial of the canine; B- Individual surfaces as viewed in Abaqus.

In Abaqus, the exported surfaces act as a separate part from the teeth allowing for “surface to surface” interactions to be defined between the adjacent surfaces. However, these interactions work only for surfaces in contact with each other.

To obtain load transmission through the teeth, adjustments to increase the sensibility of the interactions were needed. Thus, the tolerance of each surface to surface interaction was set to 0.4 to allow communication of nodes at a distance up to 0.4 mm (to account for the maximum distance separating the teeth which is equal to 0.3 mm). A total of four

interactions was created starting from the distal surface of the canine to the mesial of the second molar (Fig. 3.16).

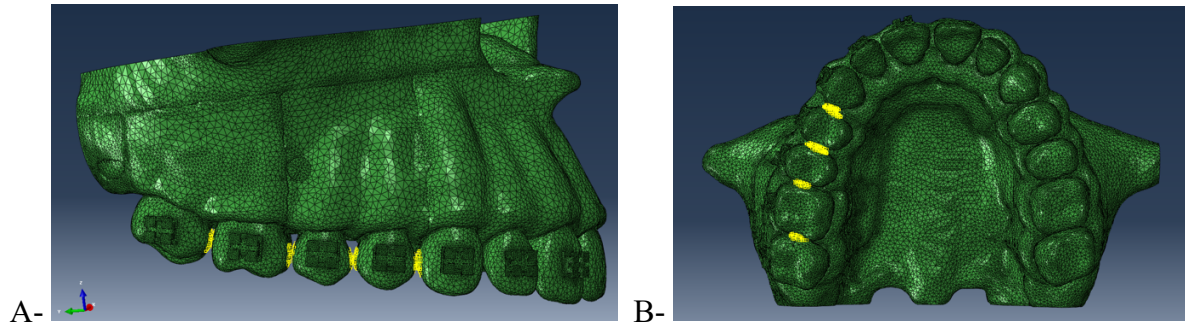


**Fig. 3.16:** “Surface to surface” interactions (in yellow) defined between the adjacent surfaces; **A-** Lateral view; **B-** Occlusal view.

#### 3.2.2.4. Loading setup and boundary conditions

- Load

Distalization of the buccal segment was simulated with an optimal force of 150 grams (1.47 Newton) directed from the miniscrew placed between the maxillary right 2<sup>nd</sup> premolar and 1<sup>st</sup> molar to the canine bracket (direct anchorage) (Fig. 3.17).



**Fig. 3.17:** Clinical picture showing the direct distalization modality in a patient treated without decortications or microperforations.

In Abaqus, a node-set was created on the upper half of the maxillary right canine bracket comprised of around 990 nodes. The applied force (150 grams =1.47 Newton) was equally divided on all the nodes of the bracket set (Fig. 3.18).

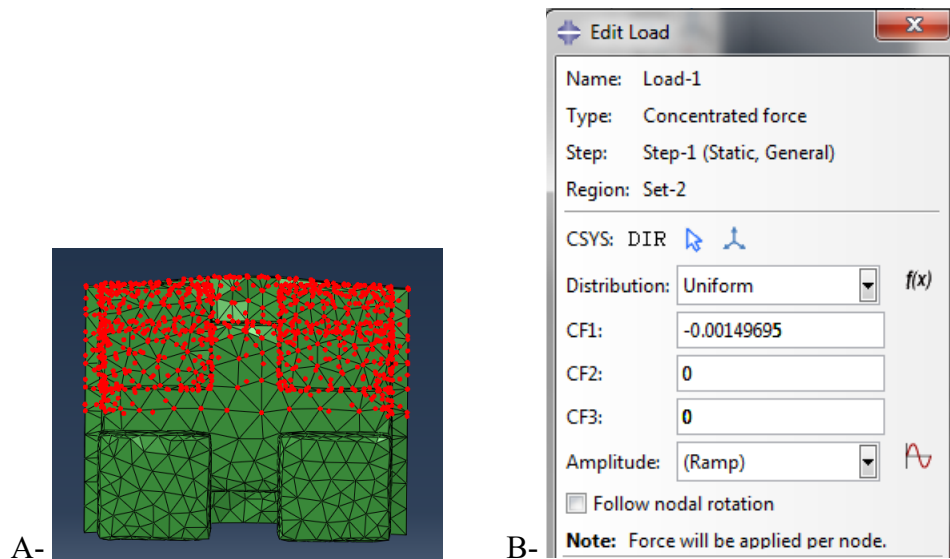


**Fig. 3.18:** A- Node set created on the upper half of the canine bracket; B- Load uniformly distributed on all the nodes.

Subsequently, a datum axis system was constructed using 3 points (Fig. 3.19):

- The origin of the axis system located at the center of the miniscrew head.
- The second point located at the center of the bracket helped define the X-axis.
- The third point was placed perpendicular to the X-axis. The direction of the direct loading force followed the X-axis with no components in the Y and Z axes.

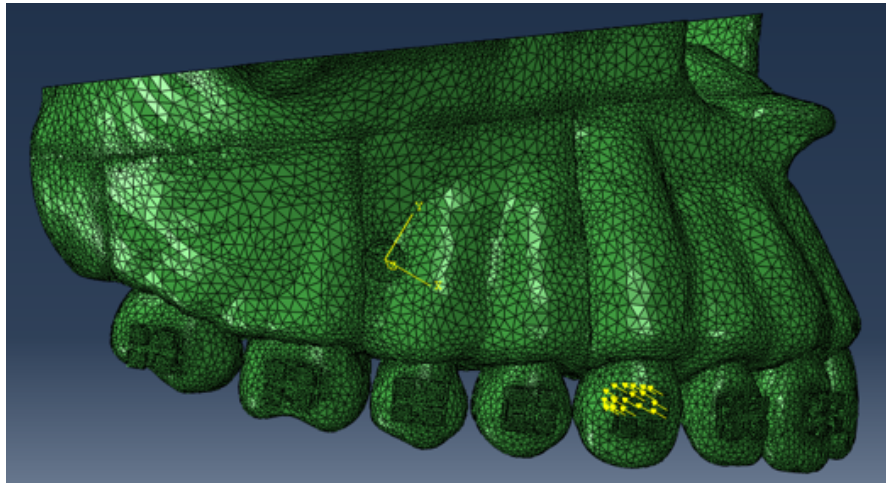


**Fig. 3.19:** Lateral view of the direct load from the miniscrew to the bracket.

- Boundary conditions

Most FEA studies on the maxilla considered the upper and posterior regions of the maxilla fully restrained (boundary condition 1). This assumption is explained by the fact that the upper and posterior parts of the maxillary bone are fused to the cranial base bones (frontal, ethmoid, sphenoid, malar and nasal bones) and therefore clamped in all directions. This type of boundary condition is encastered, that is all the translation and rotation degrees of freedom are equal to zero ( $U_1=U_2=U_3=UR_1=UR_2=UR_3=0$ ) (Fig. 3.20).

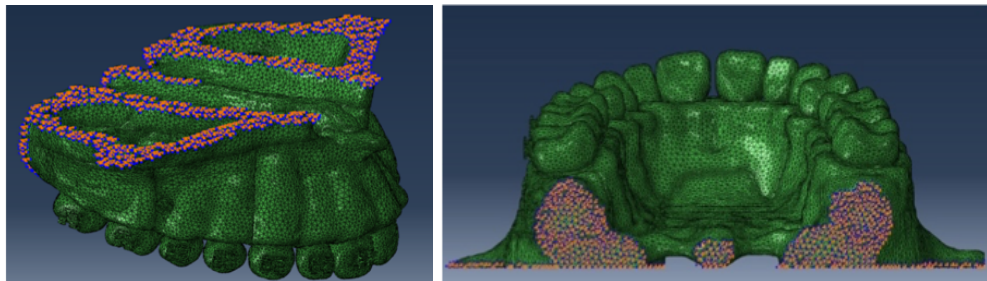


**Fig. 3.20:** Boundary condition 1 to fully restrain the upper and posterior parts of the maxilla.

To simulate the action of the brackets and the movement of the teeth along the archwire, an axis system following the long axis of every tooth was created (Fig. 3.21); Thus, specific boundary conditions were assigned to the nodes located at the level of each bracket (Fig. 3.22), allowing the following movements only:

- Mesio-distal translation along the X-axis of every tooth (parallel to the archwire).
- Mesio-distal and bucco-lingual tipping around the Z and X axes respectively.
- Rotation around the long axis (Y-axis) of each tooth.

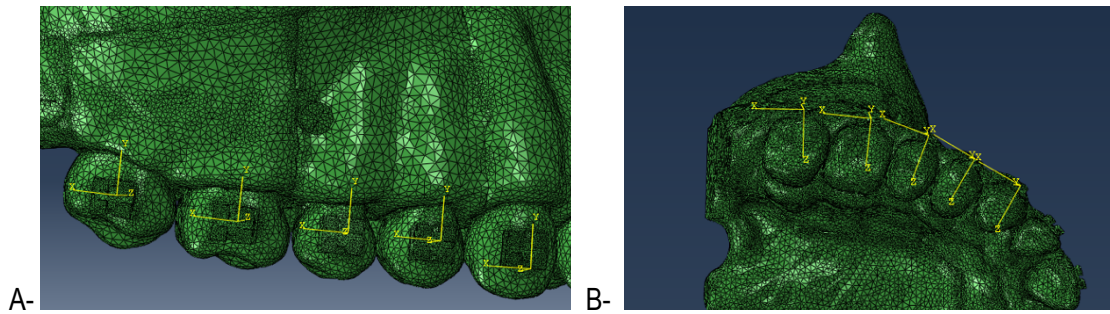


**Fig. 3.21:** Datum axes systems constructed parallel to the long axis of each tooth, and used to define boundary condition that mimic the presence of the archwire. A- Lateral view B- Occlusal view.

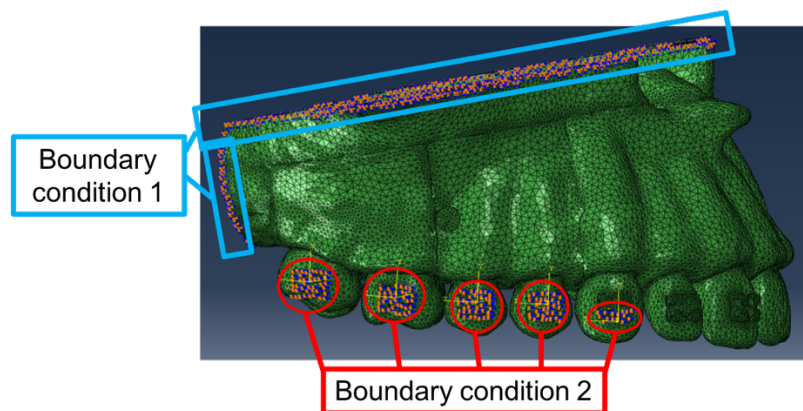


**Fig. 3.22:** **Boundary condition 1:** ENCASTER ( $U1=U2=U3=UR1=UR2=UR3=0$ ) to fully restrain the upper and posterior parts of the maxilla; **Boundary condition 2:** XASYMM ( $U2=U3=UR1=0$ ) simulating the action of the bracket and archwire.

### 3.2.2.5. Data collection and export

- Measurement

In orthodontics, stress distribution produced by forces between the periodontal ligament and the bone indicates the location where tooth movement occurs. Thus, stress at the PDL is assumed to be in proportion to the bone-remodeling rate (Kojima et al., 2012).

Von Mises stress, evaluated at an element, is a measure of the elasticity of a material and represents the point at which the elastic limit is exceeded and permanent deformation results. The total displacement includes the sum of the initial translation movements of a node in the X, Y, and Z axes in addition to the rotation movements around these axes systems.

- Sets

Abaqus offers the possibility to collect numerical stresses, displacement and other phenomena at each node or element. For stress data collection, a set containing randomly selected elements uniformly dispersed along each surface of the periodontal ligament was created. The canine and first premolar were represented by 4 sets corresponding to the buccal, palatal, mesial and distal surfaces. Furthermore, to assess the stress distribution along the PDL area, the buccal, mesial and distal surfaces of the PDL of the canine were further divided into cervical, middle and apical areas. Each set contained between 70 to 250 elements (depending on area size) (Fig. 3.23).



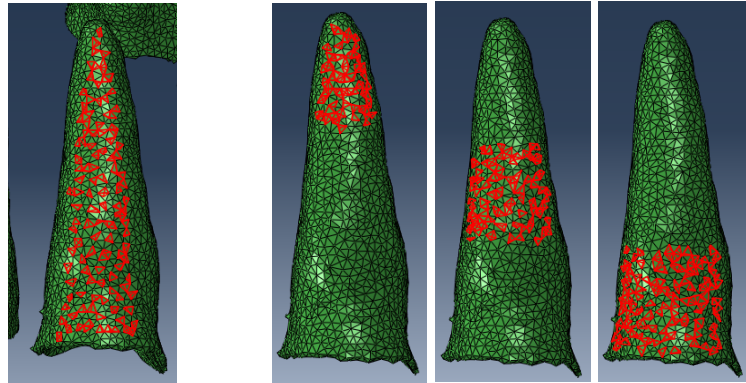


**Fig. 3.23:** Selection of element sets. A- Buccal of canine (B3); B- Apical (B3a); C- Middle (B3m); D- Cervical area of the buccal canine (B3c).

Similarly, stress on the trabecular bone was denoted with a set consisting of 45 to 70 elements selected in the area of trabecular bone underlying the corticotomy distal to the canine (Fig. 3.24).

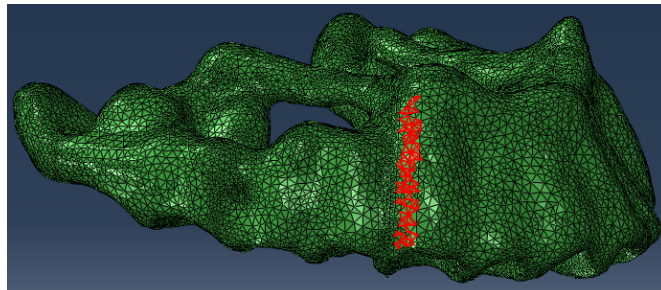


**Fig. 3.24:** Selection of the set of elements on the trabecular bone.

As for tooth displacement, 10 to 17 nodes were selected at the centroid of the crown of the right canine and first premolars. The resulting sets were used to measure the initial displacement (Fig. 3.25). The centroid of each crown was used to account for the rotation movement that may occur. Subsequently, each set was allocated its corresponding output variable of interest in the “history output” section.

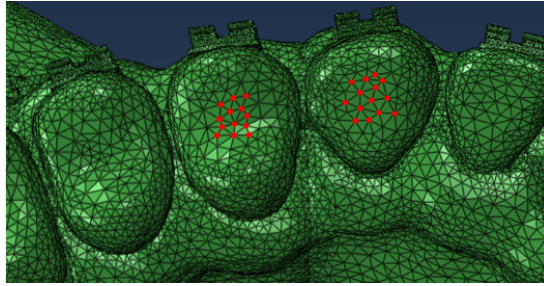


**Fig. 3.25:** Selection of node sets representing the centroid of the canine and premolar.

To obtain the volume of cortical bone removed with each corticotomy, a model containing only the mask of the cut was created in Simpleware then meshed and exported into ABAQUS, where information about the mass properties of the entire assembly used was obtained.

After running the finite element analysis, the stress and displacement results were exported as DAT. files into an excel file where the averages were calculated. Finally, the averages for each modality were put in two final data sheets, the first corresponding to the stiffness variation, and the second to the thickness variation. As usual, FEA results were evaluated using color mapped representations and arrows. However, to assess individual variations, statistical analysis was applied on the numerical data.

### **3.2.3. *Statistical analysis***

Descriptive statistics were generated for stress and tooth displacement in the subsamples of the stiffness and thickness variations in the six treatment modalities (CONTROL, 3MOP, 4MOP, 5MOP, 6MOP, DEC). Mean and standard deviations for the canine (3) and 1<sup>st</sup> premolar (4) at each surface of the PDL (buccal, mesial, distal and



palatal), and for the trabecular bone were reported. The Shapiro-Wilk normality test was run to check if the outcome variables have a normal distribution.

The stresses resulting from the stiffness and thickness variations were compared between the two teeth at each surface within each treatment modality using the independent samples t-test when the data was normally distributed, or its equivalent for non-parametric data, the Mann-Whitney U test when the data were not normally distributed. The amount of tooth displacement was also compared between canine and 1<sup>st</sup> premolar using the same statistical tests. For comparison of stress and tooth displacement between modalities, the repeated measures ANOVA was used followed by pairwise comparison. Stress resulting from stiffness was also compared for the canine at the apical, middle and coronal levels using the repeated measures ANOVA followed by pairwise comparisons.

The Pearson moment correlation coefficient (and its equivalent non-parametric Spearman correlation coefficient) was performed to test correlations between:

- i) The initial canine and 1<sup>st</sup> premolar displacement with the total stress at the PDL within each modality, and with the stress on each surface in all the modalities, both in the stiffness and thickness variations.
- ii) The total stresses at the PDL of each tooth within each modality with the stiffness (S1, S2, S3) and the thickness (TB, TP) of the corresponding palatal and buccal cortical bones areas.
- iii) The stress of the trabecular bone underlying the corticotomy within each modality with the stiffness (S1, S2, S3) and the thickness (TB, TP) of the corresponding palatal and buccal cortical bone areas.

iv) The Von mises stress at the periodontal ligament surfaces of each tooth, and the initial displacement with the volume of cortical bone removed in each modality for the stiffness and thickness variations.

v) The stress of the trabecular bone and the volume of bone removed in each modality.

All statistical analyses were performed using SPSS and the level of significance was considered 0.05.

## CHAPTER 4

### RESULTS

The intra-class correlation coefficient indicated good reliability for the repeated measures in each modality ( $r=0.8$ ). For outcome comparison between the canine and first premolar, the statistical tests were repeated six times representing each modality (CONTROL, 3MOP, 4MOP, 5MOP, 6MOP, DEC) for stiffness and thickness variations.

#### 4.1. Stiffness variation

##### 4.1.1. Stress comparison between teeth and modalities

The color mapped representation of the Von mises stress showed that the stress distribution pattern was similar in all the models, being highest on the canine, more precisely on the cervical region, and progressively decreasing in magnitude from the canine to the second molar (Fig 4.1).

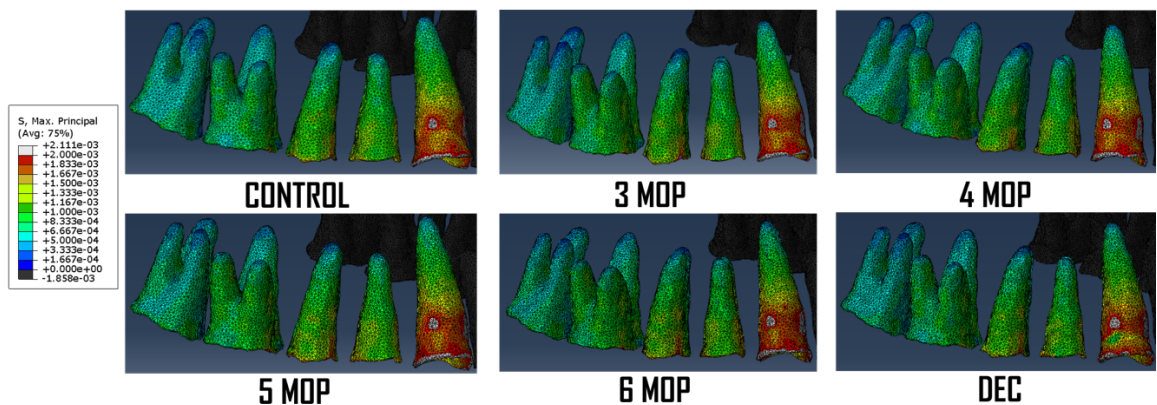


**Fig. 4.1:** Von Mises stress distribution (kilopascals) on the PDL of the teeth in each modality in the template models.

In the stiffness variation applied to each modality, the Mann-Whitney U test results showed that the stresses on all PDL surfaces were significantly different between the canine and first premolar in all the modalities. Higher stresses were recorded on the distal, followed by the buccal then the mesial surfaces of the canine. The only exception to this pattern was on the palatal surface (Table 4.1; Fig 4.2).

**Table 4.1: Comparison of the stress generated on the PDL surfaces between the canine and first premolar in each modality (stiffness variation)**

		Canine		1 <sup>st</sup> PM		p-value
		Mean	StD	Mean	StD	
CONTROL	SB	0.252	0.002	0.191	0.003	0.000*
	SD	0.265	0.003	0.214	0.003	0.000*
	SM	0.232	0.003	0.225	0.003	0.016*
	SP	0.195	0.003	0.234	0.003	0.000*
3MOP	SB	0.279	0.002	0.206	0.003	0.000*
	SD	0.294	0.003	0.225	0.004	0.000*
	SM	0.258	0.004	0.244	0.003	0.000*
	SP	0.211	0.003	0.245	0.003	0.000*
4MOP	SB	0.289	0.002	0.214	0.003	0.000*
	SD	0.305	0.003	0.232	0.003	0.000*
	SM	0.267	0.003	0.253	0.004	0.000*
	SP	0.217	0.003	0.253	0.004	0.000*
5MOP	SB	0.299	0.003	0.221	0.003	0.000*
	SD	0.315	0.003	0.240	0.004	0.000*
	SM	0.276	0.004	0.261	0.004	0.000*
	SP	0.222	0.008	0.262	0.004	0.000*
6MOP	SB	0.312	0.002	0.229	0.004	0.000*
	SD	0.329	0.003	0.249	0.004	0.000*
	SM	0.287	0.006	0.270	0.004	0.000*
	SP	0.233	0.003	0.271	0.004	0.000*
DEC	SB	0.241	0.002	0.230	0.004	0.000*
	SD	0.331	0.004	0.252	0.004	0.000*
	SM	0.300	0.01	0.273	0.004	0.000*
	SP	0.236	0.005	0.276	0.004	0.000*

Stresses in kPa; **StD**: Standard deviation; **SB**: Stress at buccal surface; **SD**: Stress at distal surface; **SP**: Stress At palatal surface; **SM**: Stress at mesial surface.

<sup>†</sup>Results obtained with Mann-Whitney U test

\*Significant at p <0.05

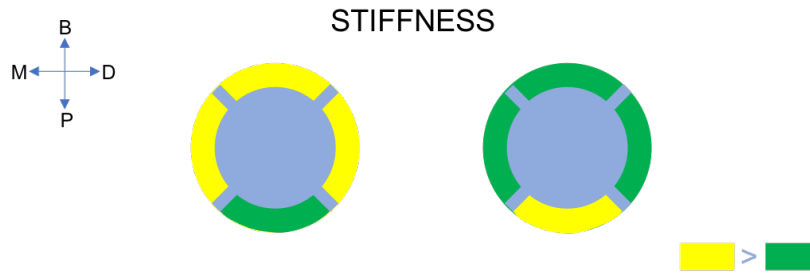


**Fig. 4.2:** Graphic representation of the canine and 1<sup>st</sup> premolar response to direct distalization/ stiffness variation. B: buccal, P: palatal, M: mesial, D: distal surface of teeth. Yellow indicates higher severity, green lower severity as per used FEA scale.

Repeated measures ANOVA for stress comparison on the teeth and the trabecular bone between the different microperforation modalities and the control showed statistically significant differences (Table 4.2). The pairwise comparison performed between every two modalities also showed significant differences except for the palatal surface of the canine between 4MOP and 5MOP modalities, where the stress was not significantly different. Stresses increased as the number of perforations increased. The 6MOP yielded the highest stresses on all PDL surfaces and the trabecular bone (Table 4.3; Fig 4.3).

**Table 4.2: Comparison of the stress generated on the teeth and the trabecular bone among the different microperforation modalities (n=11) (stiffness variation)**

		CONTROL		3MOP		4MOP		5MOP		6MOP		p-value
		Mean	StD	Mean	StD	Mean	StD	Mean	StD	Mean	StD	
Canine	SB3	0.252	0.002	0.279	0.002	0.289	0.002	0.299	0.003	0.312	0.002	0.000*
	SD3	0.265	0.003	0.294	0.003	0.305	0.003	0.315	0.003	0.329	0.003	0.000*
	SM3	0.232	0.003	0.258	0.004	0.267	0.003	0.276	0.004	0.287	0.006	0.000*
	SP3	0.195	0.003	0.211	0.003	0.217	0.003	0.222	0.008	0.233	0.003	0.000*
1 <sup>st</sup> PM	SB4	0.191	0.003	0.206	0.003	0.214	0.003	0.221	0.003	0.229	0.004	0.000*
	SD4	0.214	0.003	0.225	0.004	0.232	0.003	0.240	0.004	0.249	0.004	0.000*
	SM4	0.225	0.003	0.244	0.003	0.253	0.004	0.261	0.004	0.270	0.004	0.000*
	SP4	0.234	0.003	0.245	0.003	0.253	0.004	0.262	0.004	0.271	0.004	0.000*
<b>Trabecular bone</b>		1.348	0.116	1.610	0.131	1.718	0.135	1.891	0.144	2.009	0.133	0.000*

\*Results obtained with repeated measures ANOVA

\*Significant at p <0.05

3: canine; 4: first premolar

**Table 4.3: Pairwise comparison for stress between each microperforation modality (stiffness variation)**

		CONT-3MOP	CONT-4MOP	CONT-5MOP	CONT-6MOP	3MOP-4MOP	3MOP-5MOP	3MOP-6MOP	4MOP-5MOP	4MOP-6MOP	5MOP-6MOP
Canine	SB	0.000*	0.000*	0.000*	0.000*	0.000*	0.000*	0.000*	0.000*	0.000*	0.000*
	SD	0.000*	0.000*	0.000*	0.000*	0.000*	0.000*	0.000*	0.000*	0.000*	0.000*
	SM	0.000*	0.000*	0.000*	0.000*	0.000*	0.000*	0.000*	0.000*	0.000*	0.000*
	SP	0.000*	0.000*	0.000*	0.000*	0.000*	0.011*	0.000*	0.683	0.000*	0.016*
1 <sup>st</sup> PM	SB	0.000*	0.000*	0.000*	0.000*	0.000*	0.000*	0.000*	0.000*	0.000*	0.000*
	SD	0.000*	0.000*	0.000*	0.000*	0.000*	0.000*	0.000*	0.000*	0.000*	0.000*
	SM	0.000*	0.000*	0.000*	0.000*	0.000*	0.000*	0.000*	0.000*	0.000*	0.000*
	SP	0.000*	0.000*	0.000*	0.000*	0.000*	0.000*	0.000*	0.000*	0.000*	0.000*
Trabecular bone		0.000*	0.000*	0.000*	0.000*	0.000*	0.000*	0.000*	0.000*	0.000*	0.000*

\*Significant at  $p < 0.05$

When comparing each modality to the decortication modality (DEC), statistically significant differences were found indicating that the highest stresses on the PDL of the teeth are obtained following the decortication, except for the buccal surface of the canine where the lowest stress was registered (Table 4.4; Fig 4.3). Also, DEC leads to significantly increased stress on the trabecular bone (3.5 kPa) (Fig 4.4).

**Table 4.4: Teeth and trabecular bone stresses comparison between the decortication modality (DEC) and each microperforation modality (stiffness variation)**

		DEC-CONTROL	DEC-3MOP	DEC-4MOP	DEC-5MOP	DEC-6MOP
Canine	SB3	0.000*	0.000*	0.000*	0.000*	0.000*
	SD3	0.000*	0.000*	0.000*	0.000*	0.000*
	SM3	0.000*	0.000*	0.000*	0.000*	0.008*
	SP3	0.000*	0.000*	0.000*	0.003*	0.018*
1 <sup>st</sup> PM	SB4	0.000*	0.000*	0.000*	0.000*	0.000*
	SD4	0.000*	0.000*	0.000*	0.000*	0.000*
	SM4	0.000*	0.000*	0.000*	0.000*	0.004*
	SP4	0.000*	0.000*	0.000*	0.000*	0.000*
Trabecular bone		0.000*	0.000*	0.000*	0.000*	0.000*

\*Significant at  $p < 0.01$

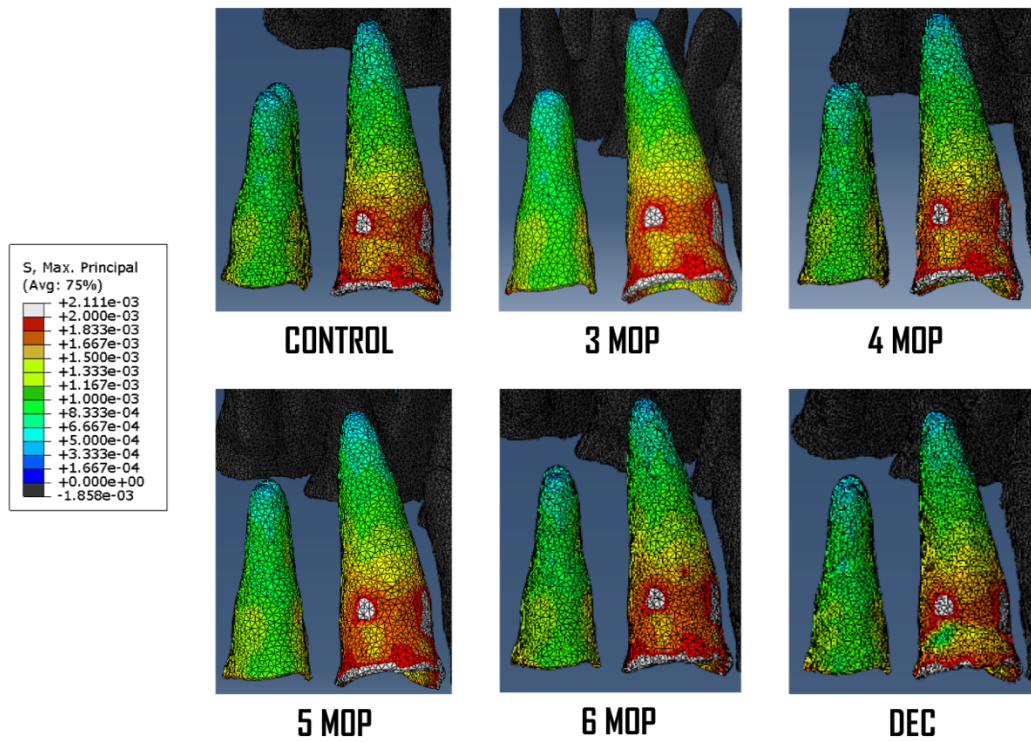


**Fig. 4.3:** PDL Von mises stress (kilopascals) on the buccal surface of the canine and 1<sup>st</sup> premolar in each modality.

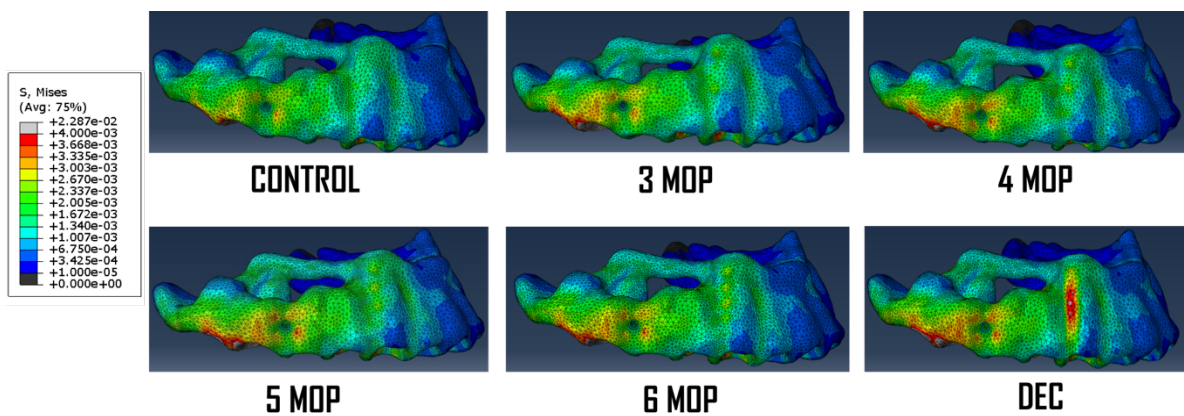


**Fig. 4.4:** Von mises stress (kilopascals) on the trabecular bone in each modality.

After dividing the buccal, mesial and distal PDL surfaces of the canine into equal thirds: apical, middle and cervical, and comparing the stress on each third first between the different modalities using repeated-measures ANOVA, significant differences were observed, except for the stress on the apical third of the canine's distal surface (Table 4.5).

**Table 4.5: Comparison of the stress generated on the sections of the PDL of the canine in all the modalities (n=11) (stiffness variation)**

		CONTROL		3MOP		4MOP		5MOP		6MOP		DEC		p-value
		Mean	StD	Mean	StD	Mean	StD	Mean	StD	Mean	StD	Mean	StD	
SB3	a	0.156	0.002	0.172	0.002	0.179	0.002	0.185	0.002	0.193	0.002	0.134	0.002	0.000*
	m	0.245	0.002	0.271	0.002	0.281	0.002	0.291	0.003	0.304	0.002	0.234	0.002	0.000*
	c	0.347	0.003	0.385	0.003	0.399	0.004	0.413	0.004	0.430	0.003	0.329	0.010	0.000*
SM3	a	0.132	0.002	0.146	0.003	0.150	0.007	0.157	0.002	0.164	0.003	0.165	0.002	0.000*
	m	0.199	0.002	0.222	0.002	0.229	0.003	0.246	0.002	0.247	0.003	0.249	0.003	0.000*
	c	0.306	0.003	0.339	0.003	0.352	0.004	0.353	0.003	0.379	0.004	0.380	0.004	0.000*
SD3	a	0.182	0.002	0.203	0.002	0.383	0.057	0.217	0.002	0.226	0.002	0.228	0.002	0.405
	m	0.256	0.003	0.284	0.003	0.294	0.003	0.304	0.003	0.317	0.003	0.320	0.006	0.000*
	c	0.327	0.003	0.363	0.003	0.376	0.004	0.389	0.004	0.405	0.004	0.408	0.004	0.000*

Stresses in kPa; **StD**: Standard deviation; a: apical; m: middle; c: cervical

<sup>†</sup>Results obtained with repeated measures ANOVA

\*Significant at  $p < 0.05$

A further comparison performed between every two modalities on the sections where significant differences were found, also showed significant differences, except for the stress on the mesial surface, specifically on the apical third between 3MOP- 4MOP, and on the middle and cervical thirds between 3MOP- 5MOP, 4MOP- 5MOP and 5MOP- 6MOP, where no significant differences were observed (Table 4.6).



**Table 4.6: Pairwise comparison for stress on the PDL sections of the canine surfaces between each microperforation modality (stiffness variation)**

		CONT-3MOP	CONT-4MOP	CONT-5MOP	CONT-6MOP	3MOP-4MOP	3MOP-5MOP	3MOP-6MOP	4MOP-5MOP	4MOP-6MOP	5MOP-6MOP
SB3	a	0.000*	0.000*	0.000*	0.000*	0.000*	0.000*	0.000*	0.000*	0.000*	0.000*
	m	0.000*	0.000*	0.000*	0.000*	0.000*	0.000*	0.000*	0.000*	0.000*	0.000*
	c	0.000*	0.000*	0.000*	0.000*	0.000*	0.000*	0.000*	0.000*	0.000*	0.000*
SM3	a	0.000*	0.000*	0.000*	0.000*	1.000	0.000*	0.000*	0.028*	0.000*	0.000*
	m	0.000*	0.000*	0.000*	0.005*	0.000*	0.301	0.000*	1.000	0.000*	1
	c	0.000*	0.000*	0.000*	0.030*	0.000*	1.000	0.000*	1.000	0.000*	0.690
SD3	a										
	m	0.000*	0.000*	0.000*	0.000*	0.000*	0.000*	0.000*	0.000*	0.000*	0.000*
	c	0.000*	0.000*	0.000*	0.000*	0.000*	0.000*	0.000*	0.000*	0.000*	0.000*

\*Significant at p <0.05

Upon comparing each modality to the decortication modality (DEC), statistically significant differences were found indicating higher stresses with decortications. The only non-significant comparisons were with the stress on the middle and cervical thirds of the mesial surface obtained with 5MOP and 6MOP, and in the middle of the distal surface obtained with 6MOP (Table 4.7).

**Table 4.7: Canine PDL stress comparison between the decortication modality (DEC) and each microperforation modality (n=11) (stiffness variation)**

		DEC-CONT	DEC-3MOP	DEC-4MOP	DEC-5MOP	DEC-6MOP
SB3	a	0.000*	0.000*	0.000*	0.000*	0.000*
	m	0.000*	0.000*	0.000*	0.000*	0.000*
	c	0.031*	0.000*	0.000*	0.000*	0.008*
SM3	a	0.000*	0.000*	0.000*	0.000*	0.000*
	m	0.000*	0.000*	0.000*	1.000	0.108
	c	0.000*	0.000*	0.000*	0.519	0.341
SD3	a					
	m	0.000*	0.000*	0.000*	0.000*	0.359
	c	0.000*	0.000*	0.000*	0.000*	0.000*

\*Significant at p <0.01

#### 4.1.2. Displacement comparison between teeth and modalities

Concerning initial tooth displacement, the Mann-Whitney U test results showed that the canine displacement was statistically significantly greater than the 1<sup>st</sup> premolar displacement in all six modalities (Table 4.8). These results were supported by the color mapped configuration showing similar patterns in all the models with higher displacements at the canine, more at the crown part, and decreasing posteriorly (Fig 4.5).

**Table 4.8: Comparison of the initial displacement between the canine and 1<sup>st</sup> premolar in each modality (stiffness variation)**

	SU3		SU4		p-value
	Mean	StD	Mean	StD	
<b>CONTROL</b>	0.0623	0.0006	0.0425	0.0008	0.000*
<b>3MOP</b>	0.0692	0.0007	0.0459	0.0008	0.000*
<b>4MOP</b>	0.0717	0.0007	0.0476	0.0009	0.000*
<b>5MOP</b>	0.0741	0.0007	0.0492	0.0009	0.000*
<b>6MOP</b>	0.0773	0.0008	0.0510	0.0009	0.000*
<b>DEC</b>	0.0779	0.0008	0.0514	0.0009	0.000*

Displacement in mm; StD: Standard deviation

**SU3:** Initial displacement at the canine; **SU4:** Initial displacement at the 1<sup>st</sup> PM

†Results obtained with Mann-Whitney U test

\*Significant at p <0.05

Repeated measures ANOVA for comparison of the initial displacement of the canine and first premolar between the different microperforation modalities and the control followed by a paired t-test between every two modalities showed statistically significant differences. More displacement was achieved when the number of perforations increased. 6MOP yielded the highest canine and first premolar initial displacement values (Table 4.9-4.10; Fig 4.5).

**Table 4.9: Comparison of the initial teeth displacement among the different microperforation modalities (n=11) (stiffness variation)**

	CONTROL		3MOP		4MOP		5MOP		6MOP		p-value
	Mean	StD	Mean	StD	Mean	StD	Mean	StD	Mean	StD	
SU3	0.0623	0.0006	0.0692	0.0007	0.0717	0.0007	0.0741	0.0007	0.0773	0.0008	0.000*
SU4	0.0425	0.0008	0.0459	0.0008	0.0476	0.0009	0.0492	0.0009	0.0510	0.0009	0.000*

<sup>†</sup>Results obtained with repeated measures ANOVA

\*Significant at p <0.05

**Table 4.10: Pairwise comparison for displacement between each microperforation modality (stiffness variation)**

	CONT-3MOP	CONT-4MOP	CONT-5MOP	CONT-6MOP	3MOP-4MOP	3MOP-5MOP	3MOP-6MOP	4MOP-5MOP	4MOP-6MOP	5MOP-6MOP
SU3	0.000*	0.000*	0.000*	0.000*	0.000*	0.000*	0.000*	0.000*	0.000*	0.000*
SU4	0.000*	0.000*	0.000*	0.000*	0.000*	0.000*	0.000*	0.000*	0.000*	0.000*

\*Significant at p <0.05

By comparing each modality to the DEC modality, statistically significant differences were found indicating that greater displacement (0.0779 mm) is achieved with decortication than with 6 perforations (Table 4.11; Fig 4.5).

**Table 4.11: Displacement comparison between DEC and each microperforation modality (stiffness variation)**

	DEC-CONTROL	DEC-3MOP	DEC-4MOP	DEC-5MOP	DEC-6MOP
SU3	0.000*	0.000*	0.000*	0.000*	0.000*
SU4	0.000*	0.000*	0.000*	0.000*	0.000*

\*Significant at p <0.05

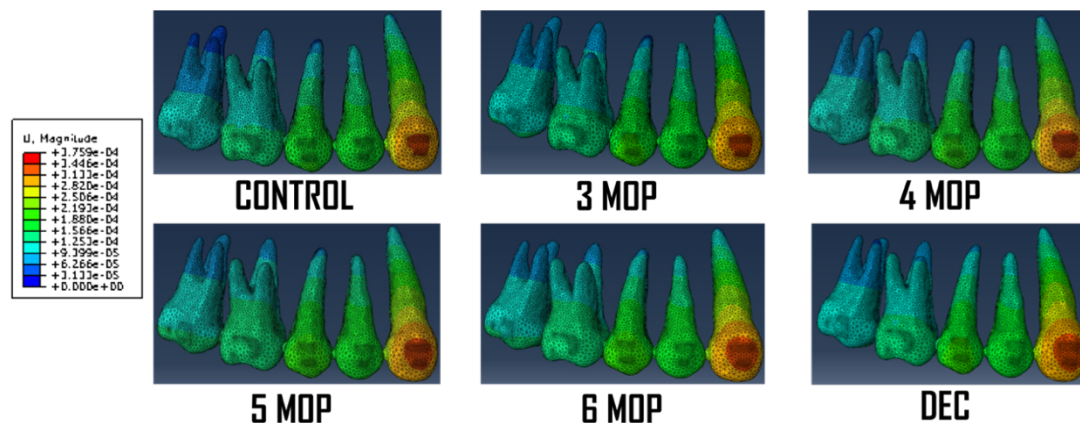


**Fig. 4.5: Initial tooth displacement (mm) in each modality.**

## 4.2. Thickness variation

### 4.2.1. Stress comparison between teeth and modalities

In the thickness variation applied to each modality, the Mann-Whitney U test results showed that the stresses on all PDL surfaces were significantly different between the canine and first premolar in all the modalities, except for the stress on the mesial surface in the control, 3MOP and 4MOP modalities. Higher stresses were recorded on the distal, followed by the buccal and the mesial surfaces of the canine. The only exception was the stress on the palatal surface which was significantly higher on the 1<sup>st</sup> premolar (Table 4.12; Fig 4.6).

**Table 4.12: Comparison of the stress generated on the PDL surfaces between the canine and 1<sup>st</sup> premolar in each modality (thickness variation)**

		Canine		1 <sup>st</sup> PM		p-value
		Mean	StD	Mean	StD	
CONTROL	TB	0.248	0.002	0.172	0.003	0.000*
	TD	0.260	0.003	0.196	0.003	0.000*
	TM	0.229	0.003	0.215	0.003	0.626
	TP	0.180	0.003	0.224	0.003	0.000*
3MOP	TB	0.272	0.002	0.185	0.003	0.000*
	TD	0.284	0.003	0.205	0.004	0.000*
	TM	0.252	0.004	0.234	0.003	0.369
	TP	0.211	0.003	0.245	0.003	0.000*
4MOP	TB	0.284	0.002	0.192	0.003	0.000*
	TD	0.298	0.003	0.213	0.003	0.000*
	TM	0.263	0.003	0.241	0.004	0.096
	TP	0.202	0.003	0.244	0.004	0.000*
5MOP	TB	0.293	0.003	0.197	0.003	0.000*
	TD	0.307	0.003	0.222	0.004	0.000*
	TM	0.271	0.004	0.249	0.004	0.043*
	TP	0.209	0.008	0.250	0.004	0.000*
6MOP	TB	0.303	0.002	0.203	0.004	0.000*
	TD	0.315	0.003	0.228	0.004	0.000*
	TM	0.280	0.006	0.256	0.004	0.022*
	TP	0.211	0.003	0.258	0.004	<0.001*
DEC	TB	0.234	0.002	0.210	0.004	0.003*
	TD	0.320	0.004	0.232	0.004	0.000*
	TM	0.284	0.01	0.261	0.004	0.029*
	TP	0.216	0.005	0.263	0.004	0.000*

Stresses in kPa; **StD**: Standard deviation; **TD**: Stress at distal surface; **TP**: Stress at palatal surface; **TM**: Stress at mesial surface; **TB**: Stress at buccal surface

<sup>†</sup>Results obtained with Mann-Whitney U test; \*Significant at p <0.05



**Fig. 4.6:** Graphic representation of the canine and first premolar response to direct distalization/ Thickness variation. B: buccal, P: palatal, M: mesial, D: distal surface of teeth. Yellow indicates higher severity, green lower severity as per used FEA scale.

Repeated measures ANOVA for stress comparison on the teeth and the trabecular bone between the different microperforations modalities and the control showed statistically significant differences. By comparing every two modalities separately, significant differences were also observed. However, there were no statistically significant differences between control and 3MOP on the distal and palatal stresses of the 1<sup>st</sup> premolar, between 3MOP and 4MOP on the buccal and palatal stresses of the premolar as well, and between 5MOP and 6MOP on the canine palatal surface. Furthermore, no difference was found in the stress on the trabecular bone between 4MOP and 5MOP (Table 4.13- 4.14).

**Table 4.13: Comparison of the stress generated on the teeth and the trabecular bone among the different microperforation modalities (n=13) (thickness variation)**

		CONTROL	3MOP	4MOP	5MOP	6MOP	p-value
Canine	TB3	0.248	0.248	0.248	0.248	0.248	0.000*
	TD3	0.260	0.260	0.260	0.260	0.260	0.000*
	TM3	0.229	0.229	0.229	0.229	0.229	0.000*
	TP3	0.180	0.180	0.180	0.180	0.180	0.000*
1 <sup>st</sup> PM	TB4	0.172	0.206	0.214	0.221	0.229	0.000*
	TD4	0.196	0.225	0.232	0.240	0.249	0.000*
	TM4	0.215	0.244	0.253	0.261	0.270	0.000*
	TP4	0.224	0.245	0.253	0.262	0.271	0.000*
Trabecular bone		1.319	1.592	1.705	1.819	1.976	0.000*

<sup>†</sup>Results obtained with repeated measures ANOVA

\*Significant at p <0.01

**Table 4.14: Pairwise comparison for stress between each microperforation modality (thickness variation)**

		CONT-3MOP	CONT-4MOP	CONT-5MOP	CONT-6MOP	3MOP-4MOP	3MOP-5MOP	3MOP-6MOP	4MOP-5MOP	4MOP-6MOP	5MOP-6MOP
Canine	TB3	0.000*	0.000*	0.000*	0.000*	0.001*	0.000*	0.000*	0.000*	0.000*	0.000*
	TD3	0.000*	0.000*	0.000*	0.000*	0.000*	0.000*	0.000*	0.001*	0.000*	0.000*
	TM3	0.000*	0.000*	0.000*	0.000*	0.000*	0.000*	0.000*	0.000*	0.000*	0.000*
	TP3	0.001*	0.000*	0.000*	0.000*	0.015*	0.000*	0.000*	0.000*	0.000*	1.000
1 <sup>st</sup> PM	TB4	0.008*	0.011*	0.001*	0.000*	0.511	0.015*	0.001*	0.001*	0.000*	0.000*
	TD4	1.000	0.233	0.020*	0.005*	0.022*	0.002*	0.000*	0.003*	0.000*	0.000*
	TM4	0.009*	0.001*	0.000*	0.000*	0.014*	0.001*	0.000*	0.001*	0.000*	0.000*
	TP4	0.103	0.013*	0.002*	0.000*	0.193	0.010*	0.000*	0.000*	0.000*	0.000*
Trabecular bone		0.000*	0.000*	0.000*	0.000*	0.000*	0.000*	0.000*	0.000*	0.054	0.002*

\*Significant at p <0.05

When each modality was compared to the decortication modality, statistically significant differences were found for the stresses on the teeth and trabecular bone (3.12 kPa) indicating that the highest stresses are obtained following the decortication (same as with the stiffness variation). The only non-statistically significant difference was on the buccal surface of the canine between the control and DEC models (Table 4.15).

**Table 4.15: Teeth and trabecular bone stresses comparison between the decortication modality (DEC) and each microperforation modality (thickness variation)**

		DEC-CONTROL	DEC-3MOP	DEC-4MOP	DEC-5MOP	DEC-6MOP
Canine	TB3	0.069	0.000*	0.000*	0.000*	0.000*
	TD3	0.000*	0.000*	0.000*	0.000*	0.000*
	TM3	0.000*	0.000*	0.000*	0.000*	0.000*
	TP3	0.000*	0.000*	0.000*	0.000*	0.000*
1 <sup>st</sup> PM	TB4	0.000*	0.000*	0.000*	0.000*	0.000*
	TD4	0.000*	0.000*	0.000*	0.000*	0.001*
	TM4	0.000*	0.000*	0.000*	0.000*	0.000*
	TP4	0.000*	0.000*	0.000*	0.000*	0.000*
Trabecular bone		0.000*	0.000*	0.000*	0.000*	0.000*

\*Significant at p <0.01

#### 4.2.2. Displacement comparison between teeth and modalities

Comparison of the canine and 1<sup>st</sup> premolar initial displacement in the thickness variation with the Mann-Whitney U test showed that the canine displacement was statistically significantly greater than the 1<sup>st</sup> premolar displacement in all six modalities, similar to the results obtained with the stiffness variation (Table 4.16).

**Table 4.16: Comparison of the initial displacement between the canine and 1<sup>st</sup> premolar in each modality (thickness variation)**

	TU3		TU4		p-value
	Mean	StD	Mean	StD	
<b>CONTROL</b>	0.059	0.004	0.040	0.004	0.000*
<b>3MOP</b>	0.065	0.004	0.042	0.003	0.000*
<b>4MOP</b>	0.068	0.004	0.044	0.003	0.000*
<b>5MOP</b>	0.070	0.004	0.046	0.003	0.000*
<b>6MOP</b>	0.073	0.004	0.047	0.003	0.000*
<b>DEC</b>	0.073	0.004	0.048	0.003	0.000*

Displacement in mm; StD: Standard deviation

**TU3:** Initial displacement at the canine; **TU4:** Initial displacement at the 1<sup>st</sup> PM

<sup>†</sup>Results obtained with Mann-Whitney U test

\*Significant at p <0.05

A comparison of the displacement outcome between the microperforations modalities in the thickness variation also revealed statistically significant differences indicating that adding perforations significantly increased the initial displacement (Table 4.17- 4.18).

**Table 4.17: Comparison of the initial teeth displacement among the different microperforation modalities (n=13) (thickness variation)**

	CONTROL	3MOP	4MOP	5MOP	6MOP	p-value
<b>TU3</b>	0.059	0.065	0.068	0.070	0.073	0.000*
<b>TU4</b>	0.040	0.042	0.044	0.046	0.047	0.000*

<sup>†</sup>Results obtained with repeated measures ANOVA

\*Significant at p <0.05

**Table 4.18: Pairwise comparison for displacement between each microperforation modality (thickness variation)**

	CONT-3MOP	CONT-4MOP	CONT-5MOP	CONT-6MOP	3MOP-4MOP	3MOP-5MOP	3MOP-6MOP	4MOP-5MOP	4MOP-6MOP	5MOP-6MOP
TU3	0.000*	0.000*	0.000*	0.000*	0.000*	0.000*	0.000*	0.000*	0.000*	0.000*
TU4	0.000*	0.000*	0.000*	0.000*	0.000*	0.000*	0.000*	0.000*	0.000*	0.000*

\*Significant at p <0.05

By comparing each modality to the DEC modality, the same results were found as with stiffness, with statistically significant differences confirming that greater displacement is achieved with decortication (0.0738 mm) than with 6 perforations (Table 4.19).

**Table 4.19: Displacement comparison between DEC and each microperforation modality (thickness variation)**

	DEC-CONTROL	DEC-3MOP	DEC-4MOP	DEC-5MOP	DEC-6MOP
TU3	0.000*	0.000*	0.000*	0.000*	0.000*
TU4	0.000*	0.000*	0.000*	0.000*	0.000*

\*Significant at p <0.05

### 4.3. Correlation between stress and displacement

#### 4.3.1. Stiffness variation

In the stiffness variation, a significantly high correlation was present between the total stress on the PDL of the canine and the initial displacement in the 5MOP modality. On the other hand, significantly high correlations were found between the total stress of the first premolar PDL and the displacement in the 3MOP and 6MOP modality (Table 4.20).

**Table 4.20: Correlation between total stress at the canine and 1<sup>st</sup> PM and the corresponding displacement in each modality (stiffness variation)**

Variable		SU3	SU4
S-CONTROL	Pearson	0.626	0.608
	Sig. (2-tailed)	0.053	0.062
S-3MOP	Pearson	0.568	.635*
	Sig. (2-tailed)	0.087	0.048
S-4MOP	Pearson	0.514	0.539



	Sig. (2-tailed)	0.128	0.108
<b>S-5MOP</b>	Pearson	.673*	0.551
	Sig. (2-tailed)	0.033	0.099
<b>S-6MOP</b>	Pearson	0.543	.634*
	Sig. (2-tailed)	0.105	0.049
<b>S-DEC</b>	Pearson	0.63	0.614
	Sig. (2-tailed)	0.051	0.059

S: Total stress in the stiffness variation

†Significant at the: \*0.05, \*\*0.01.

Upon correlating between the initial displacement and the stress amounts at each surface of the PDL in all the modalities, high correlations (>0.9) were found between the canine displacement and the distal, mesial and palatal surfaces. As for the first premolar, high correlations were found between the displacement and each PDL surface (Table 4.21).

**Table 4.21: Correlation between stress amounts at each canine and 1<sup>st</sup> PM surface and the initial displacement (stiffness variation)**

		<b>SU3</b>	<b>SU4</b>
<b>SB</b>	Pearson	0.316	1.000**
	Sig. (2-tailed)	0.542	0
<b>SD</b>	Pearson	1.000**	.993**
	Sig. (2-tailed)	0	0
<b>SM</b>	Pearson	.988**	1.000**
	Sig. (2-tailed)	0	0
<b>SP</b>	Pearson	.995**	.990**
	Sig. (2-tailed)	0	0

†Significant at the: \*0.05, \*\*0.01.

#### **4.3.2. Thickness variation**

In the thickness variation, significantly high and positive correlations (>0.7) were present between the total canine stress and the initial displacement in all the modalities. As for the premolar, significantly high correlations (>0.8) were found between the total stress on the first premolar PDL and the corresponding displacement in all the modalities except the control and 4MOP modalities (Table 4.22).

**Table 4.22: Correlation between total stress at the canine and 1<sup>st</sup> PM and the corresponding displacement in each modality (thickness variation)**

Variable		TU3	TU4
T-CONTROL	Pearson	.887**	0.012
	Sig. (2-tailed)	0	0.97
T-3MOP	Pearson	.853**	.888**
	Sig. (2-tailed)	0	0
T-4MOP	Pearson	.840**	0.507
	Sig. (2-tailed)	0.001	0.093
T-5MOP	Pearson	.822**	.871**
	Sig. (2-tailed)	0.001	0
T-6MOP	Pearson	.812**	.861**
	Sig. (2-tailed)	0.001	0
T-DEC	Pearson	.739**	.828**
	Sig. (2-tailed)	0.006	0.001

T: Total stress in the thickness variation

†Significant at the: \*0.05, \*\*0.01.

When correlating between the displacement and the stress amounts at each surface in all the modalities, high correlations (>0.9) were found between the canine displacement and the distal, mesial and palatal surfaces of the canine, same as with the stiffness variation. High correlations but slightly lower than stiffness correlations (>0.8) existed between the premolar displacement and the stress amounts at each PDL surface (Table 4.23).

**Table 4.23: Correlation between stress amounts at each canine and 1<sup>st</sup> PM surface and the initial canine displacement (thickness variation)**

		TU3	TU4
TB	Pearson	0.263	.990**
	Sig. (2-tailed)	0.613	0
TD	Pearson	.998**	.850**
	Sig. (2-tailed)	0	0
TM	Pearson	.999**	.990**
	Sig. (2-tailed)	0	0
TP	Pearson	.994**	.988**
	Sig. (2-tailed)	0	0

†Significant at the: \*0.05, \*\*0.01.

#### 4.4. Correlation between cortical bone properties and stress

##### 4.4.1. Correlation with cortical bone stiffness

###### 4.4.1.1. Canine

No significant or high correlations were found between the stress values at the canine and the stiffness components of the corresponding cortical bone areas (S1Pinc- S2Pinc - S3Pinc- S1Binc - S2Binc - S3Binc) (Tables 4.24).

**Table 4.24: Correlation between stresses and cortical bone stiffness values at the buccal and palatal incisors and canine areas**

		S3-CONT	S3-3MOP	S3-4MOP	S3-5MOP	S3-5MOP	S3-DEC
S1Pinc	Pearson	0.507	0.568	0.572	0.081	0.409	0.304
	Sig. (2-tailed)	0.135	0.087	0.084	0.825	0.24	0.393
S2Pinc	Pearson	0.12	0.149	0.205	-0.336	-0.077	-0.112
	Sig. (2-tailed)	0.742	0.68	0.569	0.342	0.832	0.758
S3Pinc	Pearson	0.076	-0.012	0.044	-0.3	-0.208	-0.224
	Sig. (2-tailed)	0.835	0.974	0.905	0.4	0.565	0.553
S1Binc	Pearson	-0.32	-0.044	-0.014	-0.441	-0.108	-0.407
	Sig. (2-tailed)	0.368	0.905	0.969	0.203	0.766	0.243
S2Binc	Pearson	-0.196	0.01	0.098	-0.332	-0.102	-0.409
	Sig. (2-tailed)	0.587	0.979	0.787	0.349	0.778	0.241
S3Binc	Pearson	-0.469	-0.168	-0.168	-0.555	-0.352	-0.592
	Sig. (2-tailed)	0.172	0.642	0.642	0.096	0.319	0.071

Significant at \*0.05, \*\*0.01.

###### 4.4.1.2. 1<sup>st</sup> Premolar

On the contrary, significantly high and negative Pearson correlation coefficients ( $-0.542 < r < 0.843$ ) existed between the stress at the first premolar in the different modalities, and S1Pmol and S3Pmol stiffness components of the premolar areas. High correlations with S2Pmol were also found in the 4MOP, 5MOP and DEC modalities (Table 4.25).

**Table 4.25: Correlation between PDL stresses and cortical bone stiffness values at the buccal and palatal premolar areas**

		S4-CONT	S4-3MOP	S4-4MOP	S4-5MOP	S4-6MOP	S4-DEC
S1Ppmol	Pearson	-0.756*	-0.738*	-0.843**	-0.542*	-0.674*	-0.724*
	Sig. (2-tailed)	0.011	0.015	0.002	0.006	0.033	0.018
S2Ppmol	Pearson	-0.488	-0.508	-0.696*	-0.671*	0.601	-0.710*
	Sig. (2-tailed)	0.153	0.133	0.025	0.034	0.066	0.021
S3Ppmol	Pearson	-0.661*	-0.672*	-0.774**	-0.706*	-0.601*	-0.774**
	Sig. (2-tailed)	0.037	0.033	0.009	0.022	0.036	0.009
S1Bpmol	Pearson	0.034	0.104	0.255	0.517	0.27	0.332
	Sig. (2-tailed)	0.926	0.774	0.477	0.126	0.451	0.348
S2Bpmol	Pearson	0.406	0.442	0.495	0.580	0.517	0.559
	Sig. (2-tailed)	0.245	0.201	0.146	0.131	0.126	0.093
S3Bpmol	Pearson	0.099	0.148	0.102	0.365	0.223	0.164
	Sig. (2-tailed)	0.786	0.648	0.778	0.3	0.537	0.652

\*Significant at the: \*0.05, \*\*0.01.

#### 4.4.1.3. Trabecular bone

As for the stress on the trabecular bone, high and significant (p-value < 0.05) negative correlations were found with the buccal stiffness components of the incisor and canine cortical bone areas: S1Binc (-0.859 < r < -0.907), S2Binc (-0.703 < r < -0.776), and S3Binc (-0.849 < r < -0.907) increasing from the control modality to 6MOP. However, no correlations were found in the decortication modality (Table 4.26).

**Table 4.26: Correlation between trabecular bone stress and cortical bone stiffness values at the buccal and palatal incisors and canine areas**

		TB-CONT	TB-3MOP	TB-4MOP	TB-5MOP	TB-6MOP	TB-DEC
S1Pinc	Pearson	-0.108	-0.104	-0.1	-0.101	-0.078	0.111
	Sig. (2-tailed)	0.767	0.775	0.783	0.78	0.831	0.761
S2Pinc	Pearson	-0.431	-0.42	-0.391	-0.396	-0.349	-0.042
	Sig. (2-tailed)	0.214	0.25	0.264	0.257	0.322	0.909
S3Pinc	Pearson	-0.12	-0.077	-0.073	-0.093	-0.04	0.146
	Sig. (2-tailed)	0.74	0.833	0.841	0.797	0.913	0.909
S1Binc	Pearson	-0.859**	-0.884**	-0.881**	-0.881**	-0.877**	-0.336
	Sig. (2-tailed)	0.001	0.001	0.001	0.001	0.001	0.343
S2Binc	Pearson	-0.703*	-0.757*	-0.762*	-0.769**	-0.776**	-0.263
	Sig. (2-tailed)	0.023	0.011	0.01	0.009	0.008	0.463
S3Binc	Pearson	-0.849**	-0.889**	-0.895**	-0.903**	-0.907**	-0.41
	Sig. (2-tailed)	0.002	0.001	0.000	0.000	0.000	0.239

\*Significant at the: \*0.05, \*\*0.01.

#### 4.4.2. Correlation with cortical bone thickness

##### 4.4.2.1. Canine

No significant or high correlations were found between the canine stress and the buccal and palatal thicknesses of the incisor and canine cortical bone area (TPinc- TBinc) (Table 4.27).

**Table 4.27: Correlation between stresses and cortical bone thickness values at the buccal and palatal incisors and canine areas**

		T3-CONT	T3-3MOP	T3-4MOP	T3-5MOP	T3-5MOP	T3-DEC
TPinc	Pearson	0.121	-0.039	-0.213	-0.234	-0.231	-0.163
	Sig. (2-tailed)	0.708	0.904	0.505	0.463	0.469	0.612
TBinc	Pearson	0.252	0.168	0.108	0.097	0.092	0.26
	Sig. (2-tailed)	0.43	0.603	0.739	0.764	0.776	0.414

Significant at \*0.05, \*\*0.01.

##### 4.4.2.2. 1<sup>st</sup> Premolar

No significant or high correlations were found between the first premolar stress and the buccal and palatal thicknesses of the premolar cortical bone areas (TPinc- TBinc) (Table 4.28).

**Table 4.28: Correlation between stress and cortical bone thickness values at buccal and palatal premolar areas**

		T4-CONT	T4-3MOP	T4-4MOP	T4-5MOP	T4-6MOP	T4-DEC
TPpmol	Pearson	-0.02	0.264	0.202	0.347	0.341	0.356
	Sig. (2-tailed)	0.95	0.407	0.528	0.27	0.278	0.257
TBpmol	Pearson	-0.214	0.21	0.32	0.289	0.285	0.3
	Sig. (2-tailed)	0.505	0.512	0.31	0.362	0.369	0.343

Significant at \*0.05, \*\*0.01.

##### 4.4.2.3. Trabecular bone

The stress on the trabecular bone significantly and positively ( $0.613 < r < 0.842$ ) correlated with the buccal thickness component of the incisor and canine cortical bone areas (TBinc) in the control and all the modalities except 6MOP and DEC (Table 4.29).

**Table 4.29: Correlation between trabecular bone stress and cortical bone thickness values at the buccal and palatal incisors and canine areas**

		TB-CONT	TB-3MOP	TB-4MOP	TB-5MOP	TB-6MOP	TB-DEC
TPinc	Pearson	0.337	0.143	0.295	0.071	-0.112	-0.509
	Sig. (2-tailed)	0.26	0.642	0.329	0.818	0.716	0.076
TBinc	Pearson	.842**	.699**	.803**	.613*	0.353	-0.445
	Sig. (2-tailed)	0.000	0.008	0.001	0.026	0.237	0.128

Significant at \*0.05, \*\*0.01.

## 4.5. Correlation between cortical bone properties and displacement

### 4.5.1. Correlation with cortical bone stiffness

#### 4.5.1.1. Canine

No significant or high correlations were found between the displacements at the canine and the stiffness components of the corresponding cortical bone areas (S1Pinc- S2Pinc - S3Pinc- S1Binc - S2Binc - S3Binc) (Table 4.30).

**Table 4.30: Correlation between canine displacement and cortical bone stiffness values at the buccal and palatal incisors and canine areas**

		SU3-CONTROL	SU3-3MOP	SU3-4MOP	SU3-5MOP	SU3-5MOP	SU3-DEC
S1Pinc	Pearson	0.128	0.113	0.13	0.101	0.134	0.106
	Sig. (2-tailed)	0.725	0.755	0.721	0.781	0.713	0.772
S2Pinc	Pearson	-0.233	-0.238	-0.245	-0.262	-0.232	-0.271
	Sig. (2-tailed)	0.518	0.509	0.494	0.465	0.519	0.448
S3Pinc	Pearson	-0.169	-0.18	-0.202	-0.202	-0.126	-0.22
	Sig. (2-tailed)	0.64	0.618	0.576	0.575	0.729	0.542
S1Binc	Pearson	-0.399	-0.39	-0.424	-0.415	-0.437	-0.425
	Sig. (2-tailed)	0.253	0.266	0.222	0.233	0.207	0.221
S2Binc	Pearson	-0.391	-0.383	-0.415	-0.409	-0.436	-0.435
	Sig. (2-tailed)	0.263	0.275	0.233	0.241	0.208	0.209
S3Binc	Pearson	-0.584	-0.566	-0.61	-0.606	-0.63	-0.608
	Sig. (2-tailed)	0.076	0.088	0.061	0.063	0.051	0.062

Significant at \*0.05, \*\*0.01.

#### 4.5.1.2. 1<sup>st</sup> Premolar

No significant or high correlations were found between the displacements at the first premolar and the stiffness components of the premolar cortical bone areas (S1Pmol- S2Pmol - S3Pmol- S1Bmol - S2Bmol - S3Bmol) (Table 4.31).

**Table 4.31: Correlation between premolar displacement and cortical bone stiffness values at the buccal and palatal premolar areas**

		SU4-CONTROL	SU4-3MOP	SU4-4MOP	SU4-5MOP	SU4-5MOP	SU4-DEC
S1Ppmol	Pearson	-0.188	-0.189	-0.205	-0.217	-0.172	-0.195
	Sig. (2-tailed)	0.603	0.601	0.569	0.547	0.636	0.589
S2Ppmol	Pearson	-0.082	-0.089	-0.075	-0.082	-0.056	-0.056
	Sig. (2-tailed)	0.822	0.806	0.837	0.822	0.877	0.878
S3Ppmol	Pearson	-0.119	-0.137	-0.123	-0.122	-0.096	-0.091
	Sig. (2-tailed)	0.743	0.706	0.736	0.737	0.793	0.803
S1Bpmol	Pearson	-0.01	-0.023	-0.03	-0.031	-0.019	-0.042
	Sig. (2-tailed)	0.978	0.949	0.935	0.933	0.977	0.908
S2Bpmol	Pearson	0.002	0.025	0.012	-0.002	-0.011	-0.016
	Sig. (2-tailed)	0.996	0.946	0.973	0.996	0.977	0.965
S3Bpmol	Pearson	-0.334	-0.328	-0.345	-0.331	-0.356	-0.318
	Sig. (2-tailed)	0.346	0.355	0.33	0.35	0.312	0.371

Significant at \*0.05, \*\*0.01.

#### 4.5.2. Correlation with cortical bone thickness

##### 4.5.2.1. Canine

No significant or high correlations were found between the canine displacement and the thickness of the buccal and palatal canine cortical bone areas (TPinc- TBinc) (Table 4.32).

**Table 4.32: Correlation between canine displacement and cortical bone thickness values at the buccal and palatal incisors and canine areas**

		TU3-CONTROL	TU3-3MOP	TU3-4MOP	TU3-5MOP	TU3-5MOP	TU3-DEC
TPinc	Pearson	-0.03	-0.045	-0.034	0.036	0.033	-0.013
	Sig. (2-tailed)	0.927	0.89	0.916	0.911	0.918	0.968
TBinc	Pearson	0.068	0.088	0.101	0.156	0.14	0.111
	Sig. (2-tailed)	0.835	0.785	0.755	0.628	0.664	0.731

Significant at \*0.05, \*\*0.01.

#### 4.5.2.2. 1<sup>st</sup> Premolar

No significant or high correlations existed between the first premolar displacement and the thickness of the buccal and palatal premolar cortical bone (TPpmol- TBpmol) (Table 4.33).

**Table 4.33: Correlation between premolar displacement and cortical bone thickness values at the buccal and palatal premolar areas**

		TU4-CONTROL	TU4-3MOP	TU4-4MOP	TU4-5MOP	TU4-5MOP	TU4-DEC
TPpmol	Pearson	-0.105	-0.094	-0.058	0.011	-0.003	-0.014
	Sig. (2-tailed)	0.746	0.772	0.858	0.973	0.992	0.965
TBpmol	Pearson	-0.268	-0.183	-0.139	-0.008	-0.005	-0.003
	Sig. (2-tailed)	0.401	0.57	0.666	0.98	0.987	0.992

Significant at \*0.05, \*\*0.01.

## 4.6. Correlation between cortical bone removal, stress and displacement

### 4.6.1. Stiffness variation

In the stiffness variation, significantly high and positive correlations (>0.8) were present between the volume of cortical bone removed in each modality and the stress on the mesial surface of the canine, the palatal surface of the first premolar, and the trabecular bone. No significant correlations existed on the remaining PDL surfaces of the canine and first premolar and with the displacement of the canine and first premolar (Table 4.35).

**Table 4.34: Descriptive statistics for the volume of cortical bone removed in each modality**

	Control	3MOP	4MOP	5MOP	6MOP	DEC
Volume of bone removed (mm <sup>3</sup> )	0	7.32	9.76	11.30	14.64	30.85



**Table 4.35: Correlation between volume of cortical bone removed and stress for all the modalities (stiffness variation)**

		Canine					1 <sup>st</sup> PM					Trabecular bone
		SB3	SD3	SM3	SP3	SU3	SB4	SD4	SM4	SP4	SU4	
Volume of bone removed	Pearson	-0.372	0.76	.854*	0.807	0.763	0.762	0.807	0.78	.826*	0.772	.997**
	Sig. (2-tailed)	0.467	0.08	0.031	0.052	0.078	0.078	0.052	0.067	0.043	0.072	0

<sup>†</sup>Significant at the: \*0.05, \*\*0.01.

When the DEC modality was excluded and only the microperforation and control modalities were accounted for, stronger correlations were found with these surfaces as well as significantly high correlations (>0.9 at p-value <0.01) with the remaining PDL surfaces, the trabecular bone and the initial teeth displacement (Table 4.36).

**Table 4.36: Correlation between volume of cortical bone removed and stress for all the modalities except DEC (stiffness variation)**

		Canine					1 <sup>st</sup> PM					Trabecular bone
		SB3	SD3	SB3	SD3	SU3	SB4	SD4	SB4	SD4	SU4	
Volume of bone removed	Pearson	.996**	.997**	.995**	.997**	.996**	.990**	.993**	.992**	.990**	.993**	.996**
	Sig. (2-tailed)	0.004	0.003	0.005	0.003	0.004	0.01	0.007	0.008	0.01	0.007	0.004

<sup>†</sup>Significant at the: \*0.05, \*\*0.01.

#### **4.6.2. Thickness variation**

In the thickness variation, the volume of cortical bone removed was significantly and positively correlated (>0.8) with the stress on the buccal and distal surfaces of the first premolar, as well as with the stress on the trabecular bone. As for the initial displacement, no significant correlations were found with the volume of bone calculated, same as with the stiffness variation (Table 4.37).

**Table 4.37: Correlation between volume of cortical bone removed and stress for all the modalities (thickness variation)**

		Canine					1 <sup>st</sup> PM					Trabecular bone
		TB3	TD3	TM3	TP3	TU3	TB4	TD4	TM4	TP4	TU4	
Volume of bone removed	Pearson	-0.415	0.767	0.771	0.78	0.764	.848*	.870*	0.779	0.784	0.784	.999**
	Sig. (2-tailed)	0.413	0.075	0.073	0.067	0.077	0.033	0.024	0.068	0.065	0.065	0

†Significant at the: \*0.05, \*\*0.01.

When the DEC modality was excluded from the equation, significantly high correlations ( $>0.9$  at  $p$ -value  $<0.01$ ) were found with all the variables except the stress on the distal surface of the first premolar (Table 4.38).

**Table 4.38: Correlation between volume of cortical bone removed and stress for all the modalities except DEC (thickness variation)**

		Canine					1 <sup>st</sup> PM					Trabecular bone
		TB3	TD3	TM3	TP3	TU3	TB4	TD4	TM4	TP4	TU4	
Volume of bone removed	Pearson	.991**	.992**	.996**	.982**	.993**	.994**	0.769	.992**	.997**	.975**	.997**
	Sig. (2-tailed)	0.001	0.001	0	0.003	0.001	0.001	0.129	0.001	0.004	0.005	0.003

†Significant at the: \*0.05, \*\*0.01.

#### 4.7. Data normalization

By definition, data normalization in statistics is a process of reorganization that consists of dividing the data by a common norm, rescaling it to a metric value between 0 and 1, thus bringing all the numeric values in the dataset to a common scale and eliminating the units of measurement. This process enables a better data comparison and performance evaluation across modalities.

In our study, in order to compare the efficiency of microperforations and decortications relative to the volume of cortical bone removed, the metric measures of the total stress and initial displacement values divided by the volume of cortical bone removed

in each corticotomy modality were plotted in bar charts. It was revealed that the metric was highest with three microperforations, decreasing progressively with each additional perforation, and reaching the lowest value with the decortication, more drastically for the stress values on the teeth than on the trabecular bone. This pattern was similar for the stress and displacement values obtained in both the stiffness and thickness variations (Fig. 4.7-4.8).

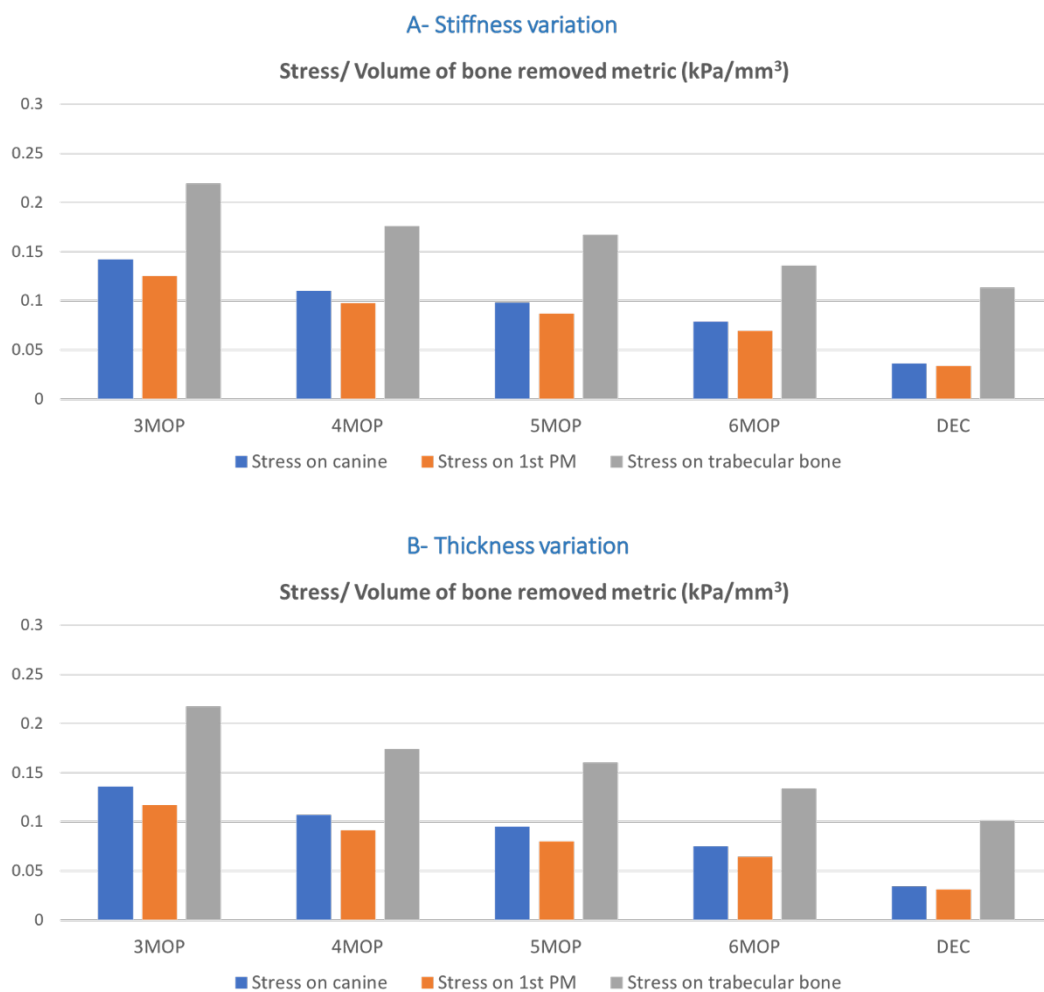


**Fig. 4.7:** Bar chart showing the metric measures for stress/volume of bone removed of the teeth and trabecular bone in all the modalities: A- Stiffness variation; B: Thickness variation

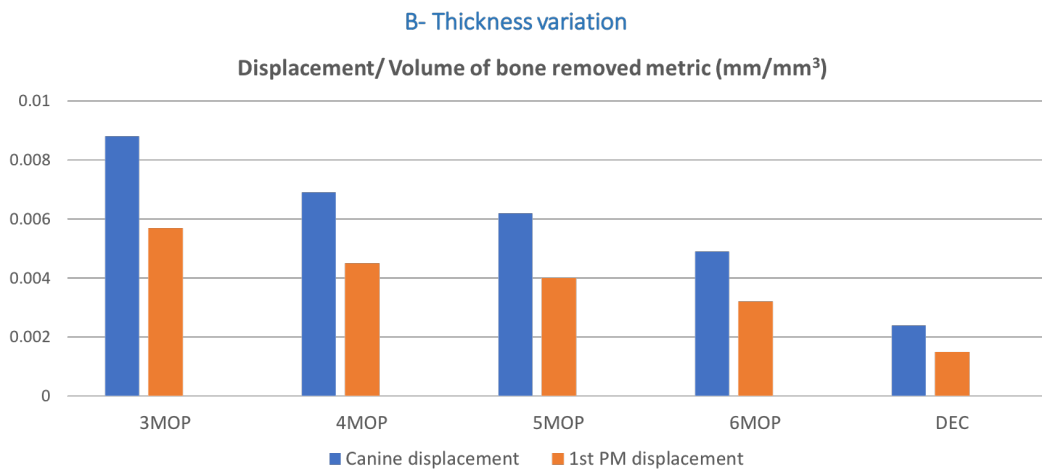
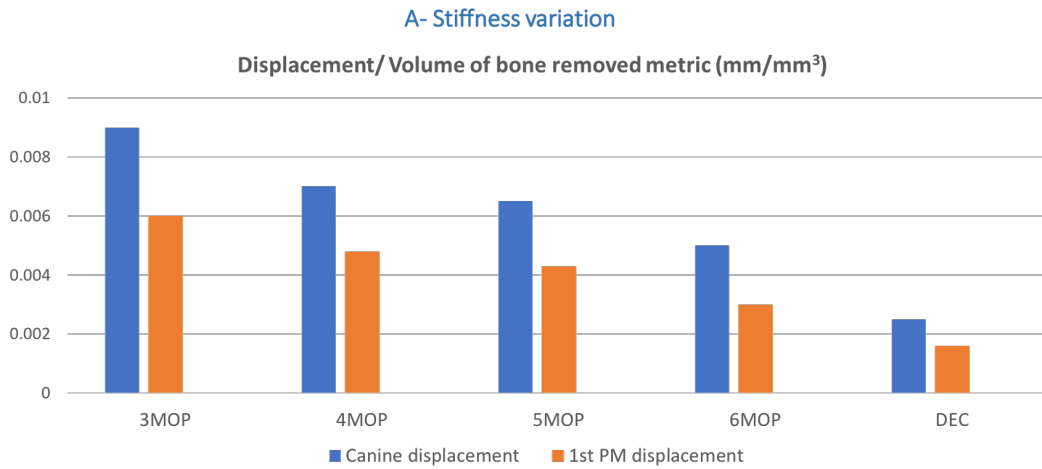


**Fig. 4.8:** Bar chart showing the metric measure for displacement/volume of bone removed of the teeth and trabecular bone in all the modalities: A: Stiffness variation; B: Thickness variation.

# CHAPTER 5

## DISCUSSION

### **5.1. Strengths**

Corticotomy has been proven as an effective method for accelerating tooth movement. This outcome has been explained from a cellular point of view in which inflammatory cells react to bone injury and thereby increase bone turnover (Buschang et al., 2012; Murphy et al., 2012), and from a mechanical point of view by the decrease in bone resistance (Köle, 1959).

Many researchers have attempted to describe and compare different corticotomy approaches. But until our present research, decortications and microperforations have not been compared clinically and on finite element analysis. Our research hereby established comparisons between modalities not used before in any previous finite element analysis study in the orthodontic field. The strengths of this research are listed in this section.

#### *5.1.1. Individual variation*

In most FEA studies applied in the medical and dental fields, simplified assumptions are made regarding geometry, anatomy and material properties, that inevitably affect the analytical results. In the human body, individual variations with respect to bone quality and quantity may lead to different outcomes for a similar clinical problem, thus the need to study larger samples to determine not only central tendencies but also potential outliers.

By incorporating values from real cadavers on thickness and stiffness of the cortical bone, which is a determining structure in OTM, we come closer to achieve a link between the virtual finite element models and clinical reality. The inclusion of a biologic sample with individual variations facilitated the application of statistical analyses that disclosed the effect of variances on a number of outcome measures, leading to definite conclusions or allowing the enunciation of new hypotheses.

#### *5.1.2. Effect of bone characteristics on tooth movement*

The orthodontic force system is a complicated three-dimensional system which is difficult to evaluate in clinical conditions. We found that the effect of force application changes depending on the force-loading environment. Studies on distalization have reported various rates of tooth movement, incriminating different factors such as: position, anatomy, physiology and metabolism of the involved systems (bone, teeth, PDL).

While factors such as physiology and metabolism cannot be studied in a static FEA, the latter provides an excellent tool to assess anatomical differences and their effect on tooth movement, because of the possibility to control all the variables. Prior to this investigation, differentiation between trabecular and cortical bone was not established in FE analysis, and cortical bone thickness and stiffness were only accounted for in a similar research by our research team (Ammoury et al., 2019).

#### *5.1.3. Orthotropic material properties*

The complex anatomy of the oral tissues (e.g. PDL and bone) and the difficulty in defining their properties, most FEA studies applied orthodontics require the utilization of

different simplified assumptions that may inadequately represent these structures. Consequently, the divergence of the published quantitative results prevents a comprehensive comparison between papers.

The oral tissues were assumed to have homogeneous isotropic material properties. However, studies on orthopedics proved otherwise. Lindh et al. (2004) found extreme variations in the density of the trabecular bone tissue of the edentulous maxilla. Chugh et al. (2013) showed variations in the density of the cortical bone in the interradicular areas of dentate maxilla. Gačnik et al. (2014) considered that each bone particle has a different elastic property than its adjacent and used a bone mapping technique to assign a material property to each voxel according to its Hounsfield Unit value obtained on the CT scan.

Moreover, while the majority of the studies judged the bone to be isotropic (material properties do not vary by direction), Schwartz-Dabney et al. (2003) reported that bone is in fact anisotropic, with material properties varying in 3 perpendicular directions X, Y and Z. Cowin & Hart (1990) stated that local anisotropy and regional variations in skeletal material properties can have drastic effects on the relationship between stress and strain.

Because orthodontic tooth movement is a periodontally-driven mechanism, the validity of the results of FEA analysis depends on proper definition of the material properties of the tooth and the surrounding tissues (Ammar et al., 2011). In our study, the material property of the PDL was assigned on the basis of the work of Kojima and Fukui (2012), most commonly used in FEA studies. In addition, the cortical bone was described as accurately as possible by defining its properties as orthotropic, measured from different directions, providing more detailed information about its behavior under different loads.

## 5.2. Comparison with FEA corticotomy studies

FEA on corticotomies was most frequently used in movements of teeth into edentulous areas such as canine retraction in the premolar extraction space (Yang et al., 2015; Pacheco et al., 2016; Samgir et al., 2018; Ahuja et al., 2019), incisors retraction (Liu et al., 2020), and arch expansion (Han et al., 2008; Ajmera et al., 2017). The main reasons were the easier interpretation of the results and to avoid difficult interaction settings between the teeth.

Distalization is a complex movement involving an indeterminate force system, in which moments and forces cannot be readily measured and evaluated, thus its amenability to study with FEA by many researchers (Yu et al., 2014; Sung et al., 2015; Kang et al., 2016; Comba et al., 2017). This investigation was the first to combine the study of maxillary distalization with corticotomy.

Therefore, we will include in this section comparing our results and those from studies of canine retraction in relation to the modality used, model construction and set up, aims, data collection, and results obtained. The methodological differences and similarities are outlined in this section, and the results are compared where pertinent.

Yang et al. (2015) simulated 24 corticotomy approaches during maxillary canine retraction on miniscrews after premolar extraction, with variations in position, distance, and width of the cut (Fig. 5.1). To simulate canine retraction, a 100-cN force was applied from miniscrew placed between the second premolar and the first molar, to the middle of the canine bracket.



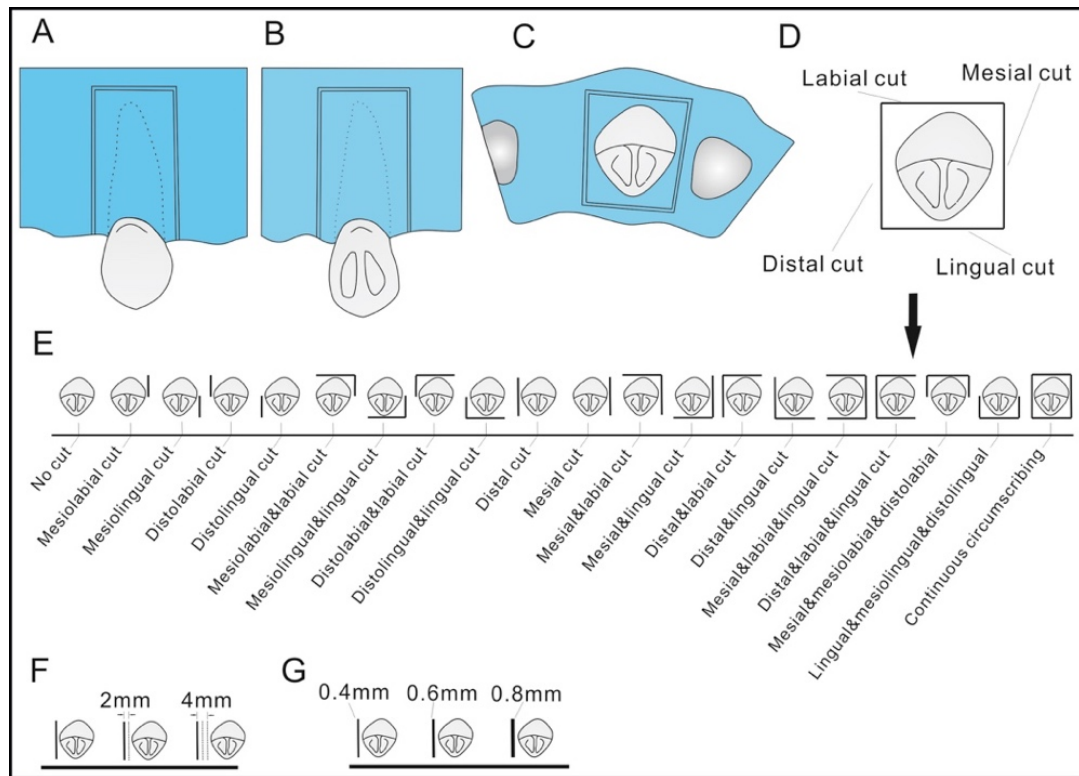


**Fig. 5.1:** Designs of corticotomy approaches: **A**, **B**, and **C**, continuous circumsccribing cut around the canine from the labial, lingual, and occlusal views; **D**, definition of canine position; **E**, corticotomy approaches with the positions of the cuts varied; **F**, with the distance to the canine varied; **G**, with the width of the cut varied (Yang et al., 2015).

Pacheco et al. (2016) assessed three canine distalization possibilities, using a force (150g) applied to a power arm attached to the canine bracket: (1) No corticotomy, (2) box-shaped corticotomy and perforations in the cortical bone of the canine, and (3) condition B along with circle-shaped corticotomy in the cortical bone of the first premolar (Fig. 5.2). The diameter of the perforations and the width of the corticotomies were equal to 1.5mm.

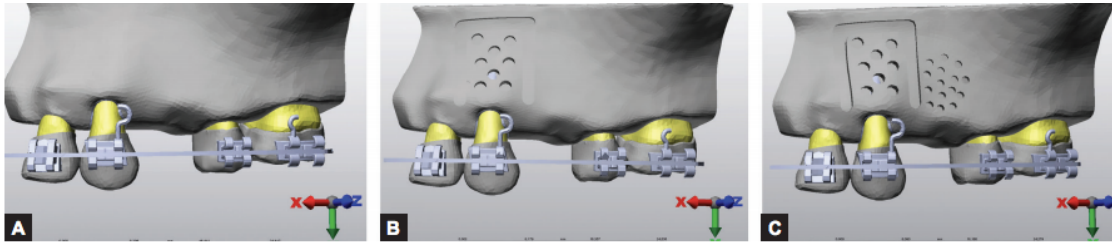


**Fig 5.2:** (A) The control model. (B) The box-shaped corticotomy. (C) The circular corticotomy (Pacheco et al., 2016).

Samgir et al. (2018) compared conventional canine retraction (model 1), with two corticotomy modifications created distal to the canine in the extraction space: three microperforations, 2mm apical to the marginal alveolar bone and in between the perforations (model 2), and a vertical groove made along the long axis of the canine (model 3) (Fig. 5.3). The cuts were 2mm deep and 1.5mm wide. The force applied from a miniscrew also placed between the second premolar and first premolar, was equal to 200g.

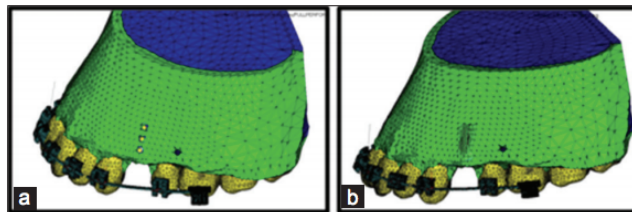


**Fig. 5.3:** (a) Model 2 showing micro-osteoperforations, (b) Model 3 showing vertical groove (Samgir et al. 2018).

In their study evaluating the effect of different corticotomy designs on maxillary canine retraction using a distal force of 150g, Ahuja et al. (2019) constructed four models: with no corticotomy cuts (model 1), with vertical cuts on both buccal and palatal side (2mm deep and 2mm wide) (model 2), with cuts only on buccal side (model 3), and with five circular holes at a distance of 2mm and a diameter of 1.5mm (model 4) (Fig. 5.4)

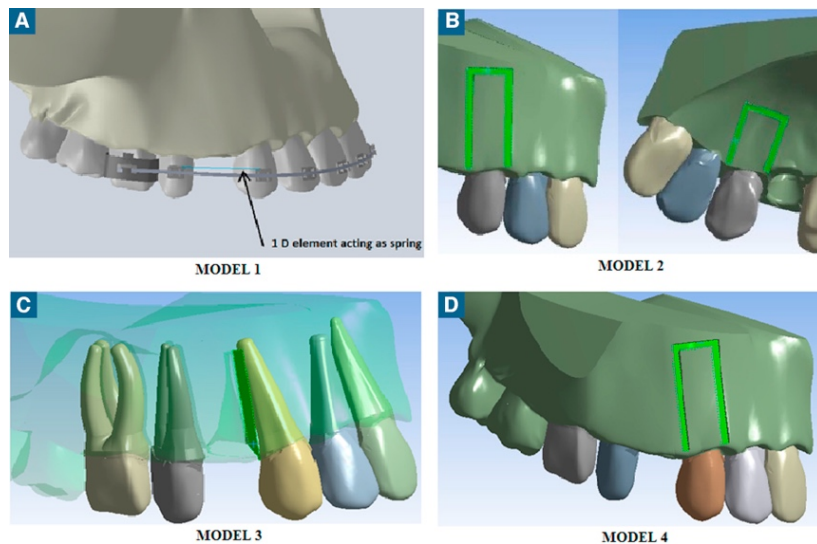


**Fig. 5.4:** FE models: A. Without corticotomy (model 1); B. Buccal and palatal cuts (model 2); C. Interseptal bone reduction (model 3); D. Buccal cuts only (model 4) (Gupta et al. 2019).

The 3D model creation in the study by Yang et al. (2015) and Pacheco et al. (2016) was similar to our method. In both studies, the model was constructed based on computed tomography (CT) scans of an adult human skull. In the study done by Ahuja et al. (2019), the geometric models were constructed on the basis of a skull as well via laser scanning.

In all these canine retraction studies, the mechanical behavior of the materials was assumed to be linear elastic (homogeneous and isotropic), and the value of each material was inferred from different previous reports. The bone was divided into cortical and trabecular and the thickness of the cortical bone was set at 2mm, to facilitate the analysis and disregard bone thickness as a confounding factor. However, the cortical bone is not uniform in thickness. In addition, it is difficult to simulate the real situation of tooth extraction, because the healing of the alveolar socket is a dynamic process, and the morphology and mechanical characteristics of the bone in this area change remarkably.

In the same context, another important reason for divergence of the quantitative results is related to the material property of the PDL. Despite using isotropic homogeneous properties for the PDL in all four studies, differences in the range of the young's moduli are present. Pacheco et al. (2016) used a Young's modulus of 0.87 MPa while the PDL stiffness in the study by Yang et al. (2015) was equal to 50 MPa. However, the PDL is a nonlinear, viscoelastic, and anisotropic material. The anisotropy of the PDL should be carefully considered because the characteristics change the values of Young's modulus and Poisson's ratio (Fill et al., 2012). In our study, we assumed a material property equal to 0.68 MPa, same as the value used by Ahuja et al. (2019) (0.677 MPa), and more commonly used in FEA studies (Kojima et al., 2012).

As for the PDL thickness, Yang et al. (2015) and Ahuja et al. (2019) considered an average thickness of 0.2 mm while Pacheco et al. (2016) and Samgir et al. (2018) set it at 0.25 mm. In our study, since the periodontal ligament (PDL) cannot be captured on the CT scan, the PDL mask was created with a thickness assumption of 0.3 mm (Bowers, 1963).

For Pacheco et al., (2016), the translational movement was restricted in the lateral faces and the upper extremity of the hemi-maxilla and the only tooth able to move was the canine. Ahuja et al. (2019) only allowed sliding without friction at the interfacial nodes between the archwire and the brackets. Yang et al. (2015) used the segmented arch technique without tying the canine to the wire to facilitate its movement.

In our method, we used the "surface to surface" interaction which assumes the presence of a rigid connection between the teeth without any sliding. Our rationale, mimicking the clinical setting, was that distalization is often applied on a heavy rectangular wire to reduce the distal tipping movement and avoid archform changes due to the

application of force buccal to the center of resistance of the tooth. The heavy rectangular wire increases the friction and limits the play between the archwire and the bracket, hindering sliding of teeth. By guiding the teeth into movement tracks defined by the archwire buccally, extrusion, intrusion and bucco-lingual translation are negated.

In dental FEA studies, comparing the stress and displacement values to other studies is not relevant to draw conclusions because many factors come into play and affect the quantitative data. For this reason, we limit the comparison of our results to qualitative findings of FEA corticotomy studies.

### *5.2.1. Comparison between teeth*

#### 5.2.1.1. Stress

Stresses on all PDL surfaces of the canine were greater or significantly greater than on the premolar PDL surfaces for all the modalities in both stiffness and thickness variations. Higher stresses were recorded on the distal which represents the compression side, followed by the buccal then the mesial surfaces of the canine suggesting that the stress is highest on the compression side of the PDL in the direction of the movement. The only exception to this pattern was on the palatal surface, where the values were higher for the premolar, probably due to the larger surface area in contact with the bone.

This result is in concordance with the findings of Sung et al. (2015) who evaluated stresses during “en masse” distalization of the maxillary arch, whereby one of the modalities (direct pull to the canine) was similar to our direct anchorage modality (point of force application) (Fig. 5.4). They reported decreased stress in the posterior segment and showed relatively uniform distribution over the entire root surface.

#### 5.2.1.2. Displacement

For both the stiffness and thickness variations, the initial displacement of the canine was significantly greater than the displacement of the first premolar in all six modalities, a finding comparable with the stress results. Indeed, the color mapped configuration showed similar patterns across all the models with higher displacements at the canine, more at the crown level, and decreasing posteriorly. This pattern indicates distal tipping in response to the direct distalizing force applied from the miniscrew to the canine bracket away from the level of the center of resistance of this tooth.

Sung et al. (2015) also found distal tipping movement with the direct anchorage method (more displacement at the crown level than the apex, and decreasing posteriorly) (Fig. 5.5). Ammar et al. (2011) reported that the application of the load on the power arm of the canine bracket placed the force closer to the center of resistance resulting in a more uniform stress distribution in the PDL and a translational movement. The load we used (150 gm) produced a desired stress distribution in other studies on canine distalization with corticotomy (Aboul-Ela et al., 2011).

#### *5.2.2. Comparison between modalities*

When comparing the displacement and stress on the PDL and the trabecular bone between the control and the different microperforation models in both the stiffness and thickness variation models, statistically significant differences were found indicating that adding perforations in the cortical bone distal to the canine while applying a distalizing force altered the mechanical environment of the canine, the adjacent tooth and the trabecular bone underlying the cut. With the amount of cortical bone around the canine

reduced with the increasing number of perforations, higher stresses and displacements were obtained. The model with six perforations yielded highest stresses values on all the PDL surfaces and the trabecular bone, and the greatest canine and first premolar initial displacement values.

Since the cut is on the buccal side of the cortical bone distal to the canine, the palatal surfaces of the canine and the first premolar which are the farthest from the cut are the least affected with the addition of each perforation, followed by the distal surface of the first premolar. The corticotomy generated stress decreased farther away from the site of the corticotomy. This was in line with the report of Yang et al. (2015) that the position of the corticotomy can affect the mechanical responses of dentoalveolar structures and that the effects decrease with the increase of distance between the cut and the tooth.

Less significant differences were observed between the models in the stress values on the middle and apical thirds of the distal surface of the canine PDL, indicating that the difference in stress distribution is concentrated on the cervical third. Yang et al. (2015) stated that the maximum stress was centered on the distolabial side of the cervix and the maximum strain in the cervical region of the PDL in all the models. Ahuja et al. (2019) also stated that the high stress distribution was noticed on the distocervical region of the canine. Similarly, Samgir et al. (2018) found that the initial displacement was highly concentrated in the distal area of the crown.

Statistically significant differences were found when comparing the results of the stress and the initial displacement of each modality to the results of the decortication modality (DEC) in both the stiffness and thickness variations, signifying that the highest stress and displacement values are obtained after decortication.

Supporting this conclusion was the work by Samgir et al. (2018) who investigated the stress distribution on the buccal side of the cortical bone around the canine under different corticotomy setups. Compared with the control method, they found that the model with the vertical groove showed the maximum amount of canine retraction followed by the model with 3 microperforations.

Also, in a single model setup of canine retraction in a premolar extraction space, Ahuja et al. (2019) demonstrated that under the influence of retractive forces, the rate of canine displacement in the corticotomy models was approximately double in the various corticotomy models when compared with the conventional approach without corticotomy. The greatest displacement value was observed in the model with the buccal and palatal corticotomy model, followed by the model with the buccal cuts only, then the model with five perforations.

Similarly, Gupta et al. (2019) found that the amount of canine retraction in the 3 tested corticotomy models, was approximately double the amount in the non-corticotomy method. The model with inter-septal bone reduction revealed maximum canine displacement (since the main portion of cancellous bone in the pathway of the canine was removed).

These findings are in agreement with Yang et al. (2015) who concluded that the continuous circumscribing cut around the canine root exhibited the maximum rate of canine displacement, suggesting that surgical injury in the form of cuts and holes reduces the resistance offered by the cortical bone. They also showed that the position of the corticotomy cuts had similar variations on the distribution of the Von Mises stresses and the distribution of the canine displacements (Fig 5.8).



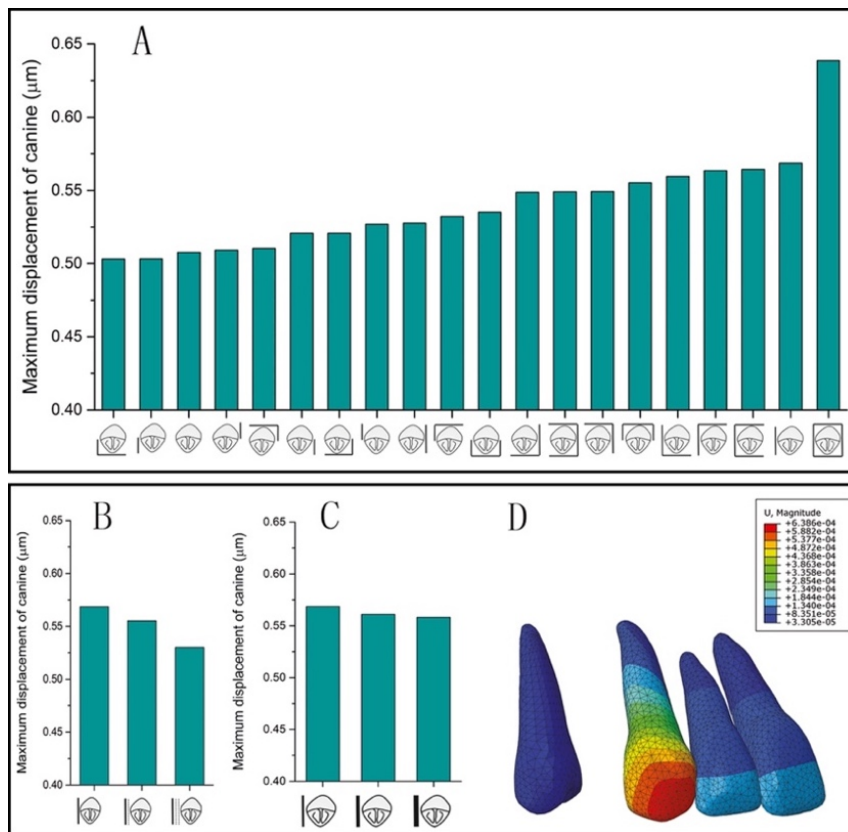


**Fig. 5.5:** Variation in the: **A.** Position of the corticotomy; **B.** Distance from the canine; **C.** Width of the corticotomy; **D.** Distribution of the von Mises stress on the canine from the labial and distal views (Yang et al., 2015).

The increased response in our and other studies might be related to the increased surgical insult. This premise is further justified biologically by the work of Cohen et al. (2010) and McBride et al. (2014) who revealed that the magnitude of the surgical insult affects bone maturity. The bone on the affected side showed greater trabecular numbers and less trabecular thickness than did the bone on the control side, secondary to the increased strain that allowed for faster tooth movement. According to Wilcko et al. (2008), the format of the corticotomy has no influence on the outcome, but rather the degree of metabolic perturbation of the involved tissues.

In a canine retraction model, Pacheco et al. (2016) reported that there was no difference with or without corticotomy, possibly because the corticotomy was superficial and did not sever the entire thickness of the cortical bone. The mechanical decrease in bone resistance produced by the corticotomy approach on the buccal plate was insufficient to cause differences in stress distribution that was uniform and similar in the 3 models they tested: The highest stress was in the middle third of the PDL, and the lowest in the apical portion. They concluded that this difference may be achieved by increasing the number of incisions or by producing a more invasive injury to the bone.

Nevertheless, the heterogeneity of results of the different FEA studies does not allow proper comparisons. FEA simulations obtained from the same study are more valid to draw conclusions because similar assumptions and settings are used. For example, the distal corticotomy in the study by Yang et al. (2015) had a similar mechanical impact on stress and displacement as the circumscribing cut, and therefore, may be a less invasive alternative. Ahuja et al. (2019) also concluded that due to the invasiveness of the procedure if performed on the buccal and palatal plates, sometimes buccal cuts may be enough to effectively accelerate orthodontic tooth movement.

The percentage of increase in initial canine displacement and stress on the distal surface relative to the control was 24% with 6MOP, almost equal to the percentage of increase obtained with decortication (25%). This finding indicates that even though the increase is statistically significantly different, clinically it is not. The difference between decortication and 6MOP is on the buccal surface of the canine which was lower with decortication compared to the control on stiffness variation, and equal to the control on thickness variation. Therefore, the corticotomy affected the response on the buccal surface

of the canine. The stress on the distal surface was more reflective of the initial displacement (Fig. 5.6).



**Fig. 5.6:** Line graphs displaying the percentage of increase in distal and buccal PDL stress and initial displacement on the canine in the stiffness variation with the different corticotomy modalities.

We found that decortication led to the significantly higher stress on the trabecular bone, more than double when compared to the control model, and approximately 66% greater than the model with six perforations. This finding indicates that the removal of cortical bone resistance shifts most of the stress to the trabecular bone. Ahuja et al. (2019) also demonstrated that the stress in the cancellous bone were greater compared to the cortical bone and were mainly concentrated on the alveolar crest of the canine in all the models. The same finding was reported by Gupta et al. (2019).

### *5.2.3. Correlation between stress and displacement*

The total canine and first premolar PDL stress was highly and positively correlated with the total initial displacement in most modalities under thickness and stiffness variations. Additionally, high and positive correlations were found between the total stress on each PDL surface of the canine and first premolar and the corresponding displacement in each modality, except for the buccal surface of the canine, because the average is affected by the low stress value obtained on this surface following the decortication.

On the basis of these results, high stress values may be assumed to translate to more movement. Ammourey et al. (2019) concluded that direct anchorage in a similar distalization scheme targets mainly the canine and first premolar. However, while the highest total canine stress value was recorded with six perforations, the highest displacement value was obtained with decortication, indicating that by removing a continuous shear band of cortical bone, the resistance to movement is decreased thereby facilitating the initial canine displacement.

A number of studies support this finding. Dalstra et al. (2006) reported that the result of the application of a biomechanical system depends on the resistance offered by the surrounding tissues. Chung et al. (2009) observed that corticotomy cuts can reduce the resistance of alveolar bone to OTM by breaking the bone integrity. Similarly, after comparing canine retraction using different distraction techniques on FEM, Xue et al. (2013) reported that corticotomy disrupted the continuity of the cortical bone, causing a change in the stress of the dentoalveolar structures.

#### *5.2.4. Correlation between stress, displacement and cortical bone properties*

The absence of correlations between the stress on the canine and first premolar and the thickness of the corresponding regions suggests that the thickness of the cortical bone does not impact initial movement as stiffness did. In addition, the absence of correlations between the displacement, stiffness and thickness indicates that the initial displacement is not affected by the cortical bone properties. This finding may not be surprising because the initial movement occurs principally in the PDL space.

While the stress at the canine was not correlated with the stiffness components of the incisor and canine area, the stress at the first premolar was highly and negatively correlated with the palatal stiffness components of the premolar area. These results indicate that an inverse relationship exists between stress and stiffness: the less stiff the cortical bone, the higher the stress at the PDL. This finding is in line with the equation between stiffness, stress and displacement: the higher the stiffness, the lower the stress and displacement, and vice versa (table 5.1). The association with the palatal components may

be explained by the contact of the palatal root of the premolar with the palatal cortical bone at the premolar area (Fig 5.9).

**Table 5.1: Cortical bone impact on PDL stress and crown displacement based on the correlations results**

Cortical bone stiffness	PDL stress	Crown displacement
↑	↓	↓
↓	↑	↑

At the canine, the smaller bucco-lingual and mesio-distal widths of the crown and the presence of only one thin and tapered root helped steer its movement in the trabecular bone with minimal contact with the cortical bone (Ammoury et al., 2019). This fact would explain the absence of any correlation of the PDL stress with the cortical bone (Fig 5.7).

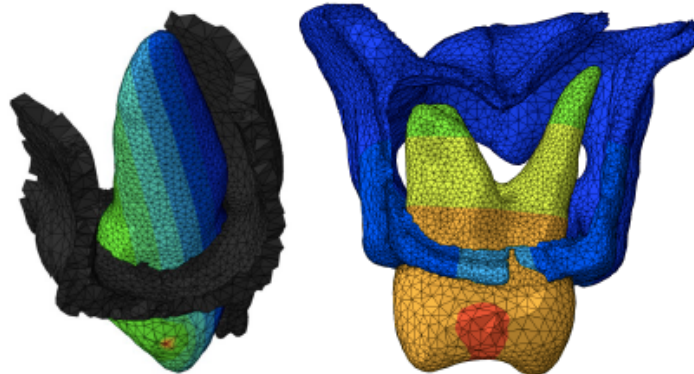


**Fig. 5.7:** Anatomical differences between the canine and the premolar possibly explaining the absence of significant correlation between stress and cortical stiffness. This illustration relates to the distalization of posterior teeth by pulling on the canine from a posteriorly located miniscrew (from Ammoury et al., 2019)

A secondary buccal displacement was observed with the decortication model, likely the result of reduced buccal bone resistance. A similar outcome was described by Verna et al. (2018) who developed a model of a lower incisor on FEA, and simulated corticotomy by modifying bone density, during three types of movements: tipping, uncontrolled tipping,

and translation. Upon analyzing the amount and type of movement, as well as the stress and strain on PDL in both corticotomized and non-corticotomized simulations, the findings were the following:

- The amount of tooth movement obtained in case of lower bone density is higher in all types of movement simulation, especially for the uncontrolled tipping (Fig. 5.8).
- The center of rotation of the movement shifts more apically in case of translation, controlled and uncontrolled tipping. Ouejaraphant et al. (2018) also reported that the center of resistance was apically repositioned in the FEA of decorticated bone.
- Reduced bone density influences not only amount of tooth movement, but also its type.

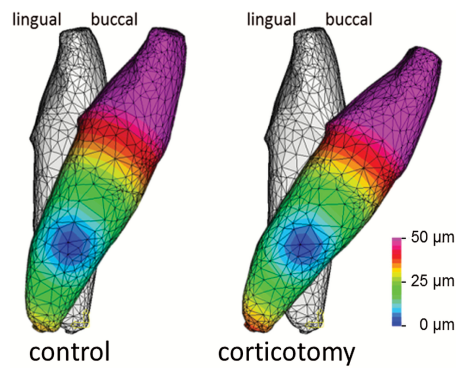


**Fig. 5.8:** The total displacement of the lateral incisor in case of an uncontrolled tipping for both the control and corticotomized models (Verna et al., 2018).

Regarding the stress on the trabecular bone distal to the canine, high and negative correlations were found with the buccal stiffness components of the incisor and canine cortical bone areas (S1Binc, S2Binc and S3Binc), increasing from the control modality to 6MOP modality. This finding suggests that the stiffer the cortical bone, the lower the stress on the underlying trabecular bone, and vice versa (Table 5.2).

In this perspective, Ammoury et al. (2019) discussed a possible theory that may account for the way stiffness may have affected the stress. By definition, a composite material is comprised of two or more constituent materials with significantly different physical or chemical properties that, when combined, produce a material with characteristics different from the individual components.

On the basis of this theory, the maxilla consists of a composite material with a high stiffness component on the outer surface and softer components in the deeper zones (trabecular bone then PDL). If one of the maxillary components is removed or if its physical or chemical properties are altered (in this instance the cortical bone), then the stiffness of the whole composite material will differ. Since stresses analyzed at one component of the of the composite material (PDL or trabecular bone) are related to the stiffness of the composite material, we would expect different PDL and trabecular bone stresses when cortical bone stiffness is changed:

$$\text{Stress } (\sigma) = \text{stiffness } (E) \times \text{strain } (\epsilon).$$

On the contrary, high and positive correlations existed between the stress on the trabecular bone and the buccal thickness component of the incisor and canine cortical bone area (TBinc) indicating that the thicker the cortical bone, the higher the stress on the underlying trabecular bone (Table 5.2). The absence of significant correlations between the stress on the trabecular bone and the stiffness and thickness components of the cortical bone in the decortication model is reflected by the high stress value obtained following the complete removal of cortical bone, transferring the stress to the trabecular bone which is no longer affected by the cortical bone properties (*refer to section 5.3.2*).



**Table 5.2: Cortical bone impact on trabecular bone stress based on the correlations results**

Cortical bone properties	Trabecular bone stress
Stiffness	-
Thickness	+

In previous studies, it was reported that the change in the mechanical status of the cortical bone is a stimulating factor that accelerates the remodeling of the trabecular bone leading to rapid canine movement (Melsen, 2001; Kawarizadeh et al., 2004). The radiological evaluation of bone density in humans has disclosed a decrease between 41 and 55 per cent of the baseline bone density after corticotomy (Baloul et al., 2011; Shoreibah et al., 2012). Decreasing bone density modifies its mechanical properties (Keller et al., 1990).

#### *5.2.5. Correlation between stress, displacement and volume of cortical bone removed*

Strong and positive correlations were found between the volume of cortical bone removed in each microperforation modality and the resultant stress at each PDL surface of the teeth and the trabecular bone and the initial displacement on stiffness and thickness variations. These outcomes indicated that the greater the volume of bone removed with the addition of perforations, the higher the stresses and displacements.

When the values of the decortication model were added to the equation, correlations between the volume and the stress and displacement of teeth were reduced significantly. The volume of bone removed with the decortication was not proportional to the increase in the stress and displacement values, as might have been expected.

To further investigate the results and to allow for a better comparison and performance evaluation between corticotomy modalities, we applied data normalization,

dividing the average stress and displacement values by the volume of cortical bone to obtain ratios that would be more comparable across the modalities. The analysis of the ratios disclosed a decrease from 3MOP with each additional perforation, and the lowest value obtained with the decortication, more significantly for the stress on teeth than on the trabecular bone. The pattern was similar for the stress and displacement graphs under both the stiffness and thickness variations, with higher ratios for the stiffness (*refer to Fig. 4.8*).

In brief, more stress and displacement were achieved proportional to the volume of bone removed with six perforations than with decortication. This finding may be explained by the dissipation of stress and initial buccal displacement with decortication. Decortication was initially introduced to affect buccal movement, as properly shown in this investigation.

### **5.3. Clinical implications**

We simulated the modified decortication technique described by the Wilcko brothers, and microperforations as performed by the Propel device (Propel®, Ossining, New York 10562, US). The aim was to explore how many microperforations are needed to equal the effect of decortication, still considered more effective than the current use of only 3 microperforations (Alkebsi et al., 2018; Sivarajan et al., 2019; Alqadasi et al. 2019). The clinical recommendations that may be implied from this research are the following:

- Although decortication lead to the greatest initial displacement, the increase in stress and displacement as an initial response is not notable relative to the amount of bone removed, in addition to the excessive stress produced on the trabecular bone. This technique is aggressive in clinical practice because it requires the elevation of mucoperiosteal flaps and

generates post-surgical discomfort. Accordingly, patients are reluctant to accept it.

However, the concomitant bone graft that aims to compensate for any corticotomy-related reduction in bone volume represents an added value because of its potential increase in post-treatment alveolar bone width, possibly enhancing long-term stability.

- The flapless microperforation technique is a viable and less invasive alternative to decortication for canine distalization depending on the number of perforations, with greater patient acceptance. An effective acceleration of maxillary canine distalization requires more than the currently advocated three microperforations. Increasing the number of perforations to six, over an equivalent distance to the decortication height, yielded an initial acceleration in tooth movement and PDL stress that were quite similar to decortication with less stress on the trabecular bone.

- Almost the same effect was obtained on the distal surface stress and initial canine displacement with 6MOP and decortication (25% increase). The difference lies in the effect on the buccal surface. These results indicate that 6MOP and decortication might have the same effect on distal movement (e.g. distalization, retraction), but differ in buccal movement (correction of crowding).

- When the distance between the corticotomy cut and the tooth increased, the effect of the corticotomy decreased gradually. Therefore, the position of the corticotomy is an important factor to consider when performing the surgical cut in order to maximize the effect on tooth movement.

- High and inverted correlations between the first premolar and the palatal stiffness of the cortical bone indicates that stress increases when stiffness decreases and vice versa. This finding, along with the high stress value registered on this surface of the PDL suggest that the cortical bone could offer resistance to initial movement of the premolar due to a possible contact of the palatal root with the palatal cortex. Consequently, it is advisable to detect this anatomical relation prior to treatment through a clinical and radiographic assessment to help steer movement in the trabecular bone with minimal contact with the cortical bone. Accordingly, heavy rectangular wires should prevent rotations and maintain the tooth in the middle of the alveolus.

- Since the initial displacement is higher in the corticotomy models where the bone density was decreased, presumably affecting both the amount and type of movement, and considering that the center of rotation of the movement in a decorticated bone shifts more apically, this suggests that the moment-to-force ratios used in conventional orthodontics should be modified when corticotomies are contemplated, perhaps with the use of a power arm or a retraction hook at the canine level to bring the point of force application closer to the center of resistance, in order to obtain a translational movement.

- The stress on the trabecular bone underlying the corticotomy showed a negative correlation with the buccal cortical bone stiffness, a positive correlation with the thickness in the microperforation modalities, and no correlation in the decortication modality. These results suggest that the stiffer and thinner the cortical bone, the lower the stress on the

underlying trabecular bone, and vice versa. The buccal cortical bone usually has a thinner but stiffer cortex (Peterson et al. 2006). Ideally, these conditions should be part of treatment planning when considering corticotomy, especially microperforations, including the definition of cortical bone thickness, stiffness, height and the width of the trabecular bone through CBCT/3D scans (if indicated).

#### **5.4. Limitations**

The main advantage of FEM (finite element method) is that it can be magnified nearly infinitely, in terms of both the actual volumetric construction itself and the mathematical variability of its material parameters. However, as with any theoretical model of a biological system, the method has limitations. The FE simulation is limited by its theoretical nature; actual teeth are surrounded by human bone, with a specific resorption-apposition pattern that is difficult to simulate in a FE model.

In addition, FEA provides a “snap-shot” view of the initial conditions (e.g. stresses, displacement) within the model and does not depict the changes that occur over time, such as bone remodeling. These initial results represent tooth movement into the PDL space before the cycle of bone resorption/apposition occurs. Subsequent clinical results may differ from the initial ones. The simulation in FEM study is based on mechanical laws, which may not be sufficient for predicting orthodontic tooth movement in clinical setups.

Ideally, time dependent (continuous/dynamic) finite element modeling for tooth movement should be implemented to reach the timepoint when FEA becomes an integral part of planning orthodontic mechanotherapy. Although such model was introduced since 1996 (Middleton et al.), accurate mathematical simulation of the biological process of tooth

movement (including the PDL and bony reactions) over time has not been possible with FEA to date (Ammar et al., 2011). Significant resources should be invested in this necessary field of research.

One aspect of this process was initiated by Cheng et al (2014) by constructing a FE model from one patient and incorporated the average rate of canine retraction into a premolar extraction space that was generated clinically from a study on 15 patients. However, their approach falls short of direct clinical interpretation, although the method offers a component of research methodology that may be used in more encompassing research, along with the inclusion of individual variation such as we proceeded.

Because of the deviations between the finite element models and the actual geometric and mechanical conditions, and owing to material property and boundary conditions, the results of this study should be interpreted within the constraints of the model setup.

## **5.5. Future research**

Despite these limitations, we integrated a finite element approach with human individual variation to investigate the comparative influences of resistance source, the pathway of canine movement, and different types of corticotomies for rapid canine distalization by reducing mechanical resistance. Future research should focus on:

- Study of factors that can influence the effect of the corticotomy: variation in the position, width and number of decortications, variation in the configuration of microperforations.
- Comparison of other corticotomy techniques such as piezocision, buccal and palatal decortication, combination of decortications and microperforations.

- Comparison of corticotomy with and without the bone grafting surgery.
- Simulation of other clinical orthodontic applications of corticotomy: mandibular anterior alignment, anterior and posterior intrusion, molar protraction, canine retraction in premolar extraction spaces.
- Because the effect of the corticotomy was proven to be temporary, simulation of repeated corticotomies at different time intervals, through the addition of time-dependent feature, would be of important clinical benefit.
- Simulation of soft tissues to study the effect of the gingival biotype.
- In the initial tooth movement, cortical bone thickness was not shown to be a factor affecting the PDL stresses because of the interposition of a layer of trabecular bone separating the PDL and the tooth from the cortical bone. However, a time-dependent FEA study should help disclose the importance of this thickness when the tooth displaces closer to the cortex.
- Because bone related anatomical factors can be evaluated using 3D radiographic imaging, future research should also focus on establishing a severity index of “cortical bone resistance”.
- FEA studies that link stress values to clinical measures (pain, hyalinization, root resorption) would contribute remarkably to the orthodontic knowledge by answering questions that experimental studies cannot answer because of ethical or logistical limitations.

Furthermore, the reason for not extracting a premolar in our model is to evaluate initial displacement in an unaltered bony environment, because following extractions, the crest remodels with possible alteration of material properties of the different elements.

Premolar extraction models would be needed with corresponding CT or CBCT scans. The removal of the premolar within the existing model does not properly simulate this change.

In order to develop biomechanical processes to simulate the orthodontic tooth movements and adjunctive procedures for acceleration of tooth movement, further clinical investigations such as RCTs, animal experiments and biomechanical researches should be performed to understand the coupling of the mechanical findings with the biological processes.



## CHAPTER 6

### CONCLUSION

Optimal tooth movement requires the application of biomechanically sound orthodontic forces and an alveolar bone that offers less resistance to tooth movement (Ren et al., 2007). For a successful orthodontic treatment, the goals must be set during the planning stage to complete the treatment in a relatively short duration without compromising the quality and stability of the results and also preserving the dentoalveolar structures. Generally, during orthodontic tooth movement, the cortical bone offers the maximum resistance to resorption and could hinder tooth movement (Sebaoun et al., 2008). This background explains the principle of surgical corticotomy which is the intentional cutting of cortical bone leaving intact trabecular bone.

This FEA study was among the first to contribute findings on 2 different modalities of corticotomy on the basis of real variation among human subjects. The major conclusions are:

1. By removing a continuous shear band of cortical bone with decortication, resistance to tooth movement is decreased thereby facilitating initial displacement.
2. Six microperforations could be as efficient as decortication when extended over the same distance.
3. By introducing individual variation in cortical bone properties, we were able to determine the effect of stiffness and thickness on stress generation, demonstrating that the

response of the dentoalveolar structures depends not only on force magnitude and vectors, but also on individual anatomy.

4. Stiffness significantly affected the stress on the first premolar with its palatal components. Moving teeth away from the stiff outer cortex might improve tooth displacement.
5. Thickness of the cortical bone seemingly did not carry as much weight as stiffness on the initial response of the teeth.
6. Stress on the trabecular bone is affected by the stiffness and thickness of the buccal cortical bone, increasing with a less stiff and thick bone. Following the corticotomy, stress is transferred to the trabecular bone.
7. These findings relate to the initial movement within the PDL. Further research should include other clinical setups and time dependent FEA modeling.

Besides these positional and anatomical factors, researchers must consider the potential influence of the occlusion, musculature, metabolism and other biologic factors. The choice of the corticotomy technique depends on the indication, as well as the patient and practitioner preferences. Nevertheless, before decortication and microperforations are included as routine practice, more RCTs are required to confirm the rate of acceleration, risk-benefit ratio, long-term follow-up, and relapse after these procedures.

Accordingly, long term orthodontic tooth movement cannot be accurately simulated only mathematically and a single formulation for all types of movements and in all patients may not provide the ultimate formula for total mechanotherapy planning. Yet, the ability for FEA in conjunction with clinical data input in the analysis should help in the

determination of “movement-specific” and “patient-specific” outcome planning and prediction.

Finally, in clinical orthodontic treatments, the individual geometry/morphology, material properties and load conditions in FE analyses should be considered. This would contribute to the development of numerical models of the orthodontic tooth movement and might lead to the possibility of individual strategies in clinical orthodontic therapy and shorten the therapy periods thus improving the effectiveness and reliability of orthodontic therapy.

## BIBLIOGRAPHY

- Abbas, N. H., Sabet, N. E., & Hassan, I. T. (2016). Evaluation of corticotomy-facilitated orthodontics and piezocision in rapid canine retraction. *American Journal of Orthodontics and Dentofacial Orthopedics*, 149(4), 473-480.
- Aboalnaga, A. A., Fayed, M. M. S., El-Ashmawi, N. A., & Soliman, S. A. (2019). Effect of micro-osteoperforation on the rate of canine retraction: a split-mouth randomized controlled trial. *Progress in orthodontics*, 20(1), 21.
- Aboul, S. M. B. E. D., El-Beialy, A. R., El-Sayed, K. M. F., Selim, E. M. N., El-mangoury, N. H., & Mostafa, Y. A. (2011). Miniscrew implant-supported maxillary canine retraction with and without corticotomy-facilitated orthodontics. *American Journal of Orthodontics and Dentofacial Orthopedics*, 139(2), 252-259.
- Ahuja, S., Gupta, S., Bhambri, E., Jaura, B., & Ahuja, V. (2019). Comparative Evaluation of Effects of Different Corticotomy Designs on Velocity of Upper Canine Retraction: A Finite Element Study. *Journal of Indian Orthodontic Society*, 53(4), 278-282.
- Ajmera, D. H., Singh, P., Wang, C., Song, J., Xiao, S. S., & Fan, Y. (2017). Analysis of dentoalveolar structures with novel corticotomy-facilitated mandibular expansion: A 3-dimensional finite element study. *American Journal of Orthodontics and Dentofacial Orthopedics*, 151(4), 767-778.
- Akay, M. C., Aras, A., Günbay, T., Akyalçın, S., & Koyuncue, B. Ö. (2009). Enhanced effect of combined treatment with corticotomy and skeletal anchorage in open bite correction. *Journal of Oral and Maxillofacial Surgery*, 67(3), 563-569.
- Aksakalli, S., Calik, B., Kara, B., & Ezirganli, S. (2015). Accelerated tooth movement with piezocision and its periodontal-transversal effects in patients with Class II malocclusion. *The Angle Orthodontist*, 86(1), 59-65
- Alansari, S., Sangsuwon, C., Vongthongleur, T., Kwal, R., chneh Teo, M., Lee, Y. B., ... & Alikhani, M. (2015, September). Biological principles behind accelerated tooth movement. In *Seminars in Orthodontics* (Vol. 21, No. 3, pp. 151-161). WB Saunders.
- Alfawal, A. M., Hajeer, M. Y., Ajaj, M. A., Hamadah, O., & Brad, B. (2018). Evaluation of piezocision and laser-assisted flapless corticotomy in the acceleration of canine retraction: a randomized controlled trial. *Head & face medicine*, 14(1), 4.
- Aljabaa, A., Almoammar, K., Aldrees, A., & Huang, G. (2018). Effects of vibrational devices on orthodontic tooth movement: A systematic review. *American Journal of Orthodontics and Dentofacial Orthopedics*, 154(6), 768-779.
- Alkebsi, A., Al-Maaitah, E., Al-Shorman, H., & Alhaija, E. A. (2018). Three-dimensional assessment of the effect of micro-osteoperforations on the rate of tooth movement during canine retraction in adults with Class II malocclusion: a randomized controlled clinical trial. *American Journal of Orthodontics and Dentofacial Orthopedics*, 153(6), 771-785.
- Alqadasi, B., Aldhorae, K., Halboub, E., Mahgoub, N., Alnasri, A., Assiry, A., & Xia, H. Y. (2019). The effectiveness of micro-osteoperforations during canine retraction: A

- three-dimensional randomized clinical trial. *Journal of International Society of Preventive and Community Dentistry*, 9(6), 637.
- Ammar, H. H., Ngan, P., Crout, R. J., Mucino, V. H., & Mukdadi, O. M. (2011). Three-dimensional modeling and finite element analysis in treatment planning for orthodontic tooth movement. *American Journal of Orthodontics and Dentofacial Orthopedics*, 139(1), e59-e71.
  - Ammoury, M. J., Mustapha, S., Dechow, P. C., & Ghafari, J. G. (2019). Two distalization methods compared in a novel patient-specific finite element analysis. *American Journal of Orthodontics and Dentofacial Orthopedics*, 156(3), 326-336.
  - Andrade Jr, I., Taddei, S. R., & Souza, P. E. (2012, December). Inflammation and tooth movement: the role of cytokines, chemokines, and growth factors. In *Seminars in Orthodontics* (Vol. 18, No. 4, pp. 257-269). WB Saunders.
  - Andrei, M., Dinischiotu, A., Didilescu, A. C., Ionita, D., & Demetrescu, I. (2018). Periodontal materials and cell biology for guided tissue and bone regeneration. *Annals of Anatomy-Anatomischer Anzeiger*, 216, 164-169.
  - Attri, S., Mittal, R., Batra, P., Sonar, S., Sharma, K., Raghavan, S., & Rai, K. S. (2018). Comparison of rate of tooth movement and pain perception during accelerated tooth movement associated with conventional fixed appliances with micro-osteoperforations—a randomized controlled trial. *Journal of orthodontics*, 45(4), 225-233.
  - Baloul, S. S., Gerstenfeld, L. C., Morgan, E. F., Carvalho, R. S., Van Dyke, T. E., & Kantarci, A. (2011). Mechanism of action and morphologic changes in the alveolar bone in response to selective alveolar decortication—facilitated tooth movement. *American Journal of Orthodontics and Dentofacial Orthopedics*, 139(4), S83-S101.
  - Bansal, M., Sharma, R., Kumar, D., & Gupta, A. (2019). Effects of mini-implant facilitated micro-osteoperforations in alleviating mandibular anterior crowding: A randomized controlled clinical trial. *Journal of orthodontic science*, 8.
  - Bartzela, T., Türp, J. C., Motschall, E., & Maltha, J. C. (2009). Medication effects on the rate of orthodontic tooth movement: a systematic literature review. *American Journal of Orthodontics and Dentofacial Orthopedics*, 135(1), 16-26.
  - Bishara, S. E., & Ostby, A. W. (2008, September). White spot lesions: formation, prevention, and treatment. In *Seminars in Orthodontics* (Vol. 14, No. 3, pp. 174-182). WB Saunders.
  - Blasi, I., & Pavlin, D. (2017). Minimally and noninvasive approaches to accelerate tooth movement. *Orthodontics: Current Principles and Techniques*.
  - Bogoch, E., Gschwend, N., Rahn, B., Moran, E., & Perren, S. (1993). Healing of cancellous bone osteotomy in rabbits—Part I: Regulation of bone volume and the regional acceleratory phenomenon in normal bone. *Journal of orthopaedic research*, 11(2), 285-291.
  - Bowers, G. M. (1963). A study of the width of attached gingiva. *Journal of Periodontology*, 34(3), 201-209.
  - Burstone, C. J. (1962). The biomechanics of tooth movement. *Vistas in orthodontics*, 197-213.

- Buschang, P. H., Campbell, P. M., & Ruso, S. (2012, December). Accelerating tooth movement with corticotomies: is it possible and desirable? In *Seminars in Orthodontics* (Vol. 18, No. 4, pp. 286-294). WB Saunders.
- Busse, J. W., Kaur, J., Mollon, B., Bhandari, M., Tornetta, P., Schünemann, H. J., & Guyatt, G. H. (2009). Low intensity pulsed ultrasonography for fractures: systematic review of randomized controlled trials. *Bmj*, 338, b351.
- Çağlaroğlu, M., & Erdem, A. (2012). Histopathologic investigation of the effects of prostaglandin E2 administered by different methods on tooth movement and bone metabolism. *The Korean Journal of Orthodontics*, 42(3), 118-128.
- Cai, Y., Yang, X., He, B., & Yao, J. (2015). Finite element method analysis of the periodontal ligament in mandibular canine movement with transparent tooth correction treatment. *BMC Oral Health*, 15(1), 106.
- Cattaneo, P. M., Dalstra, M., & Melsen, B. (2005). The finite element method: a tool to study orthodontic tooth movement. *Journal of dental research*, 84(5), 428-433.
- Cattaneo, P. M., Dalstra, M., & Melsen, B. (2009). Strains in periodontal ligament and alveolar bone associated with orthodontic tooth movement analyzed by finite element. *Orthodontics & craniofacial research*, 12(2), 120-128.
- Chandran, M., Muddaiah, S., Nair, S., Shetty, B., Somaiah, S., Reddy, G., & Abraham, B. (2018). Clinical and molecular-level comparison between conventional and corticotomy-assisted canine retraction techniques. *Journal of the World Federation of Orthodontists*, 7(4), 128-133.
- Chang, J., Chen, P. J., Dutra, E. H., Nanda, R., & Yadav, S. (2019). The effect of the extent of surgical insult on orthodontic tooth movement. *European journal of orthodontics*.
- Charavet, C., Lecloux, G., Bruwier, A., Rompen, E., Maes, N., Limme, M., & Lambert, F. (2016). Localized piezoelectric alveolar decortication for orthodontic treatment in adults: a randomized controlled trial. *Journal of dental research*, 95(9), 1003-1009.
- Cheng, S.-J., Tseng, I.-Y., Lee, J.-J., & Kok, S.-H. (2004). A prospective study of the risk factors associated with failure of mini-implants used for orthodontic anchorage. *International Journal of Oral & Maxillofacial Implants*, 19(1).
- Cheung, T., Park, J., Lee, D., Kim, C., Olson, J., Javadi, S., ... & Hong, C. (2016). Ability of mini-implant-facilitated micro-osteoperforations to accelerate tooth movement in rats. *American Journal of Orthodontics and Dentofacial Orthopedics*, 150(6), 958-967.
- Cho, K. W., Cho, S. W., Oh, C. O., Ryu, Y. K., Ohshima, H., & Jung, H. S. (2007). The effect of cortical activation on orthodontic tooth movement. *Oral diseases*, 13(3), 314-319.
- Chugh, T., Ganeshkar, S. V., Revankar, A. V., & Jain, A. K. (2013). Quantitative assessment of interradicular bone density in the maxilla and mandible: implications in clinical orthodontics. *Prog Orthod*, 14(1), 1.
- Chung, K. R., Kim, S. H., & Lee, B. S. (2009). Speedy surgical-orthodontic treatment with temporary anchorage devices as an alternative to orthognathic surgery. *American Journal of Orthodontics and Dentofacial Orthopedics*, 135(6), 787-798.

- Çifter, M., & Saraç, M. (2011). Maxillary posterior intrusion mechanics with mini-implant anchorage evaluated with the finite element method. *American Journal of Orthodontics and Dentofacial Orthopedics*, 140(5), e233-e241.
- Cobo, J., Sicilia, A., Argüelles, J., Suárez, D., & Vijande, M. (1993). Initial stress induced in periodontal tissue with diverse degrees of bone loss by an orthodontic force: tridimensional analysis by means of the finite element method. *American Journal of Orthodontics and Dentofacial Orthopedics*, 104(5), 448-454.
- Cohen, G., Campbell, P. M., Rossouw, P. E., & Buschang, P. H. (2010). Effects of increased surgical trauma on rates of tooth movement and apical root resorption in foxhound dogs. *Orthodontics & craniofacial research*, 13(3), 179-190.
- Comba, B., Parrini, S. I. M. O. N. E., Rossini, G. A. B. R. I. E. L. E., Castroflorio, T., & Deregibus, A. (2017). A three-dimensional finite element analysis of upper-canine distalization with clear aligners, composite attachments, and class II elastics. *J Clin Orthod*, 51(1), 24-8.
- Cowin, S. C., & Hart, R. T. (1990). Errors in the orientation of the principal stress axes if bone tissue is modeled as isotropic. *Journal of Biomechanics*, 23(4), 349-352.
- Cramer, C. L., Campbell, P. M., Opperman, L. A., Tadlock, L. P., & Buschang, P. H. (2019). Effects of micro-osteoperforations on tooth movement and bone in the beagle maxilla. *American Journal of Orthodontics and Dentofacial Orthopedics*, 155(5), 681-692.
- da Silva Sousa, M. V., Scanavini, M. A., Sannomiya, E. K., Velasco, L. G., & Angelieri, F. (2011). Influence of low-level laser on the speed of orthodontic movement. *Photomedicine and Laser surgery*, 29(3), 191-196.
- Dalstra, M., Cattaneo, P. M., & Beckmann, F. (2006). Synchrotron radiation-based microtomography of alveolar support tissues. *Orthodontics & craniofacial research*, 9(4), 199-205.
- Darendeliler, M. A., Zea, A., Shen, G., & Zoellner, H. (2007). Effects of pulsed electromagnetic field vibration on tooth movement induced by magnetic and mechanical forces: a preliminary study. *Australian dental journal*, 52(4), 282-287.
- Davidovitch, Z., Finkelson, M. D., Steigman, S., Shanfeld, J. L., Montgomery, P. C., & Korostoff, E. (1980). Electric currents, bone remodeling, and orthodontic tooth movement: II. Increase in rate of tooth movement and periodontal cyclic nucleotide levels by combined force and electric current. *American journal of orthodontics*, 77(1), 33-47.
- Deguchi, T., Nasu, M., Murakami, K., Yabuuchi, T., Kamioka, H., & Takano-Yamamoto, T. (2006). Quantitative evaluation of cortical bone thickness with computed tomographic scanning for orthodontic implants. *American Journal of Orthodontics and Dentofacial Orthopedics*, 129(6), 721. e727-721. e712.
- Dibart, S., Keser, E., & Nelson, D. (2015, September). Piezocision™-assisted orthodontics: Past, present, and future. In *Seminars in Orthodontics* (Vol. 21, No. 3, pp. 170-175). WB Saunders.
- Dibart, S., Surmenian, J., David Sebaoun, J., & Montesani, L. (2010). Rapid treatment of Class II malocclusion with piezocision: two case reports. *The International journal of periodontics & restorative dentistry*, 30(5), 487.

- Domínguez, A., Gómez, C., & Palma, J. C. (2015). Effects of low-level laser therapy on orthodontics: rate of tooth movement, pain, and release of RANKL and OPG in GCF. *Lasers in medical science*, 30(2), 915-923.
- Doshi-Mehta, G., & Bhad-Patil, W. A. (2012). Efficacy of low-intensity laser therapy in reducing treatment time and orthodontic pain: a clinical investigation. *American Journal of Orthodontics and Dentofacial Orthopedics*, 141(3), 289-297.
- Düker, J. (1975). Experimental animal research into segmental alveolar movement after corticotomy. *Journal of maxillofacial surgery*, 3, 81-84.
- Egermann, M., Goldhahn, J., & Schneider, E. (2005). Animal models for fracture treatment in osteoporosis. *Osteoporosis international*, 16(2), S129-S138.
- El-Angbawi, A., McIntyre, G. T., Fleming, P. S., & Bearn, D. R. (2015). Non-surgical adjunctive interventions for accelerating tooth movement in patients undergoing fixed orthodontic treatment. *Cochrane Database of Systematic Reviews*, (11).
- Ferguson, D. J., Wilcko, M. T., Wilcko, W. M., & Makki, L. (2015, September). Scope of treatment with periodontally accelerated osteogenic orthodontics therapy. In *Seminars in Orthodontics* (Vol. 21, No. 3, pp. 176-186). WB Saunders.
- Field, C., Ichim, I., Swain, M. V., Chan, E., Darendeliler, M. A., Li, W., & Li, Q. (2009). Mechanical responses to orthodontic loading: a 3-dimensional finite element multi-tooth model. *American Journal of Orthodontics and Dentofacial Orthopedics*, 135(2), 174-181.
- Fill, T. S., Toogood, R. W., Major, P. W., & Carey, J. P. (2012). Analytically determined mechanical properties of, and models for the periodontal ligament: critical review of literature. *Journal of Biomechanics*, 45(1), 9-16.
- Fischer, T. J. (2007). Orthodontic treatment acceleration with corticotomy-assisted exposure of palatally impacted canines: a preliminary study. *The Angle Orthodontist*, 77(3), 417-420.
- Fleming, P. S., Fedorowicz, Z., Johal, A., El-Angbawi, A., & Pandis, N. (2015). Surgical adjunctive procedures for accelerating orthodontic treatment. *Cochrane database of systematic reviews*, (6).
- Frost, H. M. (1983). The regional acceleratory phenomenon: a review. *Henry Ford Hospital Medical Journal*, 31(1), 3.
- Frost, H. M. (1989). *The Biology of Fracture Healing: An Overview for Clinicians. Part II. Clinical orthopaedics and related research*, 248, 294-309.
- Fu, T., Liu, S., Zhao, H., Cao, M., & Zhang, R. (2019). Effectiveness and Safety of Minimally Invasive Orthodontic Tooth Movement Acceleration: A Systematic Review and Meta-analysis. *Journal of dental research*, 0022034519878412.
- Fujita, S., M. Yamaguchi, T. Utsunomiya, H. Yamamoto, and K. Kasai. "Low-energy laser stimulates tooth movement velocity via expression of RANK and RANKL." *Orthodontics & craniofacial research* 11, no. 3 (2008): 143-155.
- Gačnik, F., Ren, Z., & Hren, N. I. (2014). Modified bone density-dependent orthotropic material model of human mandibular bone. *Medical engineering & physics*, 36(12), 1684-1692.
- Gantes, B., Rathbun, E., & Anholm, M. (1990). Effects on the periodontium following corticotomy-facilitated orthodontics. Case reports. *Journal of periodontology*, 61(4), 234-238.



- Ghafari, J. G. (2015). Centennial inventory: the changing face of orthodontics. *American Journal of Orthodontics and Dentofacial Orthopedics*, 148(5), 732-739.
- Gil, A. P. S., Haas Jr, O. L., Méndez-Manjón, I., Masiá-Gridilla, J., Valls-Ontañón, A., Hernández-Alfaro, F., & Guijarro-Martínez, R. (2018). Alveolar corticotomies for accelerated orthodontics: A systematic review. *Journal of Cranio-Maxillofacial Surgery*, 46(3), 438-445.
- Gkantidis, N., Mistakidis, I., Kouskoura, T., & Pandis, N. (2014). Effectiveness of non-conventional methods for accelerated orthodontic tooth movement: a systematic review and meta-analysis. *Journal of dentistry*, 42(10), 1300-1319.
- Gomez, J. P., Peña, F. M., Martínez, V., Giraldo, D. C., & Cardona, C. I. (2014). Initial force systems during bodily tooth movement with plastic aligners and composite attachments: A three-dimensional finite element analysis. *Angle Orthod*, 85(3), 454-460.
- Gonzales, C., Hotokezaka, H., Yoshimatsu, M., Yozgatian, J. H., Darendeliler, M. A., & Yoshida, N. (2008). Force magnitude and duration effects on amount of tooth movement and root resorption in the rat molar. *The Angle Orthodontist*, 78(3), 502-509.
- Graber Lee, W. (2016). *Orthodontics: Current Principles and Techniques/Lee W. Graber, Robert L. Vanarsdall, Katherine WL Vig. –6th Edition. –St. Luis: Mosby.*
- Gupta, S., Ahuja, S., Bhambri, E., Jaura, B. S., & Ahuja, V. (2019). Three-dimensional finite element analysis to evaluate biomechanical effects of different alveolar decortication approaches on rate of canine retraction. *International orthodontics*, 17(2), 216-226.
- Hajji, S. S. (2000). *The influence of accelerated osteogenic response on mandibular de-crowding (Doctoral dissertation, Saint Louis University).*
- Han, U. A., Kim, Y., & Park, J. U. (2009). Three-dimensional finite element analysis of stress distribution and displacement of the maxilla following surgically assisted rapid maxillary expansion. *Journal of Cranio-Maxillofacial Surgery*, 37(3), 145-154.
- Henneman, S., Von den Hoff, J. W., & Maltha, J. C. (2008). Mechanobiology of tooth movement. *The European Journal of Orthodontics*, 30(3), 299-306.
- Hohmann, A., Kober, C., Young, P., Dorow, C., Geiger, M., Boryor, A., . . . Sander, F. G. (2011). Influence of different modeling strategies for the periodontal ligament on finite element simulation results. *American Journal of Orthodontics and Dentofacial Orthopedics*, 139(6), 775-783.
- Holberg, C., Winterhalder, P., Holberg, N., Wichelhaus, A., & Rudzki-Janson, I. (2014). Indirect miniscrew anchorage: biomechanical loading of the dental anchorage during mandibular molar protraction—an FEM analysis. *Journal of Orofacial Orthopedics/Fortschritte der Kieferorthopädie*, 75(1), 16-24.
- Hoogeveen, E. J., Jansma, J., & Ren, Y. (2014). Surgically facilitated orthodontic treatment: a systematic review. *American Journal of Orthodontics and Dentofacial Orthopedics*, 145(4), S51-S64.
- Huang, H., Williams, R. C., & Kyrkanides, S. (2014). Accelerated orthodontic tooth movement: molecular mechanisms. *American Journal of Orthodontics and Dentofacial Orthopedics*, 146(5), 620-632.

- Iglesias-Linares, A., Moreno-Fernandez, A. M., Yañez-Vico, R., Mendoza-Mendoza, A., Gonzalez-Moles, M., & Solano-Reina, E. (2011). The use of gene therapy vs. corticotomy surgery in accelerating orthodontic tooth movement. *Orthodontics & craniofacial research*, 14(3), 138-148.
- Iino, S., Sakoda, S., Ito, G., Nishimori, T., Ikeda, T., & Miyawaki, S. (2007). Acceleration of orthodontic tooth movement by alveolar corticotomy in the dog. *American Journal of Orthodontics and Dentofacial Orthopedics*, 131(4), 448-e1.
- İşeri, H., Kişnişci, R., Bzizi, N., & Tüz, H. (2005). Rapid canine retraction and orthodontic treatment with dentoalveolar distraction osteogenesis. *American journal of orthodontics and dentofacial orthopedics*, 127(5), 533-541.
- Iwasaki, L. R., Haack, J. E., Nickel, J. C., & Morton, J. (2000). Human tooth movement in response to continuous stress of low magnitude. *American Journal of Orthodontics and Dentofacial Orthopedics*, 117(2), 175-183.
- Jean-David, M. S., SURMENIAN, J., & DIBART, S. (2011). Accelerated orthodontic treatments with Piezocision: a mini-invasive alternative to alveolar corticotomies. *Orthod Fr*, 82, 311-319.
- Jing, D., Xiao, J., Li, X., Li, Y., & Zhao, Z. (2017). The effectiveness of vibrational stimulus to accelerate orthodontic tooth movement: a systematic review. *BMC oral health*, 17(1), 143.
- Jones, M. L., Hickman, J., Middleton, J., Knox, J., & Volp, C. (2001). A validated finite element method study of orthodontic tooth movement in the human subject. *Journal of Orthodontics*, 28(1), 29-38.
- Kale, S., Kocadereli, I., Atilla, P., & Aşan, E. (2004). Comparison of the effects of 1, 25 dihydroxycholecalciferol and prostaglandin E2 on orthodontic tooth movement. *American journal of orthodontics and dentofacial orthopedics*, 125(5), 607-614.
- Kamble, R. H., Lohkare, S., Hararey, P. V., & Mundada, R. D. (2012). Stress distribution pattern in a root of maxillary central incisor having various root morphologies: a finite element study. *Angle Orthod*, 82(5), 799-805.
- Kang, J.-M., Park, J. H., Bayome, M., Oh, M., Park, C. O., Kook, Y.-A., & Mo, S.-S. (2016). A three-dimensional finite element analysis of molar distalization with a palatal plate, pendulum, and headgear according to molar eruption stage. *The Korean Journal of Orthodontics*, 46(5), 290-300.
- Kanzaki, H., Chiba, M., Arai, K., Takahashi, I., Haruyama, N., Nishimura, M., & Mitani, H. (2006). Local RANKL gene transfer to the periodontal tissue accelerates orthodontic tooth movement. *Gene Therapy*, 13(8), 678.
- Kanzaki, H., Chiba, M., Takahashi, I., Haruyama, N., Nishimura, M., & Mitani, H. (2004). Local OPG gene transfer to periodontal tissue inhibits orthodontic tooth movement. *Journal of dental research*, 83(12), 920-925.
- Kawarizadeh, A., Bourauel, C., Zhang, D., Götz, W., & Jäger, A. (2004). Correlation of stress and strain profiles and the distribution of osteoclastic cells induced by orthodontic loading in rat. *European journal of oral sciences*, 112(2), 140-147.
- Keller, T. S., Mao, Z., & Spengler, D. M. (1990). Young's modulus, bending strength, and tissue physical properties of human compact bone. *Journal of Orthopaedic Research*, 8(4), 592-603.

- Keser, E. I., & Dibart, S. (2013). Sequential piezocision: a novel approach to accelerated orthodontic treatment. *American Journal of Orthodontics and Dentofacial Orthopedics*, 144(6), 879-889.
- Kharkar, V. R., Kotrashetti, S. M., & Kulkarni, P. (2010). Comparative evaluation of dento-alveolar distraction and periodontal distraction assisted rapid retraction of the maxillary canine: a pilot study. *International journal of oral and maxillofacial surgery*, 39(11), 1074-1079.
- Kim, K. Y., Bayome, M., Park, J. H., Kim, K. B., Mo, S.-S., & Kook, Y.-A. (2015). Displacement and stress distribution of the maxillofacial complex during maxillary protraction with buccal versus palatal plates: finite element analysis. *The European Journal of Orthodontics*, 37(3), 275-283.
- Kim, S. J., Chou, M. Y., & Park, Y. G. (2015, September). Effect of low-level laser on the rate of tooth movement. In *Seminars in Orthodontics* (Vol. 21, No. 3, pp. 210-218). WB Saunders.
- Kim, S. J., Park, Y. G., & Kang, S. G. (2009). Effects of corticision on paradental remodeling in orthodontic tooth movement. *The Angle Orthodontist*, 79(2), 284-291.
- Kişnişçi, R. Ş., İşeri, H., Tüz, H. H., & Altug, A. T. (2002). Dentoalveolar distraction osteogenesis for rapid orthodontic canine retraction. *Journal of oral and maxillofacial surgery*, 60(4), 389-394.
- Ko, C. C., Rocha, E. P., & Larson, M. (2012). Past, present and future of finite element analysis in dentistry. *Biomedical Applications to Industrial Developments*, 1-25.
- Kojima, Y., & Fukui, H. (2008). Effects of transpalatal arch on molar movement produced by mesial force: a finite element simulation. *American Journal of Orthodontics and Dentofacial Orthopedics*, 142(4), 501-508.
- Kojima, Y., Kawamura, J., & Fukui, H. (2012). Finite element analysis of the effect of force directions on tooth movement in extraction space closure with miniscrew sliding mechanics. *American Journal of Orthodontics and Dentofacial Orthopedics*, 142(4), 501-508.
- Köle, H. (1959). Surgical operations on the alveolar ridge to correct occlusal abnormalities. *Oral Surgery, Oral Medicine, Oral Pathology*, 12(5), 515-529.
- Krishnan, V., & Davidovitch, Z. E. (2006). Cellular, molecular, and tissue-level reactions to orthodontic force. *American Journal of Orthodontics and Dentofacial Orthopedics*, 129(4), 469-e1.
- Ledley, R. S., & Huang, H. K. (1968). Linear model of tooth displacement by applied forces. *Journal of Dental Research*, 47(3), 427-432.
- Lee, H. K., Bayome, M., Ahn, C. S., Kim, S. H., Kim, K. B., Mo, S. S., & Kook, Y. A. (2012). Stress distribution and displacement by different bone-borne palatal expanders with micro-implants: a three-dimensional finite-element analysis. *European journal of orthodontics*, 36(5), 531-540.
- Lee, W., Karapetyan, G., Moats, R., Yamashita, D. D., Moon, H. B., Ferguson, D. J., & Yen, S. (2008). Corticotomy-/osteotomy-assisted tooth **movement** microCTs differ. *Journal of dental research*, 87(9), 861-867
- Liang, W., Rong, Q., Lin, J., & Xu, B. (2009). Torque control of the maxillary incisors in lingual and labial orthodontics: a 3-dimensional finite element analysis. *American Journal of Orthodontics and Dentofacial Orthopedics*, 135(3), 316-322.

- Liem, A. M. L., Hoogeveen, E. J., Jansma, J., & Ren, Y. (2015). Surgically facilitated experimental movement of teeth: systematic review. *British Journal of Oral and Maxillofacial Surgery*, 53(6), 491-506.
- Lim, J. W., Kim, W. S., Kim, I. K., Son, C. Y., & Byun, H. I. (2003). Three-dimensional finite element method for stress distribution on the length and diameter of orthodontic miniscrew and cortical bone thickness. *Korean Journal of Orthodontics*, 33(1), 11-20.
- Lindh, C., Obrant, K., & Petersson, A. (2004). Maxillary bone mineral density and its relationship to the bone mineral density of the lumbar spine and hip. *Oral Surgery, Oral Medicine, Oral Pathology, Oral Radiology, and Endodontology*, 98(1), 102-109.
- Liou, E. J., & Huang, C. S. (1998). Rapid canine retraction through distraction of the periodontal ligament. *American journal of orthodontics and dentofacial orthopedics*, 114(4), 372-382.
- Lombardo, L., Scuzzo, G., Arreghini, A., Gorgun, Ö., Ortan, Y. Ö., & Siciliani, G. (2014). 3D FEM comparison of lingual and labial orthodontics in en masse retraction. *Prog Orthod*, 15(1), 1-12.
- Long, H., Pyakurel, U., Wang, Y., Liao, L., Zhou, Y., & Lai, W. (2012). Interventions for accelerating orthodontic tooth movement: a systematic review. *The Angle Orthodontist*, 83(1), 164-171.
- Lu, S., Li, T., Zhang, Y., Lu, C., Sun, Y., Zhang, J., & Xu, D. (2013). Biomechanical optimization of the diameter of distraction screw in distraction implant by three-dimensional finite element analysis. *Computers in biology and medicine*, 43(11), 1949-1954.
- Mathews, D. P., & Kokich, V. G. (2013). Accelerating tooth movement: the case against corticotomy-induced orthodontics. *American Journal of Orthodontics and Dentofacial Orthopedics*, 144(1), 7.
- McBride, M. D., Campbell, P. M., Opperman, L. A., Dechow, P. C., & Buschang, P. H. (2014). How does the amount of surgical insult affect bone around moving teeth? *American Journal of Orthodontics and Dentofacial Orthopedics*, 145(4), S92-S99.
- Melsen, B. (1999). Biological reaction of alveolar bone to orthodontic tooth movement. *The Angle Orthodontist*, 69(2), 151-158.
- Middleton, J., Jones, M., & Wilson, A. (1996). The role of the periodontal ligament in bone modeling: the initial development of a time-dependent finite element model. *American Journal of Orthodontics and Dentofacial Orthopedics*, 109(2), 155-162.
- Mohandesan, H., Ravanmehr, H., & Valaei, N. (2007). A radiographic analysis of external apical root resorption of maxillary incisors during active orthodontic treatment. *The European Journal of Orthodontics*, 29(2), 134-139.
- Moss-Salentijn, L. (1997). Melvin L. Moss and the functional matrix. *Journal of dental research*, 76(12), 1814-1817.
- Mostafa, Y. A., Fayed, M. M. S., Mehanni, S., ElBokle, N. N., & Heider, A. M. (2009). Comparison of corticotomy-facilitated vs standard tooth-movement techniques in dogs with miniscrews as anchor units. *American Journal of Orthodontics and Dentofacial Orthopedics*, 136(4), 570-577.

- Murphy, K. G., Wilcko, M. T., Wilcko, W. M., & Ferguson, D. J. (2009). Periodontal accelerated osteogenic orthodontics: a description of the surgical technique. *Journal of Oral and Maxillofacial Surgery*, 67(10), 2160-2166.
- Murphy, N. C., Bissada, N. F., Davidovitch, Z. E., Kucska, S., Bergman, R. T., Dashe, J., & Enlow, D. H. (2012, December). Corticotomy and tissue engineering for orthodontists: a critical history and commentary. In *Seminars in Orthodontics* (Vol. 18, No. 4, pp. 295-307). WB Saunders.
- Nelson, D., & Dibart, S. (2014). Sequential piezocision in a challenging adult case. *Journal of clinical orthodontics: JCO*, 48(9), 555.
- Nihara, J., Gielo-Perczak, K., Cardinal, L., Saito, I., Nanda, R., & Uribe, F. (2015). Finite element analysis of mandibular molar protraction mechanics using miniscrews. *The European Journal of Orthodontics*, 37(1), 95-100.
- Nishimura, M., Chiba, M., Ohashi, T., Sato, M., Shimizu, Y., Igarashi, K., & Mitani, H. (2008). Periodontal tissue activation by vibration: intermittent stimulation by resonance vibration accelerates experimental tooth movement in rats. *American Journal of Orthodontics and Dentofacial Orthopedics*, 133(4), 572-583.
- Office of the Surgeon General (US). (2004). *Bone health and osteoporosis: a report of the Surgeon General*.
- Oliveira, D. D., Oliveira, B. F. D., & Soares, R. V. (2010). Alveolar corticotomies in orthodontics: Indications and effects on tooth movement. *Dental Press Journal of Orthodontics*, 15(4), 144-157.
- Ouejjaraphant, T., Samruajbenjakun, B., & Chaichanasiri, E. (2018). Determination of the center of resistance during en masse retraction combined with corticotomy: finite element analysis. *Journal of orthodontics*, 45(1), 11-15.
- Pachêco-Pereira, C., Pereira, J. R., Dick, B. D., Perez, A., & Flores-Mir, C. (2015). Factors associated with patient and parent satisfaction after orthodontic treatment: a systematic review. *American Journal of Orthodontics and Dentofacial Orthopedics*, 148(4), 652-659.
- Pacheco, A. A., Saga, A. Y., Paese, V. N., & Tanaka, O. M. (2016). Stress Distribution Evaluation of the Periodontal Ligament in the Maxillary Canine for Retraction by Different Alveolar Corticotomy Techniques: A Three-dimensional Finite Element Analysis. *The journal of contemporary dental practice*, 17(1), 32-37.
- Park, Y. G., Kang, S. G., & Kim, S. J. (2006). Accelerated tooth movement by corticision as an osseous orthodontic paradigm. *Kinki Tokai Kyosei Shika Gakkai Gakujyutsu Taikai, Sokai*, 48(6), 6-15.
- Pearce, A. I., Richards, R. G., Milz, S., Schneider, E., & Pearce, S. G. (2007). Animal models for implant biomaterial research in bone: a review. *Eur Cell Mater*, 13(1), 1-10.
- Penarrocha-Diago, M., Rambla-Ferrer, J., Perez, V., & Perez-Garrigues, H. (2008). Benign paroxysmal vertigo secondary to placement of maxillary implants using the alveolar expansion technique with osteotomes: a study of 4 cases. *International Journal of Oral & Maxillofacial Implants*, 23(1).
- Proffit, W. R., Fields, H., & Sarver, D. (2007). *Contemporary orthodontics 4th Edition*. Mosby: St Louis.

- Qian, H., Chen, J., & Katona, T. R. (2001). The influence of PDL principal fibers in a 3-dimensional analysis of orthodontic tooth movement. *American Journal of Orthodontics and Dentofacial Orthopedics*, 120(3), 272-279.
- Ren, A., Lv, T., Kang, N., Zhao, B., Chen, Y., & Bai, D. (2007). Rapid orthodontic tooth movement aided by alveolar surgery in beagles. *American Journal of Orthodontics and Dentofacial Orthopedics*, 131(2), 160-e1.
- Ren, Y., Maltha, J. C., Van't Hof, M. A., & Kuijpers-Jagtman, A. M. (2004). Optimum force magnitude for orthodontic tooth movement: a mathematic model. *American journal of orthodontics and dentofacial orthopedics*, 125(1), 71-77.
- Roberts, W. E. (2011). Bone physiology, metabolism and biomechanics in orthodontic practice. *Orthodontics current principles and techniques*, 5, 287-343.
- Roberts, W. E., Huja, S., & Roberts, J. A. (2004, June). Bone modeling: biomechanics, molecular mechanisms, and clinical perspectives. In *Seminars in orthodontics* (Vol. 10, No. 2, pp. 123-161). WB Saunders.
- Safavi, S. M., Heidarpour, M., Izadi, S. S., & Heidarpour, M. (2012). Effects of flapless bur decortications on movement velocity of dogs' teeth. *Dental research journal*, 9(6), 783.
- Sameshima, G. T., & Sinclair, P. M. (2001). Predicting and preventing root resorption: Part II. Treatment factors. *American Journal of Orthodontics and Dentofacial Orthopedics*, 119(5), 511-515.
- Samgir, R., Fulari, S., Agrawal, J., Agrawal, M., Nanjannawar, L., Kagi, V. (2018). A comparative evaluation of effects of micro-osteoperforations on canine retraction using finite element analysis: An in vitro study. *International Journal of Scientific Study* (Vol. 5, Issue. 11).
- Sanjideh, P. A., Rossouw, P. E., Campbell, P. M., Opperman, L. A., & Buschang, P. H. (2009). Tooth movements in foxhounds after one or two alveolar corticotomies. *The European Journal of Orthodontics*, 32(1), 106-113.
- Schwartz-Dabney, C. A., & Dechow, P. C. (2003). Variations in cortical material properties throughout the human dentate mandible. *American Journal of Physical Anthropology: The Official Publication of the American Association of Physical Anthropologists*, 120(3), 252-277.
- Sebaoun, J. D., Kantarci, A., Turner, J. W., Carvalho, R. S., Van Dyke, T. E., & Ferguson, D. J. (2008). Modeling of trabecular bone and lamina dura following selective alveolar decortication in rats. *Journal of periodontology*, 79(9), 1679-1688.
- Shahabee, M., Shafae, H., Abtahi, M., Rangrazi, A., & Bardideh, E. (2019). Effect of micro-osteoperforation on the rate of orthodontic tooth movement—a systematic review and a meta-analysis. *European Journal of Orthodontics*.
- Sherwood, L. (2015). *Human physiology: from cells to systems*. Cengage learning.
- Shoreibah, E. A., Ibrahim, S. A., Attia, M. S., & Diab, M. M. (2012). Clinical and radiographic evaluation of bone grafting in corticotomy-facilitated orthodontics in adults. *Journal of the International Academy of Periodontology*, 14(4), 105-113.
- Showkatbakhsh, R., Jamilian, A., & Showkatbakhsh, M. (2010). The effect of pulsed electromagnetic fields on the acceleration of tooth movement. *World J Orthod*, 11(4), e52-e56.

- Singh, J. R., Kambalyal, P., Jain, M., & Khandelwal, P. (2016). Revolution in Orthodontics: Finite element analysis. *Journal of International Society of Preventive & Community Dentistry*, 6(2), 110.
- Sivarajan, S., Doss, J. G., Papageorgiou, S. N., Cobourne, M. T., & Wey, M. C. (2019). Mini-implant supported canine retraction with micro-osteoperforation: A split-mouth exploratory randomized clinical trial. *The Angle Orthodontist*.
- Stark, T. M., & Sinclair, P. M. (1987). Effect of pulsed electromagnetic fields on orthodontic tooth movement. *American Journal of Orthodontics and Dentofacial Orthopedics*, 91(2), 91-104.
- Staud, R., Robinson, M. E., Goldman, C. T., & Price, D. D. (2011). Attenuation of experimental pain by vibro-tactile stimulation in patients with chronic local or widespread musculoskeletal pain. *European Journal of Pain*, 15(8), 836-842.
- Sung, E.-H., Kim, S.-J., Chun, Y.-S., Park, Y.-C., Yu, H.-S., & Lee, K.-J. (2015). Distalization pattern of whole maxillary dentition according to force application points. *The Korean Journal of Orthodontics*, 45(1), 20-28.
- Sung, S.-J., Jang, G.-W., Chun, Y.-S., & Moon, Y.-S. (2010). Effective en-masse retraction design with orthodontic mini-implant anchorage: a finite element analysis. *American Journal of Orthodontics and Dentofacial Orthopedics*, 137(5), 648-657.
- Suya, H. (1991). *Corticotomy in orthodontics. Mechanical and biological basics in orthodontic therapy*. Heidelberg, Germany: Huthig Buch Verlag, 207-26.
- Suzuki, A., Masuda, T., Takahashi, I., Deguchi, T., Suzuki, O., & Takano-Yamamoto, T. (2011). Changes in stress distribution of orthodontic miniscrews and surrounding bone evaluated by 3-dimensional finite element
- Swapp, A., Campbell, P. M., Spears, R., & Buschang, P. H. (2015). Flapless cortical bone damage has no effect on medullary bone mesial to teeth being moved. *American Journal of Orthodontics and Dentofacial Orthopedics*, 147(5), 547-558.
- Tanne, K., Sakuda, M., & Burstone, C. J. (1987). Three-dimensional finite element analysis for stress in the periodontal tissue by orthodontic forces. *American Journal of Orthodontics and Dentofacial Orthopedics*, 92(6), 499-505.
- Techalerpaisarn, P., & Versluis, A. (2013). Mechanical properties of Opus closing loops, L-loops, and T-loops investigated with finite element analysis. *American Journal of Orthodontics and Dentofacial Orthopedics*, 143(5), 675-683.
- Teixeira, C. C., Khoo, E., Tran, J., Chartres, I., Liu, Y., Thant, L. M., ... & Alikhani, M. (2010). Cytokine expression and accelerated tooth movement. *Journal of dental research*, 89(10), 1135-1141.
- Ten Hoeve, A., Mulie, R. M., & Brandt, S. (1977). Technique modifications to achieve intrusion of the maxillary anterior segment. *Journal of clinical orthodontics: JCO*, 11(3), 174.
- Tominaga, J. Y., Ozaki, H., Chiang, P. C., Sumi, M., Tanaka, M., Koga, Y., ... & Yoshida, N. (2014). Effect of bracket slot and archwire dimensions on anterior tooth movement during space closure in sliding mechanics: a 3-dimensional finite element study. *American Journal of Orthodontics and Dentofacial Orthopedics*, 146(2), 166-174.
- Trivedi, S. (2014). Finite element analysis: A boon to dentistry. *Journal of oral biology and craniofacial research*, 4(3), 200-203.

- Tsai, C. Y., Yang, T. K., Hsieh, H. Y., & Yang, L. Y. (2015). Comparison of the effects of micro-osteoperforation and corticision on the rate of orthodontic tooth movement in rats. *The Angle Orthodontist*, 86(4), 558-564.
- Uribe, F., Padala, S., Allareddy, V., & Nanda, R. (2014). Patients', parents', and orthodontists' perceptions of the need for and costs of additional procedures to reduce treatment time. *American Journal of Orthodontics and Dentofacial Orthopedics*, 145(4), S65-S73.
- Uzuner, F. D., & Darendeliler, N. (2013). Dentoalveolar surgery techniques combined with orthodontic treatment: A literature review. *European journal of dentistry*, 7(02), 257-265.
- van Gemert, L. N., Campbell, P. M., Opperman, L. A., & Buschang, P. H. (2019). Localizing the osseous boundaries of micro-osteoperforations. *American Journal of Orthodontics and Dentofacial Orthopedics*, 155(6), 779-790.
- Van Staden, R. C., Guan, H., & Loo, Y. C. (2006). Application of the finite element method in dental implant research. *Computer methods in biomechanics and biomedical engineering*, 9(4), 257-270.
- Vasudeva, G. (2009). Finite element analysis: a boon to dental research. *Internet J Dent Sci*, 6(3).
- Vercellotti, T., & Podesta, A. (2007). Orthodontic microsurgery: a new surgically guided technique for dental movement. *International Journal of Periodontics & Restorative Dentistry*, 27(4).
- Verna, C. (2016). Regional acceleratory phenomenon. In *Tooth Movement* (Vol. 18, pp. 28-35). Karger Publishers.
- Verna, C., & Melsen, B. (2003). Tissue reaction to orthodontic tooth movement in different bone turnover conditions. *Orthodontics & craniofacial research*, 6(3), 155-163.
- Verna, C., Cattaneo, P. M., & Dalstra, M. (2018). Corticotomy affects both the modulus and magnitude of orthodontic tooth movement. *European journal of orthodontics*, 40(1), 107-112.
- Verna, C., Dalstra, M., & Melsen, B. (2000). The rate and the type of orthodontic tooth movement is influenced by bone turnover in a rat model. *The European Journal of Orthodontics*, 22(4), 343-352.
- Viceconti, M., Davinelli, M., Taddei, F., & Cappello, A. (2004). Automatic generation of accurate subject-specific bone finite element models to be used in clinical studies. *Journal of Biomechanics*, 37(10), 1597-1605.
- Wachter, N. J., Krischak, G. D., Mentzel, M., Sarkar, M. R., Ebinger, T., Kinzler, L., ... & Augat, P. (2002). Correlation of bone mineral density with strength and microstructural parameters of cortical bone in vitro. *Bone*, 31(1), 90-95.
- Wakabayashi, N., Ona, M., Suzuki, T., & Igarashi, Y. (2008). Nonlinear finite element analyses: advances and challenges in dental applications. *Journal of dentistry*, 36(7), 463-471.
- Wang, B., Shen, G., Fang, B., Yu, H., Wu, Y., & Sun, L. (2014). Augmented corticotomy-assisted surgical orthodontics decompensates lower incisors in Class III malocclusion patients. *Journal of Oral and Maxillofacial Surgery*, 72(3), 596-602.
- Wang, L., Lee, W., Lei, D. L., Liu, Y. P., Yamashita, D. D., & Yen, S. L. K. (2009). Tissue responses in corticotomy-and osteotomy-assisted tooth movements in rats:



- histology and immunostaining. *American Journal of Orthodontics and Dentofacial Orthopedics*, 136(6), 770-e1.
- Wang, X. X., Li, N., Xu, J. G., Ren, X. S., Ma, S. L., & Zhang, J. (2014). 3-Dimensional Finite Element Analysis on Periodontal Stress Distribution of Impacted Teeth During Orthodontic Treatment. In *Frontier and Future Development of Information Technology in Medicine and Education* (pp. 1247-1252). Springer, Dordrecht.
  - Wilcko, M. T., Wilcko, W. M., & Bissada, N. F. (2008, December). An evidence-based analysis of periodontally accelerated orthodontic and osteogenic techniques: a synthesis of scientific perspectives. In *Seminars in Orthodontics* (Vol. 14, No. 4, pp. 305-316). WB Saunders.
  - Wilcko, M. T., Wilcko, W. M., Pulver, J. J., Bissada, N. F., & Bouquot, J. E. (2009). Accelerated osteogenic orthodontics technique: a 1-stage surgically facilitated rapid orthodontic technique with alveolar augmentation. *Journal of Oral and Maxillofacial Surgery*, 67(10), 2149-2159.
  - Wilcko, W. M., Ferguson, D. J., Bouquot, J. E., & Wilcko, M. T. (2003). Rapid orthodontic decrowding with alveolar augmentation: case report. *World Journal of Orthodontics*, 4(3).
  - Wilcko, W. M., Wilcko, M. T., Bouquot, J. E., & Ferguson, D. J. (2001). Rapid orthodontics with alveolar reshaping: two case reports of decrowding. *International Journal of Periodontics and Restorative Dentistry*, 21(1), 9-20.
  - Xue, J., Ye, N., Yang, X., Wang, S., Wang, J., Wang, Y., ... & Lai, W. (2014). Finite element analysis of rapid canine retraction through reducing resistance and distraction. *Journal of Applied Oral Science*, 22(1), 52-60.
  - Yan, X., He, W., Lin, T., Liu, J., Bai, X., Yan, G., & Lu, L. (2013). Three-dimensional finite element analysis of the craniomaxillary complex during maxillary protraction with bone anchorage vs conventional dental anchorage. *American Journal of Orthodontics and Dentofacial Orthopedics*, 143(2), 197-205.
  - Yang, C., Wang, C., Deng, F., & Fan, Y. (2015). Biomechanical effects of corticotomy approaches on dentoalveolar structures during canine retraction: A 3-dimensional finite element analysis. *American Journal of Orthodontics and Dentofacial Orthopedics*, 148(3), 457-465.
  - Yi, J., Xiao, J., Li, Y., Li, X., & Zhao, Z. (2017). Efficacy of piezocision on accelerating orthodontic tooth movement: a systematic review. *The Angle Orthodontist*, 87(4), 491-498.
  - Yoshida, T., Yamaguchi, M., Utsunomiya, T., Kato, M., Arai, Y., Kaneda, T., ... & Kasai, K. (2009). Low-energy laser irradiation accelerates the velocity of tooth movement via stimulation of the alveolar bone remodeling. *Orthodontics & craniofacial research*, 12(4), 289-298.
  - Yu, I.-J., Kook, Y.-A., Sung, S.-J., Lee, K.-J., Chun, Y.-S., & Mo, S.-S. (2014). Comparison of tooth displacement between buccal mini-implants and palatal plate anchorage for molar distalization: a finite element study. *The European Journal of Orthodontics*, 36(4), 394-402.

- Zhao, N., Lin, J., Kanzaki, H., Ni, J., Chen, Z., Liang, W., & Liu, Y. (2012). Local osteoprotegerin gene transfer inhibits relapse of orthodontic tooth movement. *American Journal of Orthodontics and Dentofacial Orthopedics*, 141(1), 30-40.